FUNCTIONALIZED POLY(p-PHENYLENE ETHYNYLENE)S FOR CHEMICAL SENSING AND CARBON NANOTUBE (CNT) DISPERSION

YOUSEF POURGHAZ

Functionalized poly(*p*-phenylene ethynylene)s for chemical sensing and

carbon nanotube (CNT) dispersion

by

Yousef Pourghaz

A thesis submitted to the School of Graduate Studies

in partial fulfillment of the requirements for

the degree of Master of Science

Department of Chemistry

Memorial University

St. John's, Newfoundland and Labrador, Canada

August 2011

Abstract

This dissertation explores the design, synthesis, characterization and applications of conjugated polymers as fluorescence "turn-on" chemosensors and carbon nanotube (CNT) dispersants. A series of poly(p-phenylene ethynylene)s (PPEs) were synthesized using the Sonogashira cross coupling reaction and "click chemistry" was applied to introduce receptor groups such as amino groups to the side chain of the polymers. The ability of synthesized polymers to detect metal ions through a fluorescence "turn-on" mechanism was tested using various metal ions with UV-Vis and fluorescence spectroscopic techniques. The receptor was also introduced to the backbone of the water-soluble polymer to study the efficiency of the polymer in aqueous media. To investigate the binding stoichiometry between the polymer and a metal ion, a ^{1}H NMR titration experiment was conducted to obtain a "Job plot". Further evidence for the stoichiometry ratio was provided by applying UV-Vis titration data to the "SPECFIT" analysis software. Click chemistry was also used to functionalize the PPEs with electron-rich groups such as anthracene and pyrene to interact with CNTs. The difficulties in working with click-produced monomers and synthesized polymers are discussed in terms of low solubility in organic solvents. An alternative synthetic approach to overcome the solubility problem is also described in chapter 3.

Acknowledgements

My gratitude begins with my supervisor Dr. Yuming Zhao, who gave me the opportunity to explore this interesting field. I appreciate his guidance, encouragement and patience with me through my program. I would like to extend my thanks to my supervisory committee members, Dr. Christina Bottaro and Dr. Travis D. Fridgen for taking time to review my thesis, for useful discussions and all other help throughout my graduate studies in Memorial University.

I would like to thank Dr. Dave W. Thompson for his valuable comments and discussions on the spectroscopy section of my project. I would also like to thank Dr. Graham J. Bodwell and his group members for comments on the synthesis of pyrene-related compounds. I also extend my thanks to Ph.D. student Mr. Prateek Dongare for conducting spectroscopy experiments, all my lab mates, especially Ph.D. student Mr. Karimulla Mulla for giving one of the precursors and his helpful comments, and Dr. Guang Chen for his excellent support in the lab.

I am also thankful to all organic professors and respectful staff and CCART personnel. I am very grateful to my family who were supportive all the time during my program. Finally, I would like to thank my fantastic girlfriend Hilary who was a source of encouragement and for her appreciable help in correcting my term papers and thesis.

Table of Contents

Chapter 3 Poly(*p*-phenylene ethynylene)s (PPEs) as Carbon Nanotube Dispersants

List of Figures

List of Schemes

List of Tables

List of Symbols, Abbreviations and Acronyms

δ	chemical shift
λ_{em}	maximum emission wavelength
λ_{max}	maximum absorption wavelength
ε	extinction coefficient
λ	wavelength
χ	mole fraction
Φ	quantum yield (fluorescence)
Acc	acceptor
AFM	atomic force microscopy
alt	alternating
APCI	atmospheric pressure chemical ionization
aq	aqueous
Bu	butyl
BPy	bipyridine
Conc	concentrated
CP	conjugated polymer
CoMoCAT	cobalt-molybdenum catalyzed
CNT	carbon nanotube

Calcd	calculated
d	deuterium (in NMR solvent, e.g. THF-d_8)
d	doublet
DBU	1,8-diazabicyclo[5.4.0]undec-7-ene
DCC	dicyclohexylcarbodiimide
DIPEA	diisopropylethyleamine
DMAP	4-(dimethylamino)phenol
DMF	(*N,N*)dimethylformamide
DMSO	dimethylsulfoxide
EBiB	ethyl 2-bromoisobutyrate
eq.	equivalent
Et$_3$N	triethylamine
FET	field effect transistor
FTIR	fourier transform Infrared (spectroscopy)
HiPCO	high pressure CO disproportionation
HOMO	highest occupied molecular orbital
ICT	intramolecular charge transfer
IR	infrared (spectroscopy)
J	(in NMR) coupling constant (Hz)
LCMS	liquid chromatography-mass spectrometry
LED	light-emitting diode
LUMO	lowest unoccupied molecular orbital

m	multiplet
m/z	mass to charge ratio
MALDI-TOF	matrix assisted laser desorption/ionization–time of flight
Me	methyl
MHz	megahertz
M$^+$	mass peak
mL	milliliter(s)
MS	mass spectrometry
MWNT	multi-walled nanotube
NMR	nuclear magnetic resonance (spectroscopy)
p	para
Ph	phenyl
PET	photoinduced electron transfer
PPE	poly(*p*-phenylene ethynylene)
ppm	parts per million
PPP	poly(*p*-phenylene)
PPV	poly(*p*-phenylenevinylene)
q	quartet (in NMR)
rt	room temperature
s	singlet (in NMR)
satd	saturated
SDS	sodiumdodecylsulfonate

SVD	singular value decomposition
SWNT	single-walled nanotube
t	triplet (in NMR)
THF	tetrahydrofuran
TFA	trifluoroacetic acid
TLC	thin layer chromatography
TMS	trimethylsilyl
TMSA	trimethylsilylacetylene
UV-Vis	ultraviolet-visible
UV-Vis-NIR	ultraviolet-visible-near infrared (spectroscopy)
V	volt(s)

Chapter 1

Introduction

1.1 Conjugated polymers

1.1.1 Types of conjugated polymers (CPs)

Conjugated polymers constitute an important class of organic semiconductors, which show abundant electronic and optical properties owing to the extensive π-electron delocalization along the polymer backbone. Conjugated polymers have been the focus of significant interest during the past decades because of their wide application in advanced optoelectronic devices such as light-emitting diodes (LEDs), solar cells, and field-effect transistors (FETs).[1] Conjugated polymers are synthetically prepared in various types and structures. Poly(p-phenylene vinylene)s (PPVs), polydiacetylenes (PDAs), poly(p-phenylene)s (PPPs), polythiophenes (PTs), and poly(p-phenylene ethynylene)s (PPEs) are the most notable representatives of the vast family of well-studied conjugated polymers in terms of properties, synthesis, and practical applications (Figure 1-1).[2]

PDA   PPP   PPV   PPE   PT
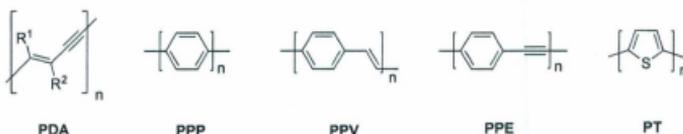
Figure 1-1: Molecular structures of some representative CPs.

1.1.2 Synthesis of CPs

The classic Pd-catalyzed Heck-Cassar-Sonogashira-Hagihara methodology (commonly referred to as the Sonogashira coupling) is one of the most common approaches used to synthesize various CPs. In this reaction, a single bond is formed between an sp carbon and an aromatic through the cross coupling of aryl or vinyl halides and terminal alkynes (Scheme 1-1).

R = Alkyl, Aryl   X = Br, I
OH, OR, CO$_2$R   Y = Acc (nitrile, ester), Don (OR, NR$_2$, alkyl)
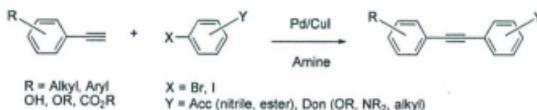
Scheme 1-1: Examples of Sonogashira coupling reactions.
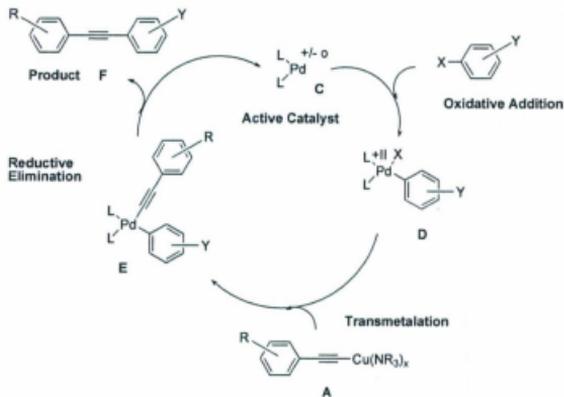
Scheme 1-2: Catalytic cycle of the Sonogashira coupling reaction.

A Pd (0) complex and a halide salt of copper (I) are the two active catalysts promoting this reaction. Commercially available Pd(PPh₃)₂Cl₂ (Pd (II) complex) is frequently used as a source of Pd, which is reduced *in situ* to palladium (0) species by the consumption of terminal alkynes in the beginning of the catalytic cycle (Scheme 1-2).[2]

1.1.3 Poly(*p*-phenylene ethynylene)s (PPEs)

PPEs have been used in semiconductor devices such as LEDs and photodiodes. The main problem to work with PPEs is their low solubility in common organic solvents due to the formation of some cross-linking and diyne defects during the polymerization process.[3] Cross-linking in PPEs is a general problem encountered in synthesis at high temperatures; however, this problem can be avoided if the polymerization is conducted at room temperature or below at least 70 °C.[2] Although solubility can be improved by addition of long-chain alkoxy groups to the backbone of the polymer, the synthesized polymer usually still shows low solubility in organic solvents. The use of excess diiodide monomer in the polymerization and employing mono-iodide compounds as endcapping reagents are two approaches to further enhance the solubility.[2]

1.1.4 Functionalization methods for PPEs

Various types of PPEs can be achieved by the combination of dialkoxy-substituted phenyl diiodides and various dialkynylbenzenes through Pd-catalyzed coupling reactions. Click chemistry is one powerful method to introduce various functional groups to the backbone of the polymer.[5]
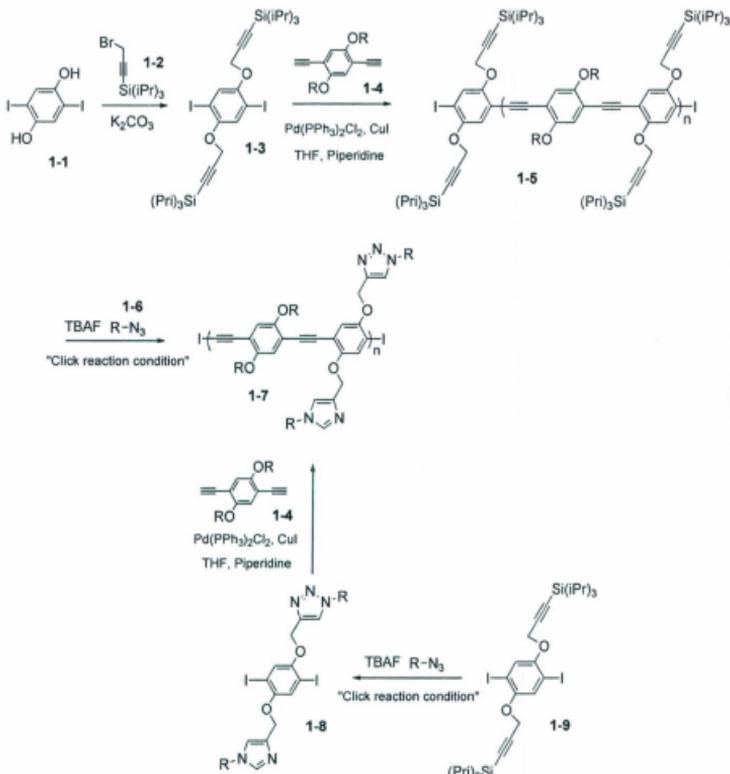
Scheme 1-3: Pre- and post-functionalization of PPEs by click chemistry.[10]

One of the most popular click reactions is based on the 1,3-dipolar cycloaddition of azides to alkynes, which was originally investigated by Huisgen and Szeimies.[4] In 2000,

Sharpless and co-workers used Cu(I) as an efficient catalyst to produce 1,4-disubstituted 1,2,3-triazoles as the only product.[5] The specificity of this transformation, the high yield, and the simple reaction conditions make this reaction widely applicable for synthesizing both small molecules and functionalized polymers.

By the click method, various functional groups can be attached to the backbone of the polymer with the same triazole linker group, which is considered an advantage in studying properties of various PPEs with different pendant groups. Bunz and co-workers synthesized a series of functionalized PPEs employing click chemistry.[6] Pre- and post-functionalization methods were both exploited to synthesize polymers containing the same functional groups (Scheme 1-3).

In the pre-functionalization approach, click reactions are conducted at the stage of monomer synthesis. The click products can be purified before polymerization, which is an advantage of this method. On the other hand, in the post-functionalization approach, synthesized polymers containing some pendant alkyne groups undergo click reactions. This approach is particularly suitable for introducing functional groups which show low stability under harsh polymerization conditions. The Bunz group reported that polymers have been functionalized up to 90% by the post-functionalization approach.[6]

1.2 Poly(*p*-phenylene ethynylene)s (PPEs) as chemosensors

1.2.1 Basics of chemosensors

A chemosensor is a molecular receptor which detects certain external stimuli and turns it to a signal which can be measured or recorded.[7] The external stimuli could be

physical quantities (such as weight), chemical analytes or biological components. A receptor element, a signal transducer, and a read-out mechanism are the three essential parts of a typical sensor. A key component of a sensor is the receptor element which directly interacts with the analyte.

Three types of sensors based on the external stimulus are physical sensors, biosensors and chemical sensors. Chemical sensors have been designed to detect cations, anions, neutral molecules, acids, chemical vapors and many other species. The selectivity, detection limit, sensitivity and reversibility are important factors to be considered in sensor design.[7]

1.2.2 Fluorescent chemosensors

Radiative relaxation of excited electrons from the excited state to the ground state by emission of photons is called fluorescence. Chemosensors that have been designed based on fluorescence signal changes are referred to as fluorescent chemosensors. The fluorescence change could be in emission intensity, fluorescence lifetime, or shift of emission wavelength.[9]

Fluorescence "turn-off" and "turn-on" are the two types of sensory responses based on the photoinduced electron transfer (PET) mechanism. In the turn-off system, the excited fluorophore with the free receptor is highly fluorescent. Upon addition of the analyte, the LUMO energy level of the receptor/analyte pair stands between the HOMO and LUMO energy levels of the fluorophore. This leads to dissipation of the excitation energy and quenching of fluorescence (Figure 1-2).[20]

Excited fluorophore with free receptor

Strongly fluorescent

Excited fluorophore with analyte bound with receptor

Weakly fluorescent
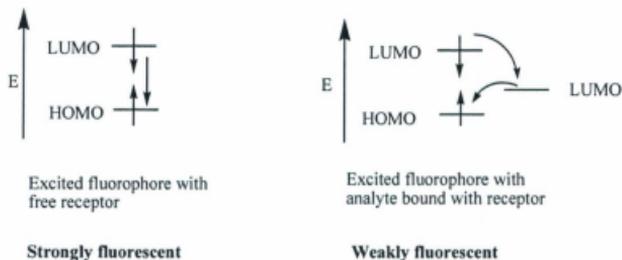
Figure 1-2: Orbital energy diagrams depicting fluorescent "turn-off" based on PET mechanism.

Excited fluorophore   Free receptor

Weakly fluorescent

Excited fluorophore   Bound receptor

Strongly fluorescent
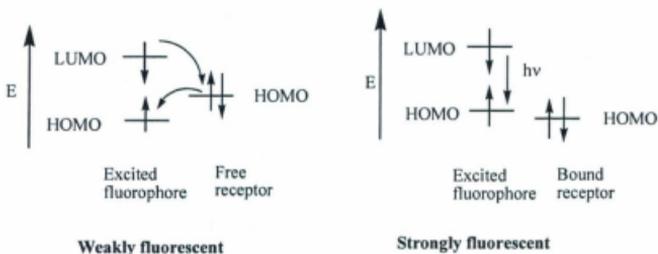
Figure 1-3: Orbital energy diagram depicting fluorescent "turn-on" based on PET mechanism.

In the fluorescence "turn-on" system, the fluorescence is quenched by the non-bonding electron pair of the receptor via rapid intramolecular charge transfer (ICT) from the receptor to the excited fluorophore. When an electron deficient analyte, such as a

7

Lewis acid, is added to the solution, the electron lone pair of the receptor coordinates with the analyte to lower the energy of the HOMO of the receptor. As a result, it turns on the fluorescence of the fluorophore (Figure 1-3).[11]

1.2.3 PPEs as fluorescent chemosensors

PPEs have been successfully designed as chemosensors to detect various types of analytes during the past decade.[12-14] Swager and co-workers have pioneered the use of CPs as chemosensors and introduced the molecule wire and signal amplification concepts.[8]

Completely quenched   Partly quenched
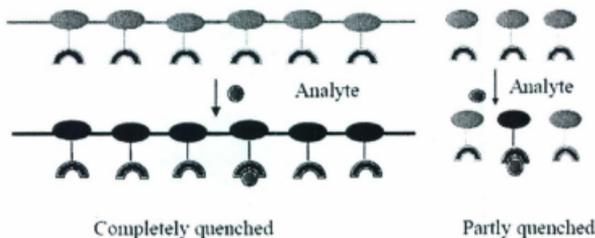
Figure 1-4: Schematic representation of molecule wire concept in CPs versus single molecules.

In PPEs, the entire polymer chain is bound together by saturated sigma bonds as well as the continuous pattern of unsaturated, conjugated bonds. The conjugation between the repeating π- units affords a "molecular wire" (Figure 1-4).[20] PPEs or analogous molecular

8

wires have several advantages over small molecules as chemosensors. The electronic communication between receptors along the polymer backbone is enhanced. In addition, the chemical structures of PPEs can be modified easily to allow them to selectively interact with particular analytes.[15]

1.2.4 PPEs as fluorescent "turn-off" chemosensors

Generally, PPEs are strongly fluorescent due to the extended π-conjugation system. They exhibit strong fluorescence quenching in the presence of electron-deficient species. Amplification of the quenching effect occurs through facile transportation of an exciton along the π conjugated polymer chain (molecular wire).

Swager and co-workers attached a cyclophane-based receptor to the backbone of the PPE for the detection of K^+ ion.[16] Bunz and co-workers synthesized a series of sugar-functionalized PPEs (compound 1-11) (Figure 1-5) and used them successfully to detect Hg^{2+} and Pb^{2+} cations through the turn-off mechanism.[17] By repeating the experiments using PPEs, they demonstrated that the presence of sugar groups is essential to the detection of these particular cations.

PPEs have been employed successfully to selectively detect nitroaromatic explosive vapors such as TNT and DNT.[18] Swager *et al.* introduced a rigid three-dimensional pentiptycene moiety in the backbone of the polymer (Figure 1-5). The fluorescence of the pentiptycene-derived polymer films (compound 1-10) is rapidly quenched upon exposure to the vapors of TNT and DNT.
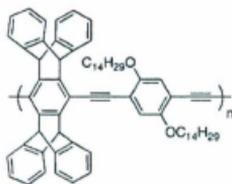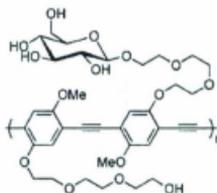
1-10   **1-11**

Figure 1-5: Molecular structure of the polymer to detect vapors of TNT and DNT (left)[18], and chemical structure of the polymer to detect Hg^{2+} and Pb^{2+} cations (right)[17].

The rigid three-dimensional pentiptycene is an electron-rich group that provides porosity in the polymer so that electron deficient compounds, such as TNT and DNT, can penetrate inside the cavities and interact with pentiptycene groups through nonbonding electronic interactions. Since electronic properties and cavity size of the polymers are the two key factors responding to electron deficient moieties, electron-rich polymers with larger cavities should give even stronger fluorescence response. Based on this concept, a sensory device to detect TNT and DNT has been developed by ICx Nomadics, Inc.[18]

1.2.5 Fluorescent "turn-on" chemosensors

In most cases, PPE-based chemosensors are based on the "turn-off" mechanism. Since PPEs have very high fluorescent background, to make PPEs showing lower initial fluorescence is challenging but crucial to achieving "turn-on" systems. The fluorescence intensity of PPEs can be quenched by many factors including impurities, aggregation, and nonspecific cations. The greatest advantage of fluorescence "turn-on" sensors over "turn-

"off" sensors is the ease of measuring low concentrations contrast relative to its "dark" background.[19]

1-12   **1-13**   **1-14**
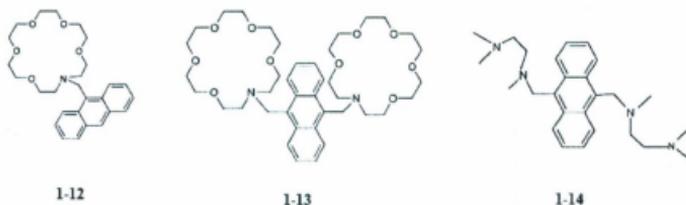
Figure 1-6: Examples of small molecules as fluorescence "turn-on" sensor.[22-23]

1.2.6 Small molecules as fluorescent "turn-on" sensors

Several groups have developed small molecules as "turn-on" chemosensors based on the photoinduced electron transfer (PET) mechanism. In general, Lewis bases function as receptors to interact with analytes that usually are Lewis acids. In most cases, amino groups are used as receptors, while anthracene or other emissive aromatic groups as fluorophore. The de Silva group[21] employed compounds **1-12** and **1-13** as fluorescent turn-on sensors (Figure 1-6). In these examples, the synthesized compounds show only weak fluorescence emission. Upon addition of potassium cations to compound **1-12**, chelation of K$^+$ with the azacrown ether induces a fluorescence enhancement by a factor of forty-seven in methanol.[21] For compound **1-13**, since the receptors have been doubled, a much higher response to potassium cations than compound **1-12** has been observed.[22]

Czarnic *et al.* used compound **1-14** (Figure 1-6) as a potassium sensor.[23] The fluorescence of anthracene is quenched through photoinduced electron transfer from the

nitrogen atoms of the receptor. The fluorescence is strongly initiated with the addition of ZnCl$_2$ by a factor of 1000-fold at the saturation point of a titration in CH$_3$CN. Zinc cations chelate with amino receptors to terminate the PET process between the amino receptor and fluorophore.

water-soluble
cationic PPE

anionic polyacrylate

1-15   **1-16**
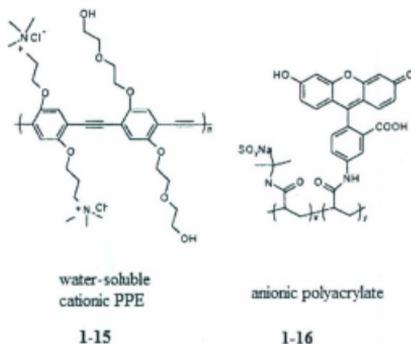
Figure 1-7: Polymers **1-15** and **1-16** which have been deposited on the glass slide.[24]

1.2.7 PPEs as fluorescent "turn-on" chemosensors

Although many examples of small molecule sensors exist in the literature, few examples of PPEs have been presented as "fluorescence" turn-on chemosensors. Swager and co-workers reported the pH-dependant system including polymers **1-15** and **1-16** which undergo intramolecular energy transfer to exhibit fluorescence enhancement (Figure 1-7).[24] The water-soluble cationic poly(*p*-phenylene ethynylen) (PPE) (**1-15**) and the anionic polyacrylate (**1-16**), to which dye has been appended to the polymer's backbone, were deposited layer by layer directly onto a glass slide. Emission of polymer

1-15 (471 nm) overlaps with the absorbance band of the dye which is at 490 nm. As a result, when this system is excited at the absorbance wavelength of polymer **1-15**, the fluorescence enhancement of the dye with increasing pH is observed 10-fold stronger than a case in which the system is excited at the absorbance wavelength of the dye. It is concluded that this overlap encourages fluorescence resonance energy transfer.
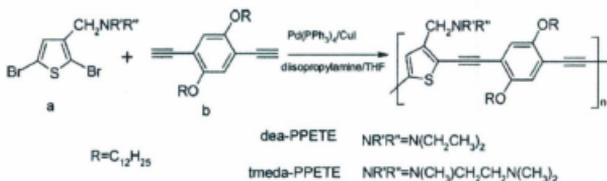
Figure 1-8: Structure of conjugated polymers as fluorescence turn-on chemosensors.[25]

In another study, Jones Jr. *et al.* report the synthesis of two different types of poly[*p*-(phenylene ethylene)-alt-(thienylene ethynylene)] (PPETE) and use them as fluorescent turn-on chemosensors for cations.[25] The receptors are *N,N*-diethylamino and *N,N,N*-trimethylethylenediamino groups in dea-PPETE tmeda-PPETE, respectively (Figure 1-8). Tmeda-PPETE showed better fluorescence enhancement, compared to dea-PPETE, upon addition of metal cations such as Hg^{2+}, Zn^{2+}, Ca^{2+} and H^+. The tmeda-PPETE exhibited selectivity toward Hg^{2+} ion as it showed 2.7-fold enhancement in fluorescence intensity for Hg^{2+} at the saturation point of titration (Figure 1-9). Jones Jr. *et al.* attributed the different responses of dea-PPETE and tmeda-PPETE towards the same cations to the relatively different HOMO/LUMO energy levels of the two amino groups

13

of the polymer backbone. Since the tmeda-PPETE possesses a high fluorescence background, its efficiency as a turn-on sensor is very low in terms of metal cation sensing.
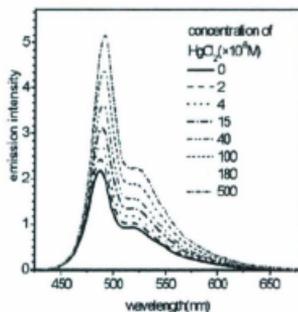
Figure 1-9: Fluorescence titration of tmeda-PPETE with Hg^{2+} cations.[25]

Jones Jr. and co-workers studied another fluorescence turn-on system to detect Fe^{2+} ions in THF.[26] The synthesized polymer (tmeda-PPETE) (Figure 1-8) was treated with various metal cations. The fluorescence intensity of the polymer was enhanced was observed upon addition of certain metal cations; however, the fluorescence was dramatically quenched upon addition of Cu^{2+} in THF. A 150-fold fluorescence enhancement by addition of Fe^{2+} to the tmeda-PPETE/Cu^{2+} hybrid system, whereas other metal cations such as Zn^{2+}, Mn^{2+}, Co^{2+} and Ca^{2+} did not cause any significant enhancement (Figure 1-10).
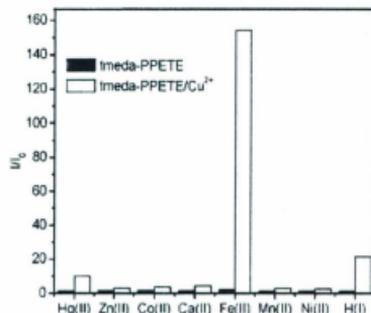
Figure 1-10: Fluorescence response of hybrid (white) and tmeda-PPETE (black) to various cations in THF.[26]

In fact, the hybrid system provides a dark fluorescence background, which is an essential factor for turn-on systems. Since the emission maximum did not shift and the UV-Vis changes were insignificant, Jones Jr. and colleagues concluded that the overall electronic structure of the polymer upon addition of Fe^{2+} is constant; hence, the iron cation has replaced the copper cation in the receptor.

Wei *et al*. reported a turn-on based chemosensor to detect Hg^{2+} selectively in THF.[27] The synthesized polymer, chiral polybinaphthyls incorporating diethylamino and benzo[2,1,3]thiadiazole (BT) moieties as receptors (Figure 1-11), showed stronger fluorescence enhancement for the Hg^{2+} cation compared with other metal ions such as Mg^{2+}, Ni^{2+}, Ag^+, Mn^{2+}, Zn^{2+} and Fe^{3+} (Figure 1-12). Because of the high fluorescence

background of the synthesized polymer, they observed only a 1.8-fold enhancement upon addition of Hg^{2+} cation.
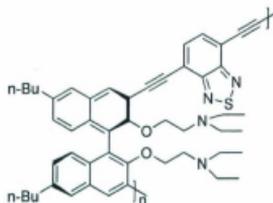
1-17
Figure 1-11: Molecular structure of the chiral polymer to detect Hg^{2+} cations.

In order to study the selectivity of the polymer to the Hg^{2+} cation, Wei *et al.* carried out the fluorescence titration of the polymer with Hg^{2+} cation in the presence of a mixture of several cations such as Cu^{2+}, Ni^{2+} and Cd^{2+}. The polymer exhibited the same fluorescence enhancement without interference from other metal cations in a particular range of concentrations. Hence, they concluded that the polymer can selectively detect the Hg^{2+} cation in the presence of other metal ions. However, the low intensity for the fluorescence enhancement and selectivity to a specific metal cation only in a narrow range of concentrations, are the obstacles for this polymer to be considered as an efficient chemosensor.

Wang *et al.* reported another fluorescence turn-on polymer chemosensor.[28] Both of the synthesized polymers (**1-18** and **1-19**) consist of the dibutylamino group as a receptor on the backbone of the polymer (Figure 1-13). They conducted fluorescence titration for two polymers with different metal ions.

16
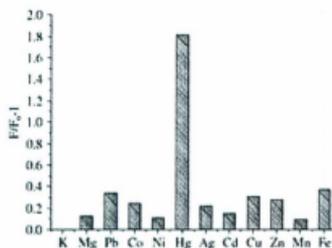
Figure 1-12: Fluorescence enhancement response of the chiral polymer to various metal cations.[27]

The fluorescence enhancement with the intensity of almost 1-fold was achieved for **1-19**, during the titration with Cu^{2+}. On the contrary, the emission spectrum of **1-18** is quenched upon addition of Cu^{2+}.
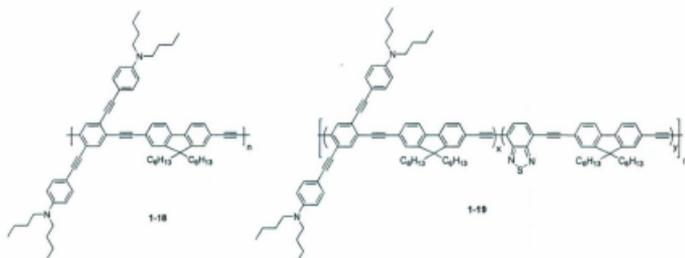
Figure 1-13: Molecular structure of synthesized polymers (**1-18** and **1-19**).

They attributed the quenching effect of **1-18** to the aggregation of polymer chains due to the addition of metal ions. Since **1-19** has nearly the same chemical structure as that of **1-18**, it would also be expected to undergo aggregation upon addition of metal ions.

1.3 PPEs as carbon nanotube (CNT) dispersants

1.3.1 Background of carbon nanotubes (CNTs)

The discoveries of fullerenes[29] and carbon nanotubes (CNTs)[30] around the late 1980s captured wide scientific research interest. The CNT is an allotrope of carbon with a tubular shape, a diameter as small as one nanometer (nm) and the length on the micron scale. Two basic categories of CNTs, in terms of layers, are single-walled nanotubes (SWNTs) and multi-walled nanotubes (MWNTs).

1.3.2 Various types of CNTs

The structure of CNTs is characterized according to the different angles in which graphene sheets wrap to form various types of SWNTs, such as "zigzag", "armchair", and "chiral". They are defined based on the chiral vector (C_h) and two indices (n,m). If n = m, CNTs are called armchair, when m = 0, they are named zigzag nanotubes, otherwise they are identified as chiral (Figure 1-14). "Metallic" and "semiconducting" are two other categories of SWNTs in terms of electronic properties. If n-m=3x (x is an integer), nanotubes are metallic, otherwise they are semiconducting.[31]

Figure 1-14. Schematic diagram of a SWNT with rolling vector (left) and three different types of carbon nanotubes based on the angle of chiral vector (right).[32]

1.3.3 Synthetic methods for CNTs

Several methods have been exploited to synthesize CNTs, including "as-prepared" SWNTs, high pressure CO disproportionation (HiPCO), as well as cobalt-molybdenum catalyzed (CoMoCAT nanotubes). However, achieving SWNTs with specific diameters and lengths is impossible using these methods. Furthermore, the produced SWNTs are not homogenous and contain MWNTs and other impurities, such as residual catalysts. Therefore, one research challenge over the past two decades has been the purification of SWNTs in terms of diameter and electronic properties.[31]

1.3.4 Properties of CNTs

CNTs not only possess exceptionally interesting mechanical and thermal properties, such as strength and flexibility, they also exhibit unique electrical and optical properties due to their specific structures.[33] While the sidewall of an ideal SWNT is considered to be composed of hexagonal networks of carbon atoms with sp^2 hybridization, the end cap

19

contains the hexagonal as well as pentagonal networks of carbon atoms, which make them more susceptible to reactions with other compounds.

Real SWNTs have defects, such as pentagonal or heptagonal rings, as well as inward or outward bends in their sidewalls due to their growth process. SWNTs bundle together in the solid state through supramolecular forces, such as π-π interactions and van der Waals forces between sidewalls to form highly complex networks.[33] These bundled SWNTs are enormously difficult to disperse in solvents.

1.3.5 Applications

Because of the remarkable properties of CNTs, they have been manipulated in various areas, as will next be concisely described.

High strength composites:

CNTs are utilized to enhance the physical properties of materials, such as polymers, in terms of strength, durability and flexibility. Furthermore, the reinforced nanocomposites are extremely light in comparison to other materials with the same toughness, because of the low-density property of CNTs. This feature makes them valuable materials in the aviation industry.[34]

Sensors:

Electron donating or withdrawing molecules, such as NH_3 and NO_2, are able to exchange electrons with the CNTs and hence alter the electronic properties of CNTs, such as conductivity. As a result, the presence of gaseous compounds, such as NH_3 and NO_2 can be detected by measuring the fluctuations of CNTs conductance property.[35]

Gas storage media:

Hydrogen is an ideal source of energy because of its relative lack of harm to the environment and the capability for regeneration. The astonishing hydrogen storage capability of SWNT-containing materials[36], as well as of graphite nanofibers or GNFs[37], has been reported. Because of their specific hollow geometry and the large "length to diameter" ratio, SWNTs are excellent candidates for storing gases such as hydrogen.

One plausible mechanism for this phenomenon is the ability of SWNTs to accumulate the gases in their inner channels and their surfaces. However, there are still some obstacles to technological applications due to the ambiguity in their storage mechanism as well as the effect of other materials on hydrogen storage.[38]

Medicine:

The ability to utilize the CNTs for destroying cancer cells has been reported.[39] The temperature of CNTs can rise to 70 °C in only 120 seconds when exposed to infrared light. By inserting CNTs inside the cancer cells, the cancer cells can be destroyed by infrared light. This capability is considered an advantage of utilizing this method rather than chemotherapy since infrared light has no effect on the other cells.

Photovoltaic applications:

The combination of organic semiconductors with CNTs has revealed promising results to replace the current expensive silicon based solar cells.[40] CNTs are dispersed in electron donating conjugated polymers in order to enhance the efficiency of organic photovoltaic devices.[41]

1.3.6 Dispersion methods for CNTs

Two major methods have been developed to disperse bundles of carbon nanotubes into smaller fractions in terms of size and diameter and introduce them to organic solvents: "covalent functionalization" and "non-covalent functionalization". However, other methodologies, such as "ultrasonication"[42], "ultracentrifugation", "magnetic purification", "microfiltration", and in some cases a combination of these methods have been also exploited.[43]

1.3.7 Covalent functionalization

The "covalent functionalization" method has been exploited during recent years in order to purify the SWNTs from impurities, such as remaining catalysts which are essential to the synthesis of CNTs, and to overcome the aggregation forces of SWNTs with the implementation of solubility. Since there are defects in the sidewalls and end caps of CNTs, covalent functionalization of CNTs on either sidewalls or endcaps is possible.
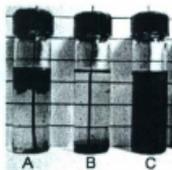
Figure 1-15. Photograph of three separate SWNT samples in THF. (A) Pristine SWNTs; (B) alkyne-functionalized SWNTs; (C) polymer-functionalized SWNTs.[47]

Chen and collaborators reported the solubility of SWNTs by functionalizing through oxidation of SWNTs with aliphatic amines to give amides.[44] In another study, SWNTs were reacted with potassium hydroxide; Pan *et al.* reported that covering the surfaces of SWNTs with hydroxyl groups enhanced their solubility in water (up to 3 mg/mL).[45]

Campidelli *et al.*[46] reported the covalent functionalization of SWNTs with polyamidoamine dendrimers. The covalent functionalization of SWNTs, utilizing the "click reaction", was reported by Li *et al.*[47] In this study, the alkyne-functionalized SWNT undergoes the click reaction with the azide-terminated polystyrene (compound 1-22) to give a polymer-functionalized SWNT (Scheme 1-4), which is soluble in organic solvents (Figure 1-15).
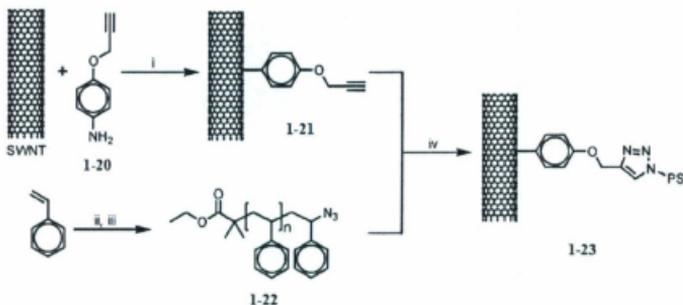
Scheme 1-4. (i) Isoamyl nitrite, 60 °C; (ii) EBiB, CuBr/BPy, DMF, 110 °C; (iii) NaN₃, DMF, room temperature; (iv) Cu(I), DMF.[47]

1.3.8 Non-covalent functionalization

A promising method to disperse SWNT bundles, in terms of retaining electrochemical and physical properties, is the "non-covalent functionalization". Since

the sp^2 hybridized carbons on CNTs are disrupted in the covalent functionalization method, the structure and properties of CNTs change. In the non-covalent functionalization approach, on the contrary, the structure and the properties of CNTs remain intact, since only non-destructive binding forces (e.g. π-π interactions, van der Waals forces and electrostatic interactions) are utilized.

Chen et al. have separated semiconducting SWNTs from metallic ones via non-covalent interactions with "porphyrins".[48] The Raman and UV-Vis-NIR spectral data confirmed the separation of these two different kinds of SWNTs. Hasobe et al. reported the self-assembly of SWNTs in the presence of protonated porphyrin.[49]

$PEG = -(CH_2-CH_2-O)_{11}-$

SWNT   Fluor-PEG

1-24
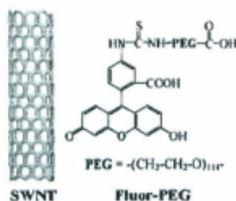
Figure 1-16. Schematic showing of SWNT and fluor-PEG.[50]

The non-covalent functionalization of SWNTs by "fluorescein-polyethylene glycol" (compound **1-24**) was reported by Nakayama-Ratchford et al.[50] In this work, the fluorescence property of SWNT/Fluor-PEG was monitored at various pHs. The result showed that by increasing pH, the absorbance peaks of SWNT/Fluor-PEG exhibited a blue-shift and approached the absorbance peaks of fluorescein. This indicates that the

binding is pH-dependent. At pH 12, precipitation of SWNT/fluor-PEG was observed. Since the SWNT/fluor-PEG complex is stable at pH around 7, soluble in aqueous solutions, and fluorescent, it can be used in physiological systems, which work in buffer media to detect the cells that are bonded to this complex. Furthermore, this complex has the aptitude to undergo further reactions, as the terminal group is a carboxylic acid (Figure 1-16).
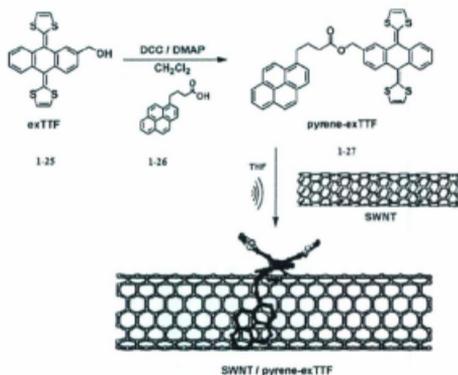
Figure 1-17. Synthesis of pyrene-exTTF and supramolecular SWNT/pyrene-exTTF nanohybrids.[51]

The electron donor ability of "tetrathiafulvalene" (TTF) is well known. Based on this property, Herranz and co-workers[51] reported the π-π interactions between SWNTs and π-extended TTFs such as "pyrene-ex-TTF" (Figure 1-17). The pyrene unit is essential to the surface immobilization of SWNTs through π-π interactions. The electronic properties of

the complex have been investigated because of the electron donor ability of ex-TTF (compound 1-25) and electron accepting properties of SWNTs.

1.3.9 Techniques to evaluate the dispersion of CNTs

Raman spectroscopy:

This technique is a powerful tool for characterizing the CNTs before and after interaction with compounds such as polymers, for which the "radial breathing mode" (RBM) and the tangential mode (G) are the two main features. Vibrations of CNTs in the radial direction from the nanotube axis are responsible for the creation of RBM bands, so that the frequencies of the peaks are reciprocally proportional to diameters of CNTs. The RBM peaks occur in the frequency range of 100-300 cm^{-1}. The G band, in the frequency range of 1500-1600 cm^{-1}, originates from the stretching of the bands among the carbon atoms in the nanotubes (Figure 1-18).
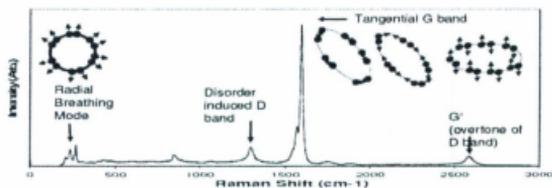
Figure 1-18: Various bands of carbon nanotubes in raman spectrum.[34]

The G band represents the types of SWNTs: metallic or semiconducting. The semiconducting SWNTs show only one peak in this region, whereas the metallic SWNTs

26

exhibit an extra shoulder peak in the lower frequencies. It has been experimentally revealed that with increasing the diameter of the SWNTs, this side peak shifts to higher frequencies and its height and width decrease as well. Moreover, the frequency of the G band is inversely proportional to the diameter of SWNTs.

Another band in the Raman spectrum of SWNTs is the D band, which appears in the frequency range of 1250-1400 cm^{-1}. Since the D band is related to the defects in SWNTs, which leads to breaking in the symmetry of sp^2 hybridized carbons in nanotubes, it can be applied to monitor the covalent interactions of CNTs with various compounds. For instance, if the D band remains without any changes during the interaction with a particular compound, it can be concluded that the nature of the interaction was non-covalent, and the functionalization is non-destructive.[34]
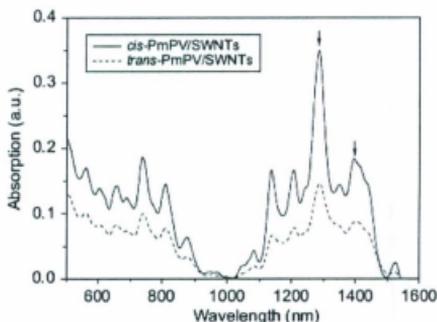
Figure 1-19: UV-VIS-NIR absorption spectra of cis and trans polymer/SWNTs mixture.[53]

Li *et al.*[47] exploited this technique to support the covalent functionalization and the non-covalent functionalization on the surface of the SWNTs. As the aniline derivative compound reacts with the SWNTs covalently, the D band's intensity increases. However, when SWNTs interact with azide-functionalized polystyrene, the D band does not change, indicating non-covalent interaction.

UV-Vis-NIR absorption spectroscopy:

CNTs have unique electronic absorptions in the range of 500-1600 nm; hence, this characteristic can be applied to prove the presence of CNTs in nanohybrids, such as "SWNT/pyren-exTTF".[51] The first transition (E_1) from the valence band to the conductance band can occur in both metallic and semiconducting SWNTs, which is called "S_{11}" and "M_{11}" for semiconducting and metallic SWNTs respectively.

However, only semiconducting SWNTs have the second transition from the valence shell to the conductance shell. Hence, this feature can be applied to distinguish between metallic and semiconducting SWNTs so that S_{11} and S_{22} are the two characteristic peaks for the semiconducting CNTs, and the M_{11} peak corresponds to the presence of metallic ones. The approximate absorption region for the S_{11} and M_{11} is 500-1000 nm, while the S_{22} peaks appear between 1000-1600 nm.[52] Yi *et al.*[53] used this technique to determine the presence of SWNTs in a solution of polymer/CNTs (Figure 1-19).

Thermogravimetric analysis (TGA):

The TGA technique is has also utilized to confirm the presence of CNTs in the complexes such as SWNTs/polymer. Since organic compounds, such as polymers,

decompose at lower temperatures than CNTs, TGA can be used to determine the ratio of functionalization per number of carbon atoms on the SWNT sidewall.[47]

Atomic Force Microscopy (AFM):

One of the techniques used to determine the average diameter of the dispersed CNTs is AFM. For example, AFM was employed to verify the dispersion of SWNTs in the "SWNT/pyren-exTTF" nanohybrid.[51]

1.3.10 Dispersion of CNTs using polymers (non-covalent method)

Polymers have been exploited to disperse the bundles of CNTs and also make them soluble in organic solvents. Polymers with highly electron-rich groups on the side chain, can interact with CNTs through non-covalent forces such as π-π interactions. The nature of the pendant groups on the backbone of the polymer is important to determination of the selectivity of the polymer toward particular SWNTs in terms of diameter, chirality and length.
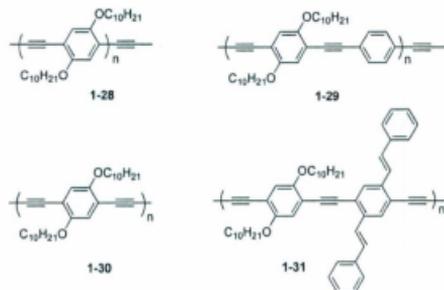
Figure 1-20: Molecular structures of some the conjugated polymers to disperse CNTs.[56]

Nicholas *et al*. employed a series of fluorene-based polymers to disperse bundles of CNTs and enriched HiPCO and CoMoCAT nanotubes in terms of specific nanotubes.[54] Chen and co-workers explored another series of fluorene-based polymers to selectively disperse CNTs and extract particular types of SWNTs in terms of chirality.[55]
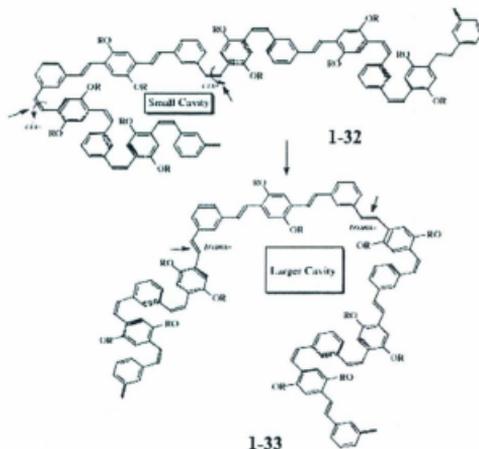
Figure 1-21: Molecular structure of *cis*-PmPV and *trans*-PmPV.[57]

Rice *et al*. reported the dispersion of as-prepared SWNTs employing linear conjugated polymers such as poly(*p*-arylene ethynylene)s (Figure 1-20).[56] Based on the analytical results, they concluded that polymers **1-30** and **1-31** (Figure 1-20) interact with SWNTs to extract the different types of CNTs in terms of diameter. In addition, changing solvents from non-polar to polar solvents exhibited different responses for the mixture of

polymer/SWNTs. In some cases (*e.g.* polymer **1-30**), polar solvents disrupt interactions between the polymer and SWNTs and cause the precipitation of CNTs in the (polymer/CNTs) solution.

Aromatic/aliphatic polyimides have been studied by Delozier *et al*. to debundle the agglomerates of SWNTs.[57] In another study, two isomers of π-conjugated *cis* and *trans* poly[(*m*-phenylenevinylene)-alt-(*p*-phenylenevinylene)] (PmPV) have been investigated in the dispersion of SWNTs. Yi *et al*.[53] found that the *cis*-PmPV is twice as effective as *trans*-PmPV in dispersion of SWNTs, and they reasoned that *cis*-PmPV provided a suitable cavity because of its specific conformation which allowed it to wrap around the SWNTs (Figure 1-21). The Raman spectroscopic result reveals that *trans*-PmPV is more selective for metallic SWNTs. Moreover, the *trans*-PmPV isomerizes to its *cis* conformer under sonication.

1.4. Outline of this thesis

In addition to this introductory chapter, this Master's thesis also contains two chapters focusing on the synthesis of poly(*p*-phenylene ethynylene)s as fluorescence chemosensors and CNTs dispersants. Chapter 2 introduces the synthesis of PPEs to detect metal ions through the fluorescence turn-on mechanism. The synthesized polymer chemosensor is able to detect various metal ions and particularly selective for Zn^{2+} and Cu^{2+} ions in organic solvent. A synthesized water-soluble polymer selectively detects Cd^{2+} ions in the water. "Click chemistry" was successfully used to attach the receptor groups to the backbone of the polymer and the Sonogashira coupling reaction was

applied for polymerization. The photophysical properties of these polymers in response to various metal ions were studied by UV-Vis and fluorescence spectroscopy. ^{1}H NMR titration and UV-Vis titration data were applied to determine the binding properties.

Chapter 3 investigates the functionalization of CNTs through a non-covalent approach using PPEs in order to improve solubility and processability. "Click chemistry" was applied to functionalize the polymer's backbone and polymerization was done using the Sonogashira cross coupling reaction. Both pre- and post-functionalization approaches were explored to functionalize the polymer. Low solubility of monomers was the main difficulty in the pre-functionalization method, while the aggregation of polymers was the obstacle in the post-functionalization approach.

Finally, Chapter 4 summarizes this thesis work and presents perspectives for future work.

Chapter 2

Poly(*p*-phenylene ethynylene)s (PPEs) as Chemosensors

2.1 Introduction

Conjugated polymers incorporating molecular recognition moieties exhibit significant advantages over small molecules in the field of chemosensory devices. For example, the conjugation between the repeating π units affords better electronic communication between receptors along the polymer backbone. This phenomenon is also known as the "signal amplification" concept, which facilitates the measurement of analytes at much lower concentrations compared to small-molecule chemosensors. In addition, the facile modification of the backbone of a conjugated polymer enables the design of selective polymer sensors towards specific target analytes.[15] The fluorescence quenching approach (i.e. "turn-off" mechanism) has been the focus of interest in current chemosensor literature. Highly fluorescent CPs interact with various analytes, depending on the structure of the polymer and as a result, the fluorescence of the polymer is quenched.

The behavior of quenching can be described by the "Stern-Volmer" equation, in which the fluorescence intensity I is related to the quencher's concentration $[Q]$.

$$I = \frac{I_0}{1 + K_{s v}\,[Q]}$$

In this equation, I and I_0 represent the fluorescence intensity after and before addition of the quencher respectively; K_{sv} is the effective association constant for the complex formed between the quencher and the fluorophore. The Stern-Volmer equation applies when the presence of quenchers has no effect on the emission of free fluorophores (unbound fluorophores). This equation can be approximately applied to many CPs at lower quencher concentrations, although the presence of excess quenchers often causes deviations from ideal Stern-Volmer behavior.[67]

In contrast to the class of "turn-off" sensors, only a few examples of CP sensors based on the "turn-on" mechanism exist in the literature.[24-27] In the "turn-on" mechanism, the fluorescence of polymer is restored upon interaction of analytes with receptor groups on the polymer backbone. In general, turn-on sensors have some advantages over turn-off sensors, such as the ease of detecting low concentrations contrast to a dark background, reduced false-positive signals, and enhanced sensitivity. Fluorophore-donor ensembles are the common design motif for fluorescence turn-on sensors. In such a system, the donor group, an amino group for example, binds with analytes such as metal ions to result in fluorescence turn-on based on photoinduced electron transfer (PET) or internal charge-transfer (ICT) mechanisms.[21-22]

CPs have been used to detect metal ions employing the turn-on mechanism. However, high background emission of CPs and the inherent fluorescence quenching effect of some metal ions are obstacles to achieving highly efficient turn-on sensing for

metal ions. In fact, the fluorescence enhancement of the CP sensors for metal ions reported in the literature so far ranges merely from 1 to 3 fold,[25,58] attesting to the difficulty of achieving high performance fluorescence turn-on sensors. Hence, new design concepts have emerged to address the difficulty in fluorescence turn-on sensors.

As previously stated in Chapter 1, Jones Jr. and co-workers synthesized a tmeda-PPETE sensor[26] which was first preloaded with Cu^{2+} ion to acquire a substantially quenched fluorescence background. This inorganic/organic hybrid system then was titrated with Fe^{2+}. Upon progressive addition of Fe^{2+}, the displacement of Fe^{2+} with Cu^{2+} restored the fluorescence of the system up to 150-fold. Although Jones group achieved considerable enhancement in the fluorescence of hybrid system upon titration with Fe^{2+} ions, the obstacles in solely CP-based turn-on sensors for metal ions still remains.

2.2 Objectives of the project

As discussed in the introduction, achieving a sufficiently "dark" fluorescence background is a key prerequisite to devise an efficient turn-on sensing system. To address this challenge, we have investigated the approach of incorporating amino groups as metal ion receptors into the side chains of poly(*p*-phenylene ethynelene)s (PPEs). To our knowledge, this is the first example of using "click" chemistry to attach amino receptor groups to the backbone of PPEs. In our target sensor (**PPE-1**), the 1,2,3-triazole linker group resulting from the popular "click" reaction, Cu-catalyzed alkyne azide cycloaddition (CuAAC), has been employed to attach the receptor (amino groups) as metal ion receptors into the side chains of **PPE-1** (Figure 2-1). Furthermore, the triazole

group not only acts as a structural element (linkage), but also plays a unique functional role in quenching the fluorescence to PPEs.
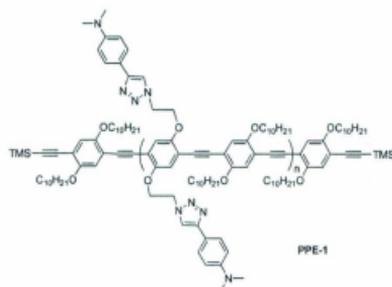
Figure 2-1: Molecular structure of sensor **PPE-1**.

For comparison purposes, two analogous polymers, **PPE-2** and **PPE-3**, have been synthesized to examine the role of receptors as well as triazole linker groups in the side chain of the polymer (Figure 2-2). In **PPE-2**, amino groups (receptors) have been removed from the polymer's side chain, but the phenyl group is still attached through the triazole linkage. Triazole groups have been removed in **PPE-3** and amino receptor groups have been incorporated to the side chain of the polymer via carboxylic ester linkages.

(A)

(B)
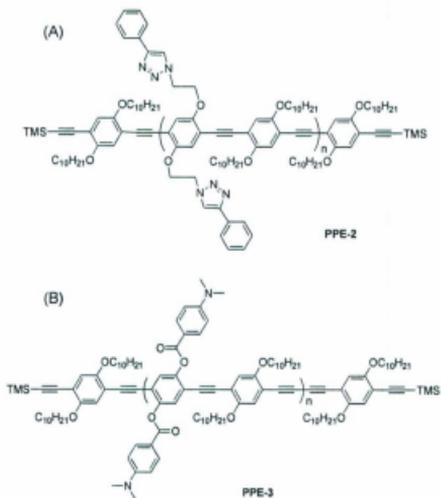
Figure 2-2: Molecular structures of **PPE-2** (A) and **PPE-3** (B).
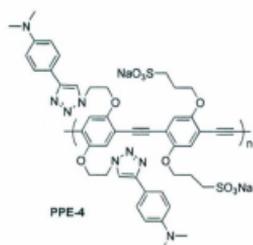
Figure 2-3: Molecular structure of **PPE-4**.

In practical applications, the detection of metal ions directly in aqueous solutions is highly desired. To achieve this goal, a water soluble polymer (**PPE-4**) has also been synthesized and tested (Figure 2-3).

2.3 Results and discussions

2.3.1 Synthesis of PPE-1 and related precursors

Sonogashira cross coupling reaction was used for the formation of PPE backbones. To do so, two monomer building blocks, compound **2-2** and compound **2-11**, were synthesized at first (Figure 2-4).

2-2   **2-11**
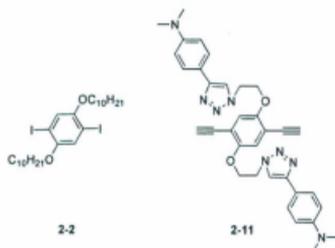
Figure 2-4: Molecular structure of monomers for **PPE-1**.

Compound **2-2** was obtained by alkylation of 1,4-hydroquinone followed by iodination catalyzed by $Hg(OAc)_2$ in dichloromethane (Scheme 2-1). In the first step, commercially available 1,4-hydroquinone underwent the alkylation reaction using 1-bromodecane in a basic ethanol solution to afford compound **2-1**. Then, the iodination of

compound **2-1** in the presence of iodine chips and Hg(OAc)₂ afforded compound **2-2** in a moderate yield of 52%.
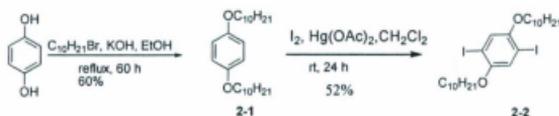
Scheme 2-1: Synthesis of monomer **2-2**.

Compound **2-11** was planned to be synthesized by using Cu-catalyzed alkyne azide cycloaddition (click reaction). To do so, two precursors, compounds **2-6** and **2-9** were first prepared.

The synthesis of compound **2-6** is shown in Scheme 2-2. First, 1,4-bis(2-hydroxyethyloxy)benzene was subjected to an Appel reaction in the presence of CBr₄ and PPh₃ in acetonitrile at room temperature to afford compound **2-3**. Then, iodination of compound **2-3** with I₂/Hg(OAc)₂ was conducted in methylene chloride furnished compound **2-4**. Compound **2-4** was subjected to Sonogashira cross coupling reaction with trimethylsilylacetylene (TMSA) to afford compound **2-5**. Finally, the bromide groups of **2-5** were converted to azido groups in the presence of sodium azide to furnish compound **2-6** in good yield.
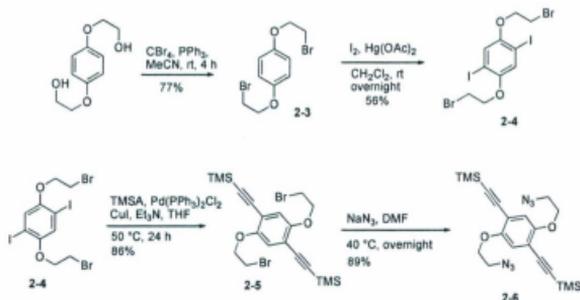
Scheme 2-2: Synthesis of compound **2-6**.

A click reaction between compound **2-6** and compound **2-9** was performed in the presence of diisopropylethylamine (DIPEA) and CuI in DMF to obtain compound **2-10** (Scheme 2-3). Compound **2-10** showed a low stability at room temperature and decomposed after 3 days of storage. Dialkyne **2-11** was synthesized by desilylation of compound **2-10** in the presence of potassium carbonate and THF/MeOH at room temperature. The solubility of **2-10** was dramatically decreased after removal of TMS groups. It was partially soluble in methylene chloride, chloroform, and THF and was completely soluble in DMF and DMSO.

In order to synthesize compound **2-9**, *N,N'*-dimethylaniline was iodinated using iodine chips in pyridine/dioxane mixture at room temperature to furnish compound **2-7**. Compound **2-7** also showed a low stability at room temperature and decomposed after 24 hours and turned to a purple mixture. For this reason, it was used immediately after synthesis. Compound **2-8** could be obtained by subjecting compound **2-7** to Sonogashira

reaction with TMSA in the presence of Pd/Cu catalysts and piperidine as the base. Compound **2-8** underwent desilylation using potassium carbonate in MeOH to afford compound **2-9** (Scheme 2-3).
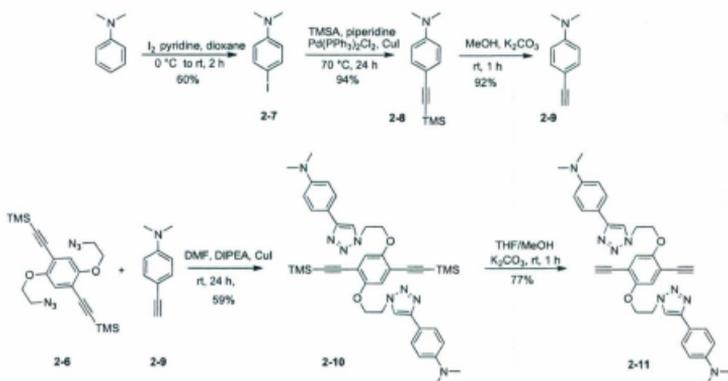
Scheme 2-3: Synthesis of compound **2-9** and monomer **2-11**.

Compound **2-12** was also synthesized to use in the polymerization as an endcapping reagent. It was achieved by subjecting compound **2-2** to Sonogashira reaction with 0.7 molar equivalents of TMSA in the presence of Et₃N and Pd/Cu catalysts to afford compound **2-12** as the major product (Scheme 2-4). A byproduct of this reaction resulted from dialkynylation and it was readily separated from **2-12** via column chromatography.
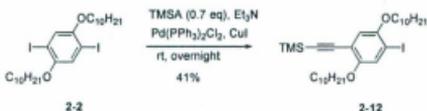
Scheme 2-4: Synthesis of compound **2-12**.

41

With two monomers (compound **2-2** and **2-11**) in hand; polymerization was carried out using a Sonogashira cross coupling reaction (Scheme 2-5). Pd (II) and Cu (I) were used as the catalyst and co-catalyst, while piperidine was used as base. In order to enhance the solubility of resulting polymer products, an endcapping reagent (compound **2-12**) was added in 10% molar equivalent in the polymerization process. The obtained polymer **PPE-1** showed quite good solubility in common organic solvents such as THF, chloroform, and methylene chloride.
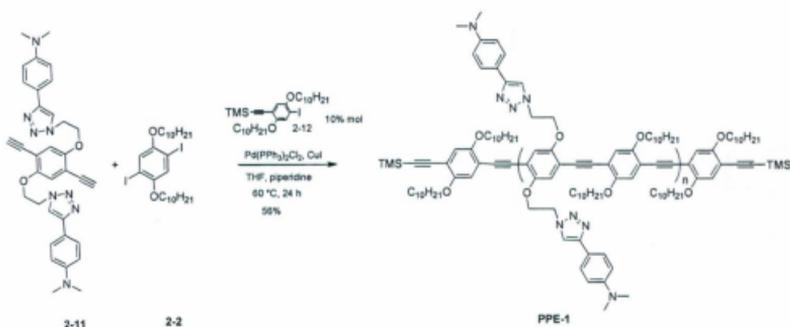
Scheme 2-5: Synthesis of **PPE-1**.

2.3.2 Synthesis of PPE-2 and its corresponding monomers

Compound **2-15** was synthesized as one of the monomers to produce a model polymer (**PPE-2**). First, compound **2-6** was coupled with phenylacetylene under click reaction conditions to form compound **2-14** (Scheme 2-6). Compound **2-15** was

synthesized by desilylation of compound **2-14** by K_2CO_3 in THF/MeOH. The solubility of compound **2-15** decreased significantly compared to its silylated precursor.
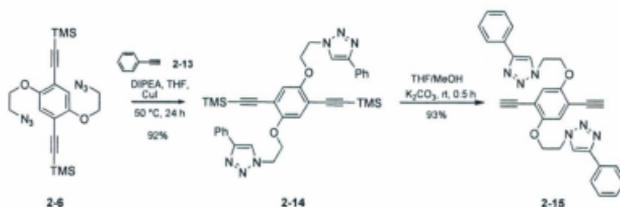
Scheme 2-6: Synthesis of compound **2-15**.

PPE-2 was synthesized through Sonogashira cross-coupling reaction between compounds **2-2** and **2-15** in the presence of endcapping reagent (compound **2-12**). Pd (II) and Cu (I) were used as catalysts and piperidine as base in THF solvent and the mixture was stirred at 60 °C for 24 hours (Scheme 2-7). **PPE-2** is soluble in common organic solvents.
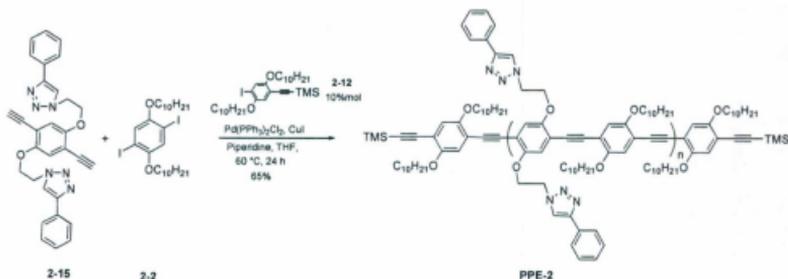
Scheme 2-7: Synthesis of **PPE-2**.

2.3.3 Synthesis of PPE-3 and its corresponding monomers

Monomer **2-17** was obtained from desilylation of compound **2-16** in MeOH/THF by K$_2$CO$_3$ (Scheme 2-8) Compound **2-16** was synthesized through Sonogashira reaction of compound **2-2** with TMSA in THF and Et$_3$N in the presence of Pd/Cu catalysts.
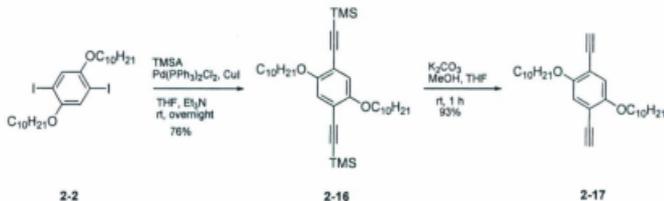
Scheme 2-8: Synthesis of monomer **2-17**.

Monomer **2-22** was synthesized by an esterification reaction of 4-(*N,N'*-dimethylamino)benzoic acid (compound **2-21**) with 1,4-hydroquinone (compound **2-20**) in the presence of SOCl$_2$ and pyridine (Scheme 2-9). To obtain compound **2-20**, compound **2-18** first underwent an iodination reaction using iodine chips and mercuric acetate in dichloromethane to afford compound **2-19**. The methoxy groups of compound **2-19** were converted to hydroxyl groups using BBr$_3$ in methylene chloride to achieve compound **2-20** (Scheme 2-9).
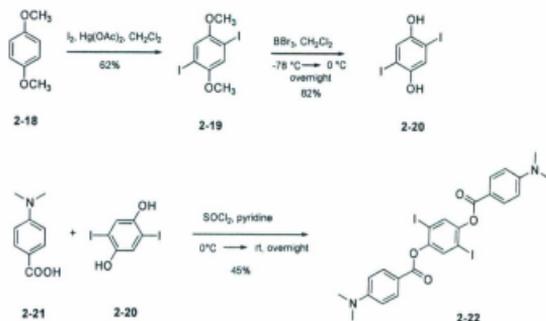
Scheme 2-9: Synthesis of compound **2-20** and monomer **2-22**.

The synthesis of **PPE-3** was achieved using monomer **2-17** and **2-22** through Sonogashira reaction. Compound **2-12** was also used as an endcapping reagent in the presence of Pd/Cu catalysts and DIPEA in THF. The mixture was stirred for 24 hours at room temperature to afford **PPE-3** (Scheme 2-10). **PPE-3** shows quite good solubility in common organic solvents.
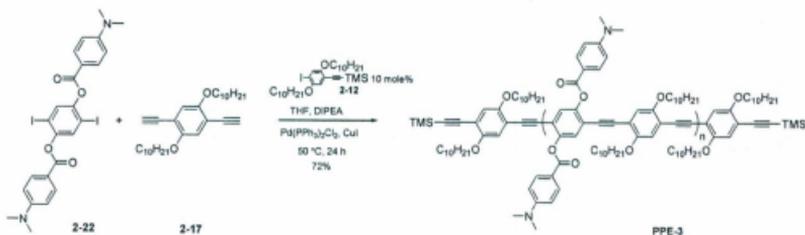
Scheme 2-10: Synthesis of **PPE-3**.

2.3.4 Synthesis of PPE-4 and its corresponding monomers

Monomer **2-24** was synthesized through the reaction of compound **2-20** with propanesultone (compound **2-23**) in a basic solution of sodium hydroxide in dioxane (Scheme 2-11).
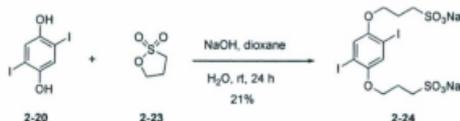
Scheme 2-11: Synthesis of compound **2-24**.

PPE-4 was synthesized according to the published synthetic procedure for water-soluble polymers[59] by the polymerization of monomers **2-24** and **2-11** in a mixture solvent system of DMF/H$_2$O/DIPEA, and Pd/Cu were used as catalysts (Scheme 2-12). **PPE-4** is moderately soluble in water and DMSO.
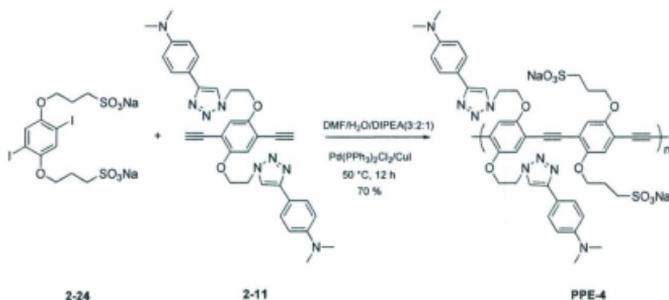
Scheme 2-12: Synthesis of PPE-4.

2.3.5 Characterization of the polymers

As previously discussed, achieving a "dark" fluorescence background is an essential factor for fluorescence "turn-on" sensors. To address this issue, the emission spectrum of the target polymer sensor (**PPE-1**) was obtained and compared to the emission spectra of the two model polymers (**PPE-2** and **PPE-3**). The fluorescence of **PPE-1** is substantially quenched compared with **PPE-2** and **PPE-3** (Figure 2-5). The difference in the fluorescence properties of the three polymers is also clearly distinguishable visually when they are placed under a UV lamp (254 nm) (Figure 2-5).

Without receptor groups (in the case of **PPE-2**), the polymer is highly emissive. By adding amino receptor groups through linkers other than triazole such as esteric groups (**PPE-3**), the polymer still exhibits high fluorescence background. However, when attaching amino receptors via triazole groups as linkers (**PPE-1**), the fluorescence of the polymer is dramatically quenched.

Emission quantum yield measurements provide further confirmation for fluorescence differences in three polymers (Table 2-1). While the emission quantum yield for **PPE-2** and **PPE-3** are 74% and 29% respectively, the emission quantum yield for **PPE-1** is only 3.8%.

Table 2-1: Emission quantum yield for three polymers

polymer	PPE-1	PPE-2	PPE-3
Φ	3.8%	74%	29%

(A)

(B)   (C)
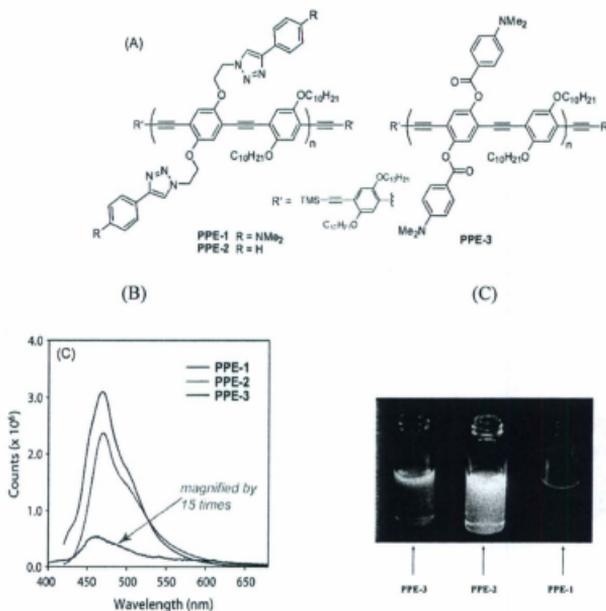
Figure 2-5: (A) Molecular structures of **PPE-1**, **PPE-2** and **PPE-3**. (B) Emission spectra of three polymers in THF (for lucidity, emission spectrum of **PPE-1** was scaled up by 15 times). (C) Photographic images of three polymers in THF under irradiation of a UV lamp.

The emission spectral profile of **PPE-1** is also different from other two model polymers (Figure 2-5 B). The broad, structureless, and relatively blue-shifted

fluorescence band of **PPE-1** is characteristic of a charge-transfer (CT) excited-state emission.[60] A quenching mechanism is hence proposed based on such spectral features as depicted in Figure 2-6.
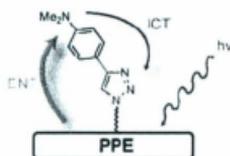
Figure 2-6: Proposed mechanism for fluorescence quenching of **PPE-1**.

Upon irradiation, the PPE unit first captures a photon to reach the first excited state (S_1). Rapid energy transfer (ENT) sensitizes the donor (amino) group, triggering an ICT process from the donor (amino) to the acceptor (triazole) group. As such, the fluorescence is quenched by a relay of energy transfer, sensitization, and charge transfer. It should be noted that the combination of aminophenyl-triazole is essential to fluorescence quenching, since high emissivity still retains for the model polymers where only triazole (**PPE-2**) or amino (**PPE-3**) groups are present on the side chains.
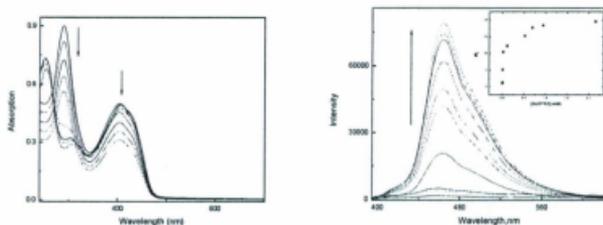
Figure 2-7: Absorption (left) and emission (right) of **PPE-1** obtained simultaneously as a function of increasing aliquots of [Zn(OTf)$_2$] in THF at 298 ± 2 K at concentrations of 0.0, 3.33 × 10^{-6}, 1.0 × 10^{-5}, 3.0 × 10^{-5}, 1.70 × 10^{-4}, 8.33 × 10^{-4}, 1.10 × 10^{-4}, 1.50 × 10^{-4} and 3.45 × 10^{-3} M. λ_{ex} = 380 nm. The arrows indicate the direction of response after addition of analyte. Inset shows the Stern-Volmer plot calculated from emission intensity at 462 nm.

The UV-Vis and fluorescence titration of nearly non-emissive **PPE-1** were conducted towards various metal ions ranging from Zn^{2+}, Cd^{2+}, Cu^{2+} to Ba^{2+}, Na$^+$ and Li$^+$. **PPE-1** was dissolved in THF and its spectral responses were monitored by both UV-Vis absorption and fluorescence spectroscopy upon addition of metal ions. In addition to metal ions, **PPE-1** was also subjected to the titration of a strong Brønsted acid, tirfluoroacetic acid (TFA). Upon addition of metal ions as well as TFA, the fluorescence of **PPE-1** was initiated. The biggest fluorescence enhancement after metal ion addition resulted from Zn^{2+} and Cd^{2+}.

The UV-Vis and fluorescence titration spectra of **PPE-1** with Zn^{2+} are depicted in Figure 2-7. At the saturation point of titration with Zn^{2+}, the fluorescence of **PPE-1** gains a 51-fold enhancement at $\lambda_{em} = 462$ nm, which is the greatest among other tested species. The calculated detection limit for Zn^{2+} ion is 1.37×10^{-6} M, meaning that **PPE-1** is able to sensitively detect Zn^{2+} ions in THF at the ppm level.
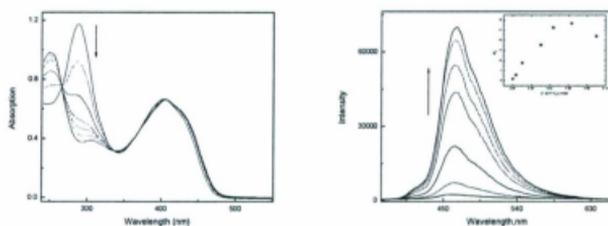
Figure 2-8: Absorption (left) and emission (right) of **PPE-1** obtained simultaneously as a function of increasing aliquots of $Cd(ClO_4)_2$ in THF at 298 ± 2 K at concentrations of 0.0, 3.33×10^{-6}, 1.0×10^{-5}, 3.0×10^{-5}, 9.0×10^{-5}, 4.33×10^{-5}, 6.33×10^{-5} M. $\lambda_{ex} = 380$ nm. The arrows indicate the direction of response after addition of analyte. Inset shows the Stern-Volmer plot calculated from the emission intensity at 475 nm.

PPE-1 also exhibits a very high sensitivity towards Cd^{2+} ions. The UV-Vis and fluorescence titration spectra of **PPE-1** with Cd^{2+} are depicted in Figure 2-8. At the saturation point of titration with Cd^{2+}, the fluorescence of **PPE-1** gains a 34-fold enhancement at $\lambda_{em} = 475$ nm, which is the second greatest enhancement among other

tested species. The calculated detection limit for Cd^{2+} ion is 1.08×10^{-6} M, meaning that **PPE-1** is also able to detect Cd^{2+} ions in THF at the ppm level.

The UV-Vis and fluorescence titration of **PPE-1** with other metal ions and TFA were also carried out (see Appendix 2-1). Figure 2-9 outlines the decreasing trend of sensitivity of **PPE-1** for various metal ions. This trend clearly confirms that **PPE-1** acts as a highly sensitive and selective chemosensor for Zn^{2+} and Cd^{2+} ions in THF.
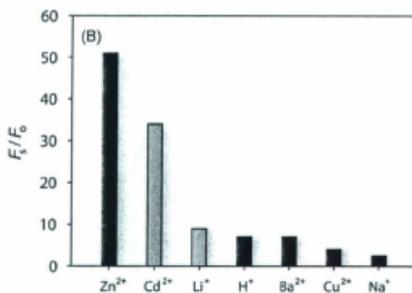
Figure 2-9: Trend of fluorescence enhancement (F_s/F_0) for different cations at maximum emission wavelength (F_s: fluorescence intensity at the saturation point of titration; F_0: initial fluorescence intensity).

The fluorescence enhancement of **PPE-1** upon addition of various metal ions as well as TFA can be visually monitored under irradiation of a UV lamp (Figure 2-10).
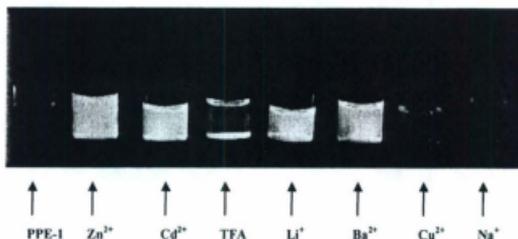
Figure 2-10: Photographic images of THF solutions of **PPE-1** without and with various metal cations under irradiation a UV lamp.

Since amino receptor groups have been incorporated in the side chain of **PPE-3**, the spectroscopic study of this polymer has been conducted to confirm the importance of a "dark" fluorescence background in turn-on system. A THF solution of **PPE-3** was titrated with Cd^{2+} ions and UV-Vis and fluorescence changes were recorded (Figure 2-11). As was expected, the fluorescence enhancement upon addition of metal ions was negligible. Because of the presence of amino receptor groups on the backbone of the polymer, interactions presumably happen between receptor groups and metal ions; however, since the polymer already exhibits high fluorescence background, the difference in the fluorescence after and before adding of metal ions is insignificant.
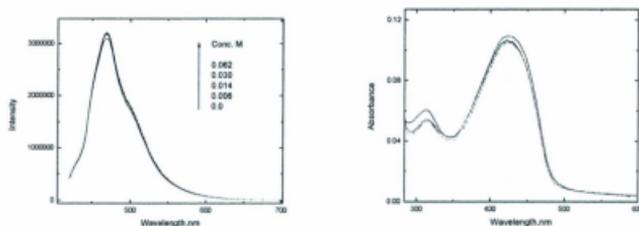
Figure 2-11: Emission (left) and absorption (right) spectra of **PPE-3** obtained as a function of increasing aliquots of $Cd(ClO_4)_2$ in THF at 298 ± 2 K. $\lambda_{ex} = 400$ nm.

One of the main sources of pollution in the environment is trace metals, especially heavy metals. The main use of heavy metals is in industry and they are consequently discharged into the environment to cause severe pollution of water resources. Cadmium, for instance, is a toxic metal and the main contamination sources are mining, plastics manufacturing, and other sources. The maximum permissible level of cadmium in drinking water is 5 μL^{-1}; hence, cadmium ions should be controlled analytically in water resources.[61]

PPE-1 is able to efficiently detect cadmium ions in organic solvents such as THF. In order to achieve the detection of cadmium ion in aqueous media, **PPE-1** was attempted to be introduced into the water. It was found that **PPE-1** can be partially solubilized in water/DMSO (1/1, v/v) with the aid of surfactants such as sodium dodecylsulfonate (SDS). The resulting aqueous solution of PPE-1/SDS showed selective fluorescence turn-on sensing behavior for Cd^{2+} ion. The fluorescence titration of **PPE-1**/SDS mixture with

Cd^{2+} ion is depicted in Figure 2-12. The sensitivity of **PPE-1**/SDS was relatively low (<
3-fold enhancement). The low sensitivity of **PPE-1** in water towards Cd^{2+} ion is
attributed to the poor solubility of **PPE-1** in water and also significant aggregation of
PPE-1 in water.
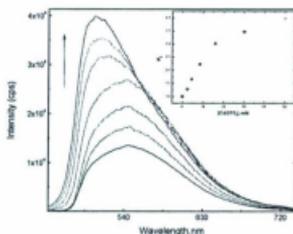
Figure 2-12: Emission spectrum of **PPE-1** obtained as a function of increasing aliquots
of $Cd(ClO_4)_2$ in deionized H_2O/DMSO (1:1 v/v) with 0.5 mg/mL of SDS added as
surfactant at 298 ± 2 K. λ_{ex} = 425 nm. The arrows indicate the direction of response after
addition of analyte. Inset showing Stern-Volmer plot calculated from the emission
intensity at 505 nm.

Since **PPE-1** shows low solubility in water, a new "water-soluble" polymer was
synthesized (**PPE-4**). The same receptor groups were incorporated on the side chain of
the polymer to detect metal ions (Figure 2-13). **PPE-4** was dissolved in water and the
solution was titrated with various metal ions as well as TFA and the spectral responses of

PPE-4 were monitored by both UV-Vis absorption and fluorescence spectroscopy. The fluorescence spectra of **PPE-4** upon titration with Cd^{2+} are depicted in (Figure 2-13).

(A)

(B)   (C)
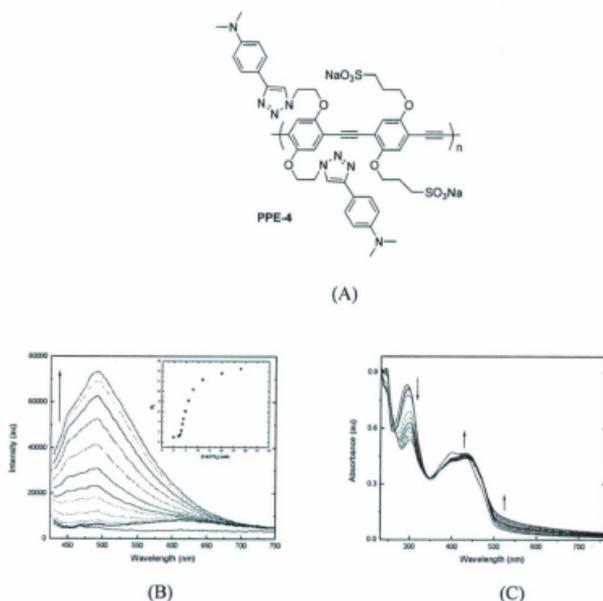
Figure 2-13: (A) Molecular structure of **PPE-4**. (B) Emission and (C) absorption spectra of **PPE-4** obtained simultaneously as a function of increasing aliquots of $Cd(ClO_4)_2$ at concentrations of 0, 2.0, 2.4, 2.8, 3.2, 3.6, 4.0, 4.8, 6.0, 8.0, 12, 20, and 28 mM, titrated in deionized H_2O at 298 ± 2 K. $\lambda_{ex} = 400$ nm. The arrows indicate the direction of response after addition of analyte. Inset shows the Stern-Volmer plot calculated from the emission intensity at 490 nm.

In the early stage of titration, a broad emission band centered at 620 nm grows notably. As the titration continues, a substantial increase at 492 nm becomes the dominant spectral feature. The two different stages of spectral changes suggest multiple binding modes are at work in the interaction of Cd^{2+} ion with **PPE-4**. The UV-Vis and fluorescence titration of **PPE-4** were carried out with other metal ions in water (Appendix 2-1). **PPE-4** exhibits the highest sensitivity towards Cd^{2+} ions among metal ions with a 14-fold fluorescence enhancement. The detection limit for measuring Cd^{2+} ion in water is 3.43×10^{-3} M; hence, **PPE-4** is able to detect Cd^{2+} ions at the mM level in water.
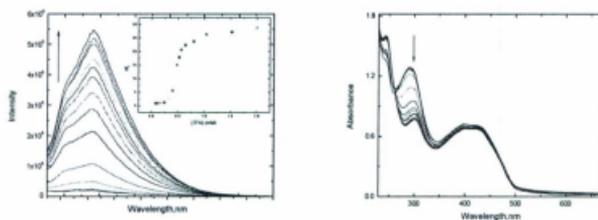
Figure 2-14: The emission (left) and absorption (right) spectra of **PPE-4** obtained simultaneously as a function of increasing aliquots of TFA at concentrations of 0.0, 0.12, 0.16, 0.18, 0.24, 0.32, 0.40, 0.44, 0.48, 0.52, 0.56, 0.64, 0.80, 1.04, 1.52, and 2.0 mM, titrated in deionized H_2O at 298 ± 2 K. λ_{ex} = 400 nm. The arrows indicate the direction of response after addition of analyte. Inset shows the Stern-Volmer plot calculated from the emission intensity at 492 nm.

PPE-4 was also titrated with TFA in water. Upon titration of PPE-4 with TFA in water, much stronger fluorescence enhancement (29-fold) was achieved. The detection limit calculation (*ca.* 3.0×10^{-4} M) also shows higher sensitivity in comparison with Cd^{2+} sensing. The UV-Vis and fluorescence titration of PPE-4 with TFA is depicted in Figure 2-14. Unlike the two-stage scenario in Cd^{2+} titration, the titration of PPE-4 with TFA showed only monotonic emission increase at 492 nm.

(A)   (B)
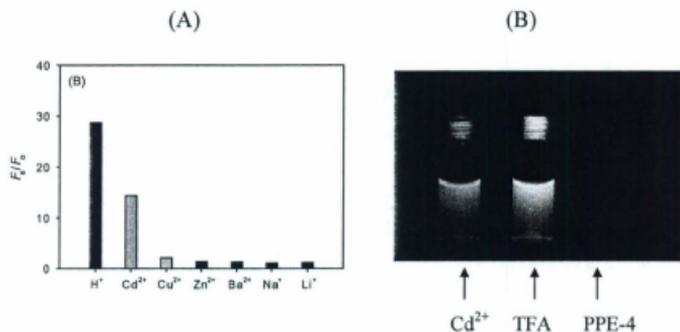
Figure 2-15: (A) Trend of fluorescence enhancement (F_s/F_0) for different cations and TFA at the maximum emission wavelength. (B) Photographic images of aqueous solutions of PPE-4 without and with Cd^{2+} and H^+ ions.

The prominent spectral responses to TFA in water indicate that PPE-4 is more prone to protic acids than metal ions under aqueous conditions. The different titration behaviors

for Cd^{2+} ions and TFA suggest that Cd^{2+} might be preferentially bound to the triazole ligand over the amino at the early stage of titration.

The sensitivity of **PPE-4** towards various metal ions as well as TFA is shown in the decreasing trend depicted in Figure 2-15. In a sharp contrast to **PPE-1**, the sensitivity of **PPE-4** for Zn^{2+} in water was rather diminutive. Since **PPE-4** responses to H$^+$ (*e.g.* TFA) in water, the pH of aqueous solution should be kept neutral or basic; hence, **PPE-4** can selectively detect Cd^{2+} ions in water at pH $\geq$ 7. The difference in fluorescence of **PPE-4** before and after addition of TFA and Cd^{2+} ions can be visually observed under the irradiation of a UV lamp (Figure 2-15).

N-Containing amino and triazole groups on the side chains of two PPE sensors (**PPE-1** and **PPE-4**) were both expected to act as receptors for metal ions. In theory, the binding of metal ions to the amino groups should reduce their electron-donating ability. The perturbation at the donor would then hinder the energy transfer step in the proposed quenching mechanism (Figure 2-6) to revive fluorescence. In addition, the binding of triazole groups with metal ions can also alter non-radiative deactivation steps in the mechanism. In this respect, characterization of the polymer-metal ion interactions is of great value to further unraveling the detailed photophysical mechanisms of the click-functionalized PPE fluorescence turn-on sensor.

To better understanding the binding properties of the receptor and metal ion, monomer **2-11** was titrated with Cd^{2+} ions and its coordination mode was examined by ^{1}H NMR spectroscopy (Figure 2-16).
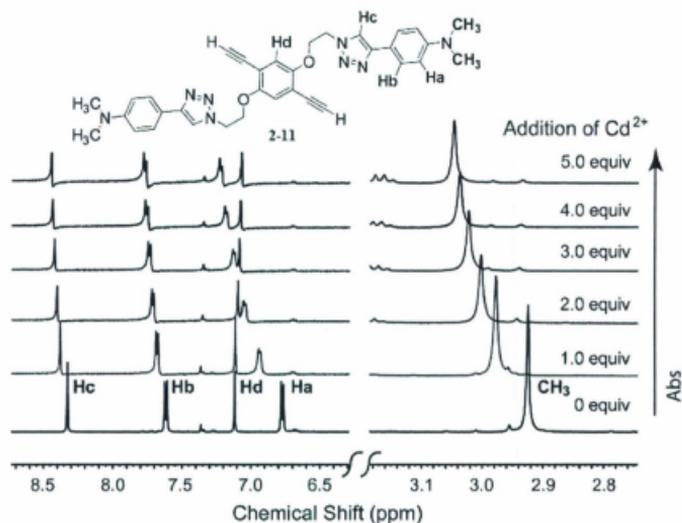
Figure 2-16: Partial ^{1}H NMR spectra monitoring the titration of monomer **2-11** (6.8×10^{-3} M) with Cd(ClO$_4$)$_2$ in DMSO-d_6.

Upon titration of compound **2-11** with Cd^{2+} ion, the ^{1}H NMR signal of CH$_3$ group significantly shifts to the down field direction. The dramatic shift of methyl group signal indicates that nitrogen in the amino group binds with the metal ion; as a result, the chemical environment changes and methyl protons become deshielded. The interaction between the amino group and the metal ion also affects the aminophenyl protons and, as can be seen in Figure 2-16, H$_a$ and H$_b$ also shift down field.

In addition to methyl and aminophenyl protons, the triazole proton (H_c) also shows a significant down field shift, indicating that the interaction of triazole groups with metal ions also occurs. The protons on the central phenyl ring (H_d), however, show only a slight up field shift. The results indicate that the amino and triazole groups are both metal ion receptors to effectively interact with Cd^{2+} ions.

To determine the stoichiometry of the binding event, the obtained data from ^1H NMR spectroscopy was subjected to the Job plot analysis shown in Figure 2-17. In the Job plot, the "x" axis is the molar fraction (χ) and the "y" axis is the difference in the chemical shift after each addition of metal ion which has been multiplied by the molar fraction ($\Delta\sigma \times \chi$) in Hz.
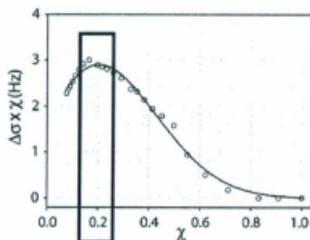
Figure 2-17: Job plot of compound **2-11** in DMSO-d_6 ($\Delta\sigma$: shift of the CH$_3$ signal; χ: molar fraction).

The signal shift of CH$_3$ protons in compound **2-11** was determined upon addition of Cd^{2+} and applied to calculation of the $\Delta\sigma$ values in the Job plot. In the Job plot, if the binding stoichiometry of "host/guest" is 1:1, the apex of the plot should appear at $1/(1+1)$

= 0.5. However, in our case, the apex is at 0.2 which corresponds to the binding stoichiometry of 1:4 ratio ($1/(1+4) = 0.2$). The 1:4 binding stoichiometry is in agreement with ^{1}H NMR observations that compound **2-11** both amino and triazole positions participate in binding.

Furthermore, the UV-Vis titration data of monomer **2-11** with Cd^{2+} was subjected to a global spectral analysis by singular value decomposition (SVD) using the program SPECFIT (Figure 2-18). The analysis validates the 1:4 binding ratio and gives a binding constant of $\log\beta = 1.10 \pm 0.06$ M^{-4} (Appendix 2-1).
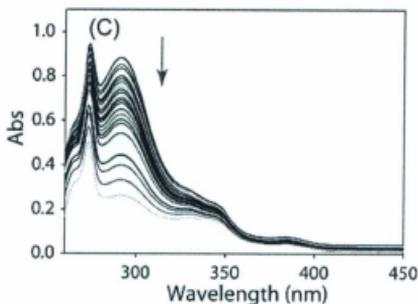
Figure 2-18: UV-Vis titration of compound **2-11** (0.0154 mM) obtained as a function of increasing aliquots of $Cd(ClO_4)_2$ in DMSO at 298 ± 2 K. Data from above spectrum was employed in calculation of association constants using SPECFIT analysis. The arrows indicate the direction of response after addition of analyte.

2.4 Conclusions

Two PPE-based chemosensors (**PPE-1** and **PPE-4**) were designed and synthesized successfully to detect metal ions in THF and water respectively. Incorporation of "click"-generated triazole linker into the side chain of PPEs enables excellent fluorescence turn-on sensing function for Zn^{2+} and Cd^{2+} ions in THF, H^+ and Cd^{2+} ions in water. The binding stoichiometry for the corresponding monomer was also determined by two different methods (Job plot and SPECFIT analysis) and the results confirmed a 1:4 (monomer/metal ion) binding ratio. Click chemistry, in addition to its prominent synthetic advantage, offers an effective approach for tackling the challenges encountered in development of fluorescence turn-on chemosensors using highly emissive CPs as fluorophores. The remarkable sensitivity and selectivity displayed by sensors **PPE-1** and **PPE-4** show promising approach for a wide range of applicability; in particular, the water-soluble **PPE-4** is expected to be a useful sensor for Cd^{2+} ion detection in environmental, biological, and industrial applications.

2.5 Experimental part

All reactions were carried out under a nitrogen atmosphere unless otherwise noted. All chemicals were of reagent grade. Chemicals and reagents were purchased from commercial suppliers and used as received unless noted otherwise. THF was distilled from sodium/benzophenone. Et_3N and toluene were distilled from CaH_2. Palladium catalyst, $Pd(PPh_3)_2Cl_2$, was prepared from $PdCl_2$ according to literature procedures. All reactions were performed in standard, oven-dried glassware. Evaporation and

concentration were performed at H_2O-aspirator pressure. Flash column chromatography was carried out with silica gel 60 (230 - 400 mesh). Thin-layer chromatography (TLC) was carried out with silica gel 60 F254 covered on plastic sheets and visualized by UV light (254 nm) or $KMnO_4$ stain. ^1H and ^{13}C NMR spectra were measured on a Bruker Avance 500 MHz or 300 MHz spectrometers. Chemical shifts (δ) are reported in parts per million (ppm) downfield from the signal of internal reference $SiMe_4$. Coupling constants (J) are given in Hertz. Mass spectra were obtained from an Agilent 1100 series LCMSD spectrometer.

UV-Visible spectra were recorded on an Agilent 8543 Diode Array Spectrophotometer interfaced with an HP computer. Data manipulations were conducted using software supplied by the manufacturer. Spectroscopic experiments were conducted using 1 cm sealed quartz fluorescence cuvettes supplied by Aldrich. Emission spectra were measured on Photon Technology International (PTI) Quantamaster 6000 spectrofluorometer equipped with a continuous xenon arc lamp as the excitation source. The emitting light was collected at 90° to the excitation beam and detected by a Hammamatsu R-928 photomultiplier tube (PMT) in photon counting mode. The PMT was housed in a water-cooled PMT housing supplied by Products for Research Inc. All emission spectra were corrected for instrumental light loss using correction factors supplied by PTI.

Deionized water was obtained from a Sybron/Barnstead apparatus. Spectral grade THF and DMSO solvents (Sigma Aldrich > 99% pure) were used as received. Titrations were performed by using triflate or perchlorate salts of the corresponding transition

metals (unless otherwise noted) purchased from Sigma-Aldrich in 99% purity and used as received. Trifluoroacetic acid (TFA) was used in the titration as a source of H^{+} was purchased from Sigma-Aldrich in 99% purity.

1,4-Bis(decyloxy)benzene (2-1)[62]

2-1
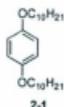
Hydroquinone (5.01 g, 45.5 mmol), KOH (6.36 g, 114 mmol), EtOH (100 mL), $C_{10}H_{21}Br$ (25.02 g, 113.2 mmol) were mixed. The resulting grey mixture was heated at 90 °C for 60 h. It was cooled to room temperature and then diluted with CH_2Cl_2, washed with NH_4Cl, H_2O, and brine and dried over $MgSO_4$. It was filtered through a short silica plug, washed with hexane. The filtrate was concentrated in vacuo. The resulting off-white solid was recrystallized from MeOH. The resulting colorless flakes were washed with cold MeOH to produce **2-1** as colorless flakes (10.62 g, 27.2 mmol, 60%). ^{1}H NMR (300 MHz, CDCl₃): δ = 6.80 (s, 4H), 3.88 (t, J = 6.59 Hz, 4H), 1.78-1.68 (m, 4H), 1.44-1.37 (m, 28H), 0.86 (t, J = 6.45 Hz, 6H); ^{13}C NMR (75 MHz, CDCl₃), δ 153.22, 115.41, 68.69, 31.93, 29.62, 29.59, 29.45, 29.44, 29.35, 26.09, 22.71, 14.14.

1,4-Bis(decyloxy)-2,5diiodobenzene (2-2)[62]

2-2
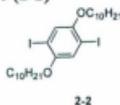
2-1 (8.05 g, 20.6 mmol), I_2 (13.12 g, 51.7 mmol), Hg(OAc)$_2$ (16.30 g, 51.3 mmol) and CH_2Cl_2 (200 mL) were mixed and stirred for 24 h. The resulting mixture was filtered and washed with aqueous $Na_2S_2O_3$ solution, water, brine, and dried over $MgSO_4$. The solvent was removed in vacuo. The crude product was recrystallized from EtOH to afford the product as colorless flakes (6.89 g, 10.7 mmol, 52%). ^{1}H NMR (500 MHz, CDCl$_3$): δ 7.17 (s, 2H), 3.92 (t, J = 6.44 Hz, 4H), 1.82-1.77 (m, 4H), 1.52-1.46 (m, 4H), 1.36-1.32 (m, 24H), 0.88 (t, J = 6.79 Hz, 6H); ^{13}C NMR (75 MHz, CDCl$_3$), δ 152.89, 122.83, 86.33, 70.40, 31.94, 29.59, 29.57, 29.35, 29.31, 29.17, 26.06, 22.72, 14.15.

1,4-Bis(2-bromoethoxy)benzene (2-3)[63]

Carbon tetrabromide (20.5 g, 61.8 mmol) was slowly added in small portions to a solution of 1,4-bis(2-hydroxyethyloxy)benzene (3.1 g, 16 mmol) and triphenylphosphine (16.1 g, 61.4 mmol) in 100 mL of dry acetonitrile in 0 °C with stirring, followed by allowing the reaction mixture to warm to room temperature. The resulting clear solution was stirred for another 4 h. Then 70 mL of cold water was added to the reaction, whereupon product 2-3 precipitated as a colorless solid. The product was collected by vacuum filtration and thoroughly washed with methanol/water (60:40 v/v), and then recrystallized from methanol. The obtained colorless flake-like crystals were dried under vacuum to afford pure 2-3 (3.9 g, 12 mmol, 77%). ^{1}H NMR (500 MHz, CDCl$_3$): δ = 6.86

(s, 2H), 4.25 (t, *J* = 6.30 Hz, 4H), 3.61 (t, *J* = 6.30 Hz, 4H); ^{13}C NMR (75 MHz, CDCl$_3$),

δ 152.84, 116.10, 68.73, 29.28.

2,5-Diiodo-1,4-Bis(2-bromoethoxy)benzene (2-4)[63]

2-4
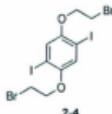
Compound **2-3** (3.0 g, 9.3 mmol), I$_2$ (9.165 g, 36.1 mmol), Hg(OAc)$_2$ (11.4 g, 35.6

mmol) and CH$_2$Cl$_2$ (150 mL) were mixed and the mixture was stirred overnight. Then it

was filtered through MgSO$_4$, washed with aqueous Na$_2$S$_2$O$_3$ solution, H$_2$O, dried over

MgSO$_4$, and evaporated *in vacuo*. The residue was recrystallized from EtOH (70 mL) to

afford **2-4** a colorless solid (16.5 g, 28.6 mmol, 56%). ^{1}H NMR (500 MHz, CDCl$_3$): δ =

7.22 (s, 2 H), 4.27 (t, *J* = 6.33 Hz, 4H), 3.66 (t, *J* = 6.29 Hz, 4H). ^{13}C NMR (75 MHz,

CDCl$_3$), δ 152.78, 123.91, 86.64, 70.34, 28.52.

(2,5-Bis(3-bromopropyl)-1,4-phenylene)bis(ethyne-2,1-diyl)bis(trimethylsilane) (2-5)

2-5
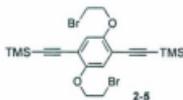
A mixture of **2-4** (800 mg, 1.39 mmol), Pd(PPh$_3$)$_2$Cl$_2$ (20 mg, 0.02 mmol), and CuI

(26 mg, 0.14 mmol) were taken in 15 mL of dry THF/Et$_3$N (1:1). To this constantly

stirred mixture was then dropwise added a solution of TMSA (408 mg, 4.17 mmol) in

THF (2 ml) and stirred at room temperature for 24 h. The solvent was removed and the resulting solid mass was dissolved in CH_2Cl_2 and washed with H_2O. The organic layer was then dried over $MgSO_4$, filtered and finally column chromatographed (hexanes/ethyl acetate 6:1) to give compound **2-5** as an off-white solid (613 mg, 1.19 mmol, 86%). IR (neat): 2956, 2150, 1499, 1396, 1211, 1072, 1025, 902, 840, 756 cm^{-1}; ^{1}H NMR (300 MHz, CDCl$_3$): δ = 6.93 (s, 2H), 4.28 (t, J = 6.46 Hz, 4H), 3.63 (t, J = 6.49 Hz, 4H), 0.26 (s, 18H); ^{13}C NMR (75 MHz, CDCl$_3$), δ 153.75, 118.90, 115.02, 101.54, 100.15, 69.80, 28.83, 0.00; HRMS (EI, +eV) m/z calcd for $C_{22}H_{32}Br_2O_2Si_2$ 513.9995, found 513.9995 (M$^+$).

2,5-Bis(2-azidoethoxy)-1,4-phenylene)bis(ethyne-2,1-diyl)bis(trimethylsilane) (2-6)
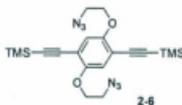
Compound 2-5 (600 mg, 1.36 mmol) was dissolved in DMF (10 mL) and NaN$_3$ (486 mg, 7.49 mmol) was added. The reaction mixture was allowed to stir at 40 °C overnight. Cold water (5 mL) was added to the reaction mixture as well as dichloromethane (15 mL). The organic layer was washed with water and brine and dried over MgSO$_4$. The solvent was evaporated *in vacuo* to furnish **2-6** as colorless needle-like crystals (533 mg, 1.21 mmol, 89%). IR (neat): 2957, 2153, 2112, 1498, 1396, 1307, 1213, 1062, 1010, 939, 870, 833, 758, 696 cm^{-1}; ^{1}H NMR (300 MHz, CDCl$_3$): δ = 6.94 (s, 2H), 4.14 (t, J = 4.88 Hz, 4H), 3.60 (t, J = 4.88 Hz, 4H), 0.25 (s, 18H). ^{13}C NMR (75 MHz, CDCl$_3$), δ 153.73,

118.13, 114.59, 101.39, 100.22, 68.73, 50.50, 0.00; HRMS (EI, +eV) *m/z* calcd for

$C_{20}H_{28}N_6O_2Si_2$ 440.1812, found 440.1816 (M^+).

4-Iodo-*N,N′*-dimethylaniline (2-7)[64]

2-7

N,N-dimethylaniline (0.5 g, 4.1 mmol) was added to pyridine/dioxane (30 mL, 1:1).

The mixture was cooled at 0 °C with an ice-water bath. Iodine chips (3.14 g, 12.4 mmol)

were added and the mixture was stirred for 1 h. Then the ice bath was removed and the

reaction mixture was stirred at room temperature for another 2 h. Afterwards, $Na_2S_2O_3$

(aq. 10%) was added to quench the excess I_2 until the brown color disappeared. After

removal of solvent *in vacuo*, the residue was dissolved in CH_2Cl_2, washed with brine and

dried over $MgSO_4$. Removal of the solvent *in vacuo* again followed by flash column

chromatography (CH_2Cl_2/hexanes, 1:4) afforded the desired product **2-7** as a white

powder (0.61 g, 2.5 mmol, 60%). ^{1}H NMR (300 MHz, CDCl$_3$): δ = 7.47 (d, *J* = 9.05 Hz,

2H), 6.50 (d, *J* = 9.01 Hz, 2H), 2.91 (s, 6H); ^{13}C NMR (75 MHz, CD$_2$Cl$_2$), δ 150.55,

137.84, 115.01, 77.22, 40.50.

***N,N*-dimethyl-4-((trimethylsily)ethynyl)benzenamine (2-8)[65]**

2-8
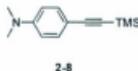
Compound **2-7** (0.6 g, 2.4 mmol), TMSA (0.59 g, 6.1 mmol), CuI (46 mg, 0.24 mmol) and Pd(PPh$_3$)$_2$Cl$_2$ (17 mg, 0.01 mmol) were dissolved in piperidine (15 mL). The mixture was stirred at 70 °C for 24 h. Then the reaction mixture was concentrated *in vacuo* and dissolved in diethyl ether, washed with saturated NaHCO$_3$ solution and brine. The solvent was removed *in vacuo* followed by flash column chromatography with (CH$_2$Cl$_2$/hexanes, 1:9) to afford product **2-8** as a pale yellow solid (496 mg, 2.28 mmol, 94%). ^{1}H NMR (300 MHz, CDCl$_3$): δ = 7.35 (d, J = 8.99 Hz, 2 H), 6.60 (d, J = 8.96 Hz, 2H), 2.96 (s, 6H), 0.23 (s, 9H); ^{13}C NMR (75 MHz, CDCl$_3$), δ 149.98, 132.90, 111.36, 109.67, 106.33, 90.95, 39.95, 0.00.

4-Ethynyl-*N*,*N*-dimethylbenzamine (2-9)[65]
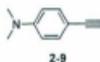
Compound **2-8** (425 mg, 1.96 mmol) was dissolved in MeOH (10 mL) and K$_2$CO$_3$ (756 mg, 5.48 mmol) was added to the mixture. The reaction mixture was stirred for 1 h and the solvent removed *in vacuo*. The residue was dissolved in diethyl ether, washed with brine and dried over MgSO$_4$. The solvent was removed *in vacuo* to afford compound **2-9** as a pale yellow solid (261 mg, 1.80 mmol, 92%). ^{1}H NMR (300 MHz, CDCl$_3$): δ = 7.38 (d, J = 8.96 Hz, 2H), 6.63 (d, J = 8.94 Hz, 2H), 2.97 (s, 7H); ^{13}C NMR (75 MHz, CDCl$_3$), δ 150.17, 132.98, 111.46, 108.53, 84.64, 74.55, 39.95.

Compound 2-10

2-10
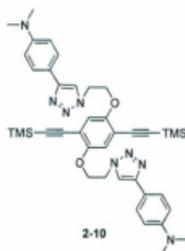
Compound **2-6** (500 mg, 1.13 mmol) and compound **2-9** (403 mg, 2.78 mmol) were dissolved in dry DMF (10 mL) and CuI (23 mg, 0.12 mmol) and DIPEA (17 mg, 0.13 mmol) were added to the mixture. The reaction mixture stirred at room temperature for 24 h. The yellow slurry was filtered and the residue was washed with CH_2Cl_2. The filtrate was washed with saturated NH_4Cl, water and brine and dried under vacuum. Flash column chromatography with ethylacetate/hexanes (2:1) gave **2-6** as a pale yellow solid (487 mg, 0.67 mmol, 59%). IR (neat): 2148, 1614, 1559, 1506, 1493, 1399, 1355, 1217, 1033, 942, 893, 845, 788, 754, 699 cm^{-1}; ^{1}H NMR (300 MHz, CDCl$_3$): δ = 8.06 (s, 2H), 7.70 (d, J = 8.89 Hz, 4H), 6.88, (s, 2H), 6.76 (t, J = 8.89 Hz, 4H), 4.81 (t, J = 4.78 Hz, 4H), 4.35 (t, J = 4.88 Hz, 4H), 2.98 (s, 12H), 0.25 (s, 18H); ^{13}C NMR (75 MHz, CDCl$_3$), δ 153.27, 150.46, 148.70, 126.86, 119.68, 118.98, 117.60, 114.29, 112.52, 101.60, 100.40, 68.09, 49.75, 40.55, 0.20; HRMS (EI, +eV) m/z calcd for C$_{40}$H$_{50}$N$_8$O$_2$Si$_2$ 730.3595, found 730.3611 (M$^+$).

Compound 2-11

2-11
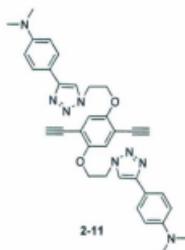
Compound **2-10** (450 mg, 0.61 mmol) and K$_2$CO$_3$ (237 mg, 1.72 mmol) were added to 15 mL of THF/MeOH (2:1) in a round-bottomed flask and stirred for 1 h. The solvent was removed *in vacuo* and the residue was dissolved in CH$_2$Cl$_2$ and washed with water. The organic layer dried over MgSO$_4$ and the solvent was removed *in vacuo* to give **2-11** as a pale yellow solid (275 mg, 0.47 mmol, 77%). IR (neat): 3287, 1612, 1559, 1504, 1446, 1393, 1331, 1270, 1219, 1133, 1041, 941, 865, 805, 737 cm^{-1}; ^{1}H NMR (500 MHz, DMSO-d_6): δ = 8.33 (s, 2 H), 7.63 (d, J = 8.72 Hz, 4H), 7.12, (s, 2H), 6.78 (t, J = 8.75 Hz, 4H), 4.75 (t, J = 4.71 Hz, 4H), 4.48 (s, 2H), 4.41 (t, J = 4.73 Hz, 4H), 2.92 (s, 12H); ^{13}C NMR (75 MHz, DMSO-d_6), δ 152.91, 149.99, 146.88, 126.00, 120.16, 118.63, 117.48, 112.74, 112.40, 86.60, 79.38, 67.50, 48.93, 29.02150.46, 148.70, 126.86, 119.68, 118.98, 117.60, 114.29, 112.52, 101.60, 100.40, 68.09, 49.75, 40.55, 0.20; MALDI-TOF MS (dithranol as the matrix) *m/z* calcd for C$_{34}$H$_{34}$N$_8$O$_2$ 586.2799, found 586.2819 (M$^+$).

1,4-Bis(decyloxy)-2-iodo-5-(trimethylsilylethynyl)benzene (2-12)[62]
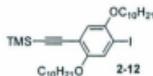
A mixture of 1,4-bis(decyloxy)-2,5-diiodobenzene (**2-2**) (2.02 g, 3.15 mmol), Pd(PPh$_3$)$_2$Cl$_2$ (88.0 mg, 0.12 mmol), and CuI (60.0 mg, 0.31 mmol) were added in 50 mL of dry THF/Et$_3$N (1:1). Then a solution of TMSA (216 mg, 2.20 mmol) in dry THF (5 mL) was added dropwise. The reaction mixture was then stirred at room temperature for 24 h. The solvent was removed under vacuum and the resulting solid mass was dissolved in CH$_2$Cl$_2$ and washed with H$_2$O. The organic layer was dried over MgSO$_4$, filtered and finally column chromatographed (hexanes/CH$_2$Cl$_2$, 10:1) to afford compound **2-12** (790 mg, 1.29 mmol, 41%) as a colorless liquid. ^{1}H NMR (500 MHz, CDCl$_3$): δ = 7.25 (s, 1H), 6.83 (s, 1H), 3.95-3.92 (m, 4H), 1.82-1.75 (m, 4H), 1.52-1.46 (m, 4H), 1.32-1.27 (m, 24H), 0.88 (t, J = 6.57, 6H); ^{13}C NMR (75 MHz, CD$_2$Cl$_2$), δ 154.93, 151.74, 123.87, 116.34, 113.46, 100.83, 99.47, 87.95, 70.14, 69.83, 31.97, 31.94, 29.69, 29.64, 29.62, 29.60, 29.47, 29.38, 29.35, 29.22, 26.15, 26.11, 26.05, 22.74, 14.17, 0.00.

Compound 2-14
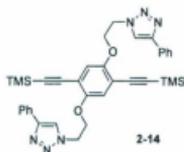
Phenylacetylene (255 mg, 2.50 mmol) was dissolved in dry THF (15 mL) and CuI (28 mg, 0.15 mmol) and DIPEA (21 mg, 0.16 mmol) were added to the mixture. Compound 2-6 (500 mg, 1.13 mmol) was dissolved in THF (5 mL) and added to the reaction mixture dropwise. The reaction mixture stirred in 50 °C for 24 h. The white slurry was filtered and the residue was washed with ethylacetate. The filtrate was washed with saturated NH_4Cl, water and brine and dried under vacuum. The obtained solid was washed with hexane, decanted and dried *in vacuo* to afford compound **2-14** as a pale yellow fine powder (670 mg, 1.04 mmol, 92%). IR (neat): 2961, 2142, 1498, 1402, 1260, 1214, 1023, 932, 864, 797, 756, 691 cm^{-1}; ^{1}H NMR (300 MHz, CD$_2$Cl$_2$): δ = 8.13 (s, 2 H), 7.74 (d, J = 7.78 Hz, 4H), 7.33 (t, J = 7.39 Hz, 4H), 7.24 (t, J = 7.49 Hz, 2H), 6.83 (s, 2H), 4.75 (t, J = 4.76 Hz, 4H), 4.28 (t, J = 4.77 Hz, 4H), 0.15 (s, 18H); ^{13}C NMR (75 MHz, CD$_2$Cl$_2$), δ 153.65, 148.18, 131.30, 129.21, 128.46, 126.13, 121.60, 117.93, 114.58, 101.88, 100.76, 68.39, 50.27, 1.21; HRMS (EI, +eV) *m/z* calcd for C$_{36}$H$_{40}$N$_6$O$_2$Si$_2$ 644.2751, found 644.2753 (M$^+$).

Compound 2-15

2-15
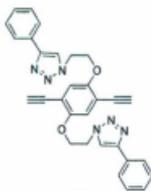
Compound **2-14** (600 mg, 0.93 mmol) and K_2CO_3 (629 mg, 4.56 mmol) were added to 15 mL of THF/MeOH (1:1) in a round-bottom flask and stirred for 0.5 h. The solvent was removed in vacuo and the residue was dissolved in ethylacetate and washed with water. The organic layer dried over $MgSO_4$ and the solvent removed in vacuo to give **2-15** as a pale yellow solid (433 mg, 0.86 mmol, 93%). IR (neat): 3290, 1666, 1565, 1496, 1396, 1353, 1269, 1224, 1156, 1041, 925, 869, 803, 759, 698 cm^{-1}; ^{1}H NMR (300 MHz, CD$_2$Cl$_2$): δ = 8.14 (s, 2 H), 7.74 (d, J = 7.14 Hz, 4H), 7.34 (t, J = 7.03 Hz, 4H), 7.24 (t, J = 7.22 Hz, 2H), 6.88 (s, 2H), 4.74 (t, J = 4.74 Hz, 4H), 4.27 (t, J = 4.97 Hz, 4H), 3.38 (s, 2H); ^{13}C NMR (75 MHz, CD$_2$Cl$_2$), δ 153.89, 147.93, 131.30, 129.23, 128.39, 125.89, 122.04, 118.17, 113.90, 83.78, 79.57, 68.34, 50.09; HRMS (EI, +eV) m/z calcd for $C_{30}H_{24}N_6O_2$ 500.1955, found 500.1958 (M$^+$).

(2,5-Bis(decyloxy)-1,4-phenylenebis(ethyne-2,1-diyl)bis(trimethylsilane) (2-16)[62]

2-16
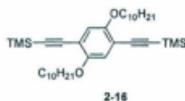
Compound **2-2** (6.52 g, 10.2 mmol), Pd(PPh$_3$)$_2$Cl$_2$ (0.73 g, 1.04 mmol) and CuI (0.42 g, 2.2 mmol) were added to an oven-dried round-bottomed flask containing dry THF/Et$_3$N (100 mL, 1:1). TMSA (2.54 g, 34.3 mmol) in dry THF was added dropwise and the reaction mixture was stirred at room temperature overnight. The solvents was removed *in vacuo* to give the crude product, which was purified by silica flash chromatography using hexanes/ethylacetate (3:1) to afford compound **2-16** as a pale pink

solid (4.51 g, 7.7 mmol, 76%). ^{1}H NMR (500 MHz, CDCl$_3$): δ 6.91 (s, 2H), 3.96 (t, J = 6.36 Hz, 4H), 1.83-1.78 (m , 4H), 1.55-1.49 (m , 4H), 1.34-1.29 (m, 24H), 0.91 (t, J = 6.80, 6H), 0.28 (s, 18H).

1,4-Bis(decyloxy)-2,5-diethylbenzene (2-17)[62]
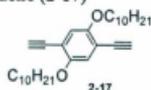
Compound **2-16** (3.2 g, 5.5 mmol) and K$_2$CO$_3$ (31.92 g, 23.1 mmol) were added to 20 mL of THF/MeOH (1:1) in a round-bottomed flask and stirred for 1 h. The solvent was removed *in vacuo* and the residue was dissolved in CH$_2$Cl$_2$ and washed with water. The organic layer was dried over MgSO$_4$ and the solvent removed in vacuo to give **2-17** as a pale yellow solid (2.2 g, 5.0 mmol, 93%). ^{1}H NMR (500 MHz, CDCl$_3$): δ 6.95 (s, 2H), 3.97 (t, J = 6.63 Hz, 4H), 3.32 (s, 2H), 1.82-1.77 (m , 4H), 1.52-1.46 (m , 4H), 1.39-1.34 (m, 24H), 0.90-0.87 (t, J = 6.76 Hz , 6H).

1,4-Diiodo-2,5-dimethoxybenzene (2-19)[68]
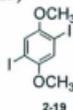
Commercially available 1,4-dimethoxybenzene (2.5 g, 18 mmol), I$_2$ (9.6 g, 38 mmol), Hg(OAc)$_2$ (11.8 g, 37.1 mmol) and CH$_2$Cl$_2$ (150 mL) were mixed and the mixture was stirred overnight. Then it was filtered through MgSO$_4$, washed with Na$_2$S$_2$O$_3$, H$_2$O,

dried over MgSO$_4$ and evaporated *in vacuo*. The residue was recrystallized from EtOH (100 mL) to afford a colorless solid **2-19** (4.4 g, 11 mmol, 62%). ^{1}H NMR (500 MHz, CDCl$_3$): δ = 7.20 (s, 2H), 3.83 (s, 6H).

2,5-Diiodobenzene-1,4-diol (2-20)[68]
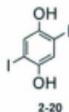
To a solution of compound **2-19** (4.3 g, 11 mmol) in CH$_2$Cl$_2$ (200 mL) under a dry ice bath was added BBr$_3$ (3.13 mL, 33.1 mmol). The mixture was allowed to warm to room temperature and stirred overnight. The resulting mixture was cooled in an ice bath. Then H$_2$O (100 mL) was added. The mixture was then filtered and washed with CH$_2$Cl$_2$. The filtrate was extracted with CH$_2$Cl$_2$ and the organic layer was dried over MgSO$_4$ and evaporated to afford **2-20** as an off-white solid (3.3 g, 9.0 mmol, 82%). ^{1}H NMR (500 MHz, (CD$_3$)$_2$CO): δ = 8.67 (s, 2H), 7.30 (s, 2H).

2,5-Diiodo-1,4-phenylene bis(4-(dimethylamino)benzoate) (2-22)
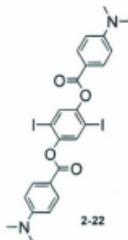
4-(Dimethylamino)benzoic acid (902 mg, 5.47 mmol), 2,5-diiodobenzene-1,4-diol (900 mg, 2.47 mmol) were dissolved in pyridine (15 mL) and the mixture was cooled to 0 °C and SOCl$_2$ (650 mg, 5.47 mmol) was dissolved in pyridine (5 mL) and slowly added to the mixture. The reaction mixture was stirred at room temperature overnight and then poured to a large amount of water. The white precipitation was collected through vacuum filtration and the off-white solid was washed several times with MeOH to give compound **2-22** (729 mg, 1.11 mmol, 45%) as an off-white solid. IR (neat): 1725, 1605, 1537, 1451, 1378, 1269, 1160, 1040, 991, 945, 823, 755, 692 cm^{-1}; ^{1}H NMR (300 MHz, CDCl$_3$): δ = 8.12-8.09 (d, J = 9.06 Hz, 4H), 7.71 (s, 2H), 6.74-6.71 (d, J = 9.10 Hz, 4H), 3.10 (s, 12H); ^{13}C NMR (75 MHz, CDCl$_3$), δ 164.20, 154.01, 149.57, 132.68, 132.44, 114.98, 110.87, 90.06, 40.10; HRMS (EI, +eV) m/z calcd for C$_{24}$H$_{22}$ I$_2$N$_2$O$_4$ 655.9669, found 655.9665 (M$^+$).

Sodium 3,3'-(2,5-diiodo-1,4-phenylene)bis(oxy)dipropane-1-sulfonate (2-24)[66]
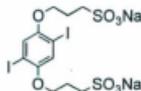
2-24

2,5-Diiodobenzene-1,4-diol (500 mg, 1.38 mmol) was dissolved in a mixed solvent of aq. NaOH (1 M, 25 mL) and dioxane (7 mL). Propane sultone (422 mg, 3.4 mmol) was slowly added to the mixture and stirred for 24 h. The reaction mixture was cooled in an ice bath and acetone was added to give **2-24** (187 mg, 0.29 mmol, 21%) as a white solid. ^{1}H NMR (300 MHz, D$_2$O): δ = 7.39 (s, 2H), 4.11 (t, J = 5.92 Hz, 4H), 3.14 (t, J = 7.67

Hz, 4H), 2.20-2.11 (m, 4H); ^{13}C NMR (75 MHz, D$_2$O), δ 152.52, 124.15, 86.45, 69.33, 48.18, 24.30.

PPE-1

PPE-1
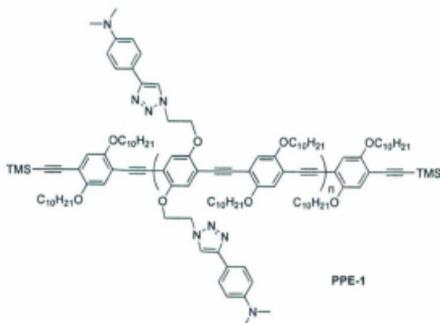
Compound **2-2** (42 mg, 0.06 mmol), compound **2-11** (43 mg, 0.07 mmol), compound **2-12** (5.0 mg, 7.5 × 10^{-3} mmol) as an endcapping reagent, Pd(PPh$_3$)$_2$Cl$_2$ (4.0 mg, 5.7 × 10^{-3} mmol) and CuI (5.0 mg, 2.63 × 10^{-2} mmol) were dissolved in dry THF/piperidine (40 mL, 5:3). The flask was purged with N$_2$ twice and was cooled to -78 °C. The content was heated up to 60 °C. The reaction mixture was stirred for 24 h at this temperature and then cooled to room temperature. The solvent was evaporated off under vacuum and the residual solid mass was dissolved in CH$_2$Cl$_2$ and washed sequentially with satd NH$_4$Cl solution to give a deep-red organic layer, which was concentrated to dryness and dissolved again in CH$_2$Cl$_2$ and precipitated out of MeOH to yield **PPE-1** (36 mg, 3.7 × 10^{-2} mmol, 56%) as a yellow-orange solid. IR (neat): 2921, 2850, 1614, 1561, 1501,

1455, 1357, 1269, 1207, 1040, 938, 858, 811, 722 cm^{-1}; ^{1}H NMR (300 MHz, CDCl$_3$): δ = 8.26 (m, 2H), 7.38 (m, 6H), 6.98 (m, 4H), 6.48 (m, 4H), 4.82 (m, 4H), 4.39 (m, 4H), 3.91 (m, 6H), 2.94 (m, 12H), 1.74 (m, 2H), 1.21 (m, 42H), 0.85 (m, 11H), 0.07 (m, 1H); ^{13}C NMR (75 MHz, CDCl$_3$), δ 150.14, 148.57, 126.46, 112.32, 112.26, 90.12, 90.09, 69.85, 50.02, 49.61, 40.56, 40.34, 31.90, 29.62, 29.55, 29.36, 29.34, 22.72, 22.69, 14.15.

PPE-2

PPE-2
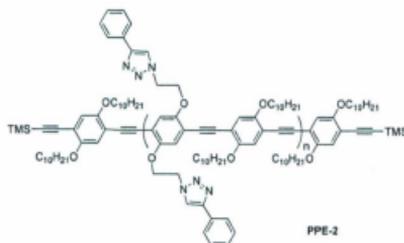
Compound **2-2** (70 mg, 0.11 mmol), compound **2-15** (60 mg, 0.12 mmol), compound **2-12** (6.5 mg, 0.012 mmol) as an endcapping reagent, Pd(PPh$_3$)$_2$Cl$_2$ (1.5 mg, 0.01 mmol) and CuI (6 mg, 0.03 mmol) were dissolved in dry THF/piperidine (40 mL, 5:3). The flask was purged with N$_2$ twice and cooled to -78 °C. The content was heated up to 60 °C. The reaction mixture was stirred for 24 h at this temperature and then cooled to room temperature. The solvent was evaporated under vacuum and the residual solid mass was dissolved in CH$_2$Cl$_2$ and washed sequentially with 1% HCl and satd. NH$_4$Cl solution to give a deep-red organic layer, which was concentrated to dryness and dissolved again in CH$_2$Cl$_2$ and precipitated out of MeOH to yield **PPE-2** (69 mg, 0.08 mmol, 65%) as a

deep-yellow solid. IR (neat): 2921, 2851, 1562, 1498, 1459, 1423, 1369, 1269, 1210, 1040, 920, 857, 761, 693 cm^{-1}; ^{1}H NMR (300 MHz, CD$_2$Cl$_2$): δ = 8.34 (m, 2H), 7.79 (m, 2H), 4.77 (m, 4H), 4.33 (m, 4H), 3.86 (m, 6H), 1.68 (m, 9H), 1.13 (m, 42H), 0.76 (m, 12H), 0.19 (m, 1H); ^{13}C NMR (75 MHz, CD$_2$Cl$_2$), δ 148.03, 147.98, 129.01, 128,15, 126.07, 125.77, 125.74, 125.72, 122.29, 122.24, 70.32, 70.06, 50.17, 32.34, 32.29, 30.03, 29.99, 29.74, 29.73, 26.50, 23.11, 23.08, 14.30.

PPE-3

PPE-3
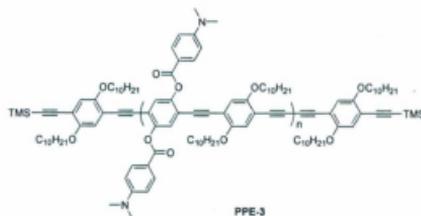
Compound **2-22** (80 mg, 0.12 mmol), compound **2-17** (61 mg, 0.13 mmol), compound **2-12** (9.0 mg, 0.01 mmol) as an endcapping reagent, Pd(PPh$_3$)$_2$Cl$_2$ (8.0 mg, 0.01 mmol) and CuI (5.0 mg, 0.03 mmol) were dissolved in dry THF/piperidine (50 mL, 5:3). The flask was purged with N$_2$ twice and was cooled to -78 °C. The content was heated up to 50 °C. The reaction mixture was stirred for 24 h at this temperature and then cooled to room temperature. The solvent was evaporated off under vacuum and the residual solid mass was dissolved in CH$_2$Cl$_2$ and washed sequentially with water and brine to give a deep-red organic layer, which was concentrated to dryness and redissolved in CH$_2$Cl$_2$ and precipitated out of MeOH to yield **PPE-3** (97 mg, 0.08 mmol, 72%) as a

green-orange solid. IR (neat): 2923, 2853, 1722, 1603, 1539, 1500, 1458, 1426, 1374, 1269, 1211, 1160, 945, 854 cm^{-1}; ^{1}H NMR (300 MHz, CDCl$_3$): δ = 6.97 (m, 8H), 6.70 (m, 4H), 4.00 (m, 32H), 3.09 (m, 12H), 2.04 (m, 18H), 1.27 (m, 196H), 0.86 (m, 45H), 0.26 (m, 5H).

PPE-4

PPE-4
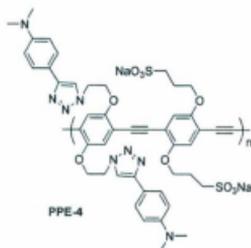
Compound **2-24** (108 mg, 0.17 mmol), compound **2-11** (98 mg, 0.17 mmol), Pd(PPh$_3$)$_2$Cl$_2$ (15 mg, 0.02 mmol) and CuI (7 mg, 0.04 mmol) were suspended in 10 mL of DMF/H$_2$O/DIPEA (3:2:1) under a nitrogen atmosphere and the mixture was stirred at 50 °C for 12 h. The reaction mixture was slowly added to 100 mL of methanol/acetone/ether mixture (1:4:5) after being cooled to room temperature. The precipitate was centrifuged and redissolved in 20 mL of water/methanol (7:3), followed by treatment with 0.01 g of Na$_2$S. The mixture was filtered and the filtrate was slowly added to 200 mL of methanol/acetone/ether mixture (1:4:5). The precipitate was centrifuged to obtain **PPE-4** (147 mg, 0.12 mmol, 70%) as a deep red powder. IR (neat): 2922, 2850, 1659, 1613, 1500, 1360, 1325, 1204, 1040, 942, 815, 783 cm^{-1}; ^{1}H NMR

(500 MHz, DMSO-d_6): δ = 7.61 (m, 8H), 6.50 (m, 4H), 4.83 (m, 4H), 4.52 (m, 4H), 4.02 (m, 8H), 2.88 (m, 12H), 2.26 (m, 2H), 2.08 (m, 12H), 1.23 (m, 3H).

Chapter 3

Poly(*p*-phenylene ethynylene)s (PPEs) as Carbon Nanotube Dispersants

3-1 Introduction

Carbon nanotubes (CNTs) are tiny cylinders made of sp^2-hybridized carbon atoms with diameters on the nanometer scale. Conceptually, they can be formed from rolling up graphene sheets in various fashions. The small dimensions and long aspect ratio of CNTs give rise to unique physical properties such as high mechanical strength, electrical and thermal conductivity, which make them very attractive materials for a wide range of promising applications from nanomedicine, sensing devices, energy storage to electrically and thermally conductive materials.[34-37] In spite of great improvements made in synthetic techniques, the purity of synthesized CNTs is usually poor. Commercially available single-walled carbon nanotubes (SWNTs), for example, invariably contain transition metal catalysts such as Fe, Co and Ni. In addition, SWNTs are composed of various types in terms of diameter, chirality and electronic properties. In practice, SWNTs bundle together strongly through van der Waals forces and π-π interactions which make them insoluble in common organic solvents.

The major obstacle to using commercially available SWNTs in CNT-based devices is their low purity. In order to use SWNTs in practical applications, specific types of SWNTs, *e.g.* electronically or structurally pure SWNTs, should be accessible. Hence, the development of purification methods to extract particular types of SWNTs from commercial products, and to debundle and disperse SWNTs in organic media, has captured great interest during the last decades. Ultra-centrifugation, ultra-sonication, covalent functionalization and non-covalent functionalization have been reported in the recent literature as potentially useful methods to purify SWNTs.[42-43]

In covalent functionalization, the reactive sites of SWNTs, *e.g.* endcaps and defects on the sidewall, undergo various chemical reactions. The resulting SWNTs exhibit high solubility in organic solvents.[44] Since the chemical reactions lead to the formation of covalent bonds, the π-delocalization among sp^2-hybridized carbons of SWNTs are disrupted, and as a result the structural integrity and electrical conductivity of SWNTs are changed dramatically. This is a disadvantage of the covalent method.

In the noncovalent method, SWNTs interact with other chemical species through weak π-π interactions, but do not form any covalent bonds. In contrast to the covalent functionalization approach, noncovalently functionalized SWNTs are structurally intact and their physical properties are hence remain the same as those of pristine SWNTs. The advantage of using noncovalent functionalization approach to preserve the properties of pristine SWNTs has attracted considerable attention. Supramolecular complexes of SWNTs with other species such as polymers have been found to result in dispersable SWNT materials in organic solvents.[54-56] For example, a series of fluorene-based

polymers was utilized by Nicholas and co-workers to disperse HiPCO and CoMoCAT SWNTs which exhibited a certain degree of diameter selectivity.[54] Another series of fluorene-based polymers was investigated by Chen and co-workers to show selectivity towards specific chirality of SWNTs.[55] Poly(*p*-arylene ethynylene)s have been investigated to disperse SWNTs and give selectivity in terms of diameters by Nicole Rice, a former student of the Zhao group at Memorial.[56]

3.2 Objectives of the project

The main aim of this project was to develop a series of poly(*p*-phenylene ethynylene)s to disperse SWNTs in organic solvents and to test their selectivity for different types of SWNTs. The Zhao group has previously reported the capability of linear conjugated polymers such as poly(*p*-phenylene ethynylene)s (PPEs), poly(*p*-phenylene vinylene)s (PPVs), and poly(phenylene butadiynylene)s (PPBs) to disperse as-prepared SWNTs in organic solvents.[56] The effectiveness of various conjugated polymers at dispersing CNTs was found to be correlated with the structure and electronic nature of the polymer.

To deepen our understanding of the polymer effect, in this project, a systematic design of conjugated polymers was planned, in which highly π-extended aromatic groups such as anthracene and pyrene were to be incorporated into the backbone of the polymer (Figure 3-1). The target polymer **3-1** contains only phenyl rings on the side chain of the polymer and target polymers **3-2** and **3-3** have anthracene and pyrene moieties respectively attached to the backbone of the polymer.

polymer 3-1

polymer 3-2
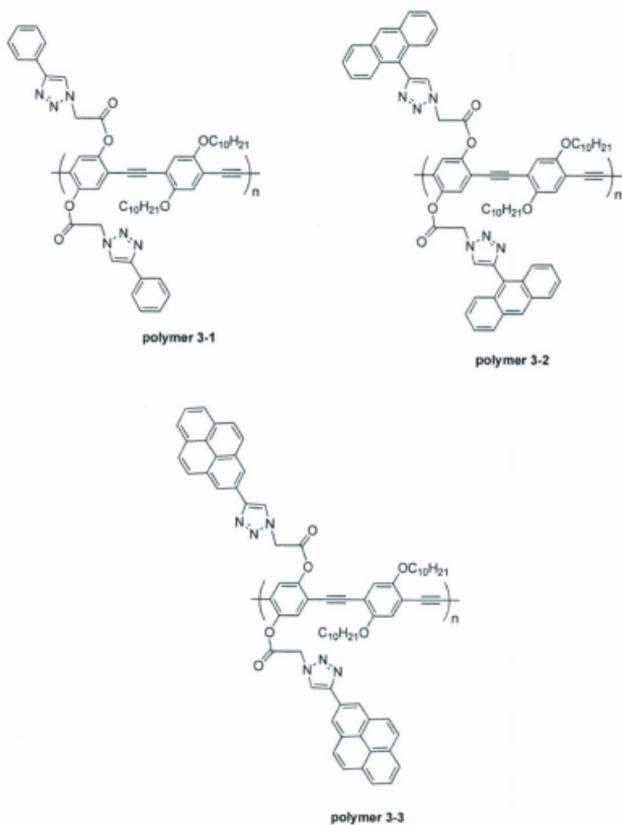
polymer 3-3

Figure 3-1: Molecular structures of target polymers.

Polymer **3-1** was designed as a reference polymer to study the effect of introducing aromatic moieties to the side chain of the polymer. Since polymers **3-2** and **3-3** have relatively large planar aromatic moieties (anthracene and pyrene, respectively), they were expected to provide stronger π-π interactions with the side walls of SWNTs. As such, more efficient dispersion of SWNTs by these two polymers were anticipated compared to polymer **3-1** which only carries phenyl rings in its side chains.

The Sonogashira cross coupling reaction was planned to be used for synthesis of the polymer backbone, while modular "click reactions" were designed to functionalize the polymers in a rapid and efficient manner.

3.3 Results and Discussions

3.3.1 Synthesis of polymer 3-1 and related monomers

To achieve polymer **3-1**, two monomeric precursors, compound **3-1** and **3-2** (Figure 3-2), needed to be prepared first.
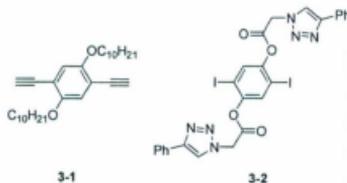
Figure 3-2: Molecular structures of monomers **3-1** and **3-2**.

Monomer **3-1** was obtained from desilylation of compound **3-5** in the mixture of MeOH/THF by K₂CO₃ (Scheme 3-1) Compound **3-5** was synthesized through Sonogashira reaction of compound **3-4** with trimethylsilylacetylene (TMSA) in THF and Et₃N in the presence of Pd/Cu catalysts. Compound **3-4** was obtained by an alkylation reaction of hydroquinone followed by iodination. In the synthesis, commercially available hydroquinone underwent a two-fold alkylation reaction with 1-bromodecane in a basic ethanolic solution to afford intermediate **3-3**. Iodination of compound **3-3** in the presence of iodine chips and mercuric acetate afforded compound **3-4** in a reasonable yield (Scheme 3-1).

Scheme 3-1: Synthesis of compound **3-1** from hydroquinone.

To introduce the phenyl ring to the side chain of the polymer, a pre-functionalization method was used to achieve compound **3-2** as another monomer. To synthesize compound **3-2**, commercially available 1,4-dimethoxybenzene underwent an iodination

reaction with iodine chips under the catalysis of mercuric acetate in dichloromethane to afford compound **3-6**. The methoxy groups of compound **3-6** were converted to hydroxyl groups using BBr₃ in dichloromethane to afford compound **3-7**. Steglich esterification of compound **3-7** with bromoacetic acid (compound **3-8**) in the presence of dicyclohexylcarbodiimide (DCC) and 4-(dimethylaminophenol) (DMAP) established compound **3-9**. Azidification of compound **3-9** using NaN₃ in DMF at room temperature afforded compound **3-10** (Scheme 3-2).
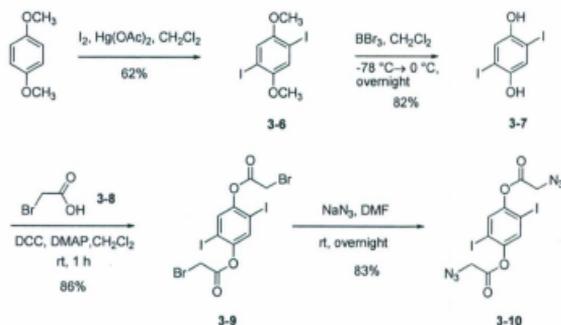
Scheme 3-2: Synthesis of compound **3-10**.

Compound **3-10** was subjected to a click reaction with phenylacetylene (compound **3-11**) in the presence of diisopropylethylamine (DIPEA) as a base and a catalytic amount of CuI in THF to afford monomer **3-2** in a good yield (Scheme 3-3).
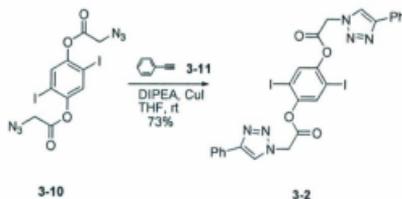
Scheme 3-3: Synthesis of compound **3-2**.

Compound **3-2** shows very low solubility in organic solvents and it is only soluble in hot DMSO. Several efforts to polymerize this compound with dialkyne **3-1** in THF/DMSO solvent system were unsuccessful. The ^{1}H NMR spectrum of **3-2** was unclear and no suitable approach has been found to purify the reaction mixture (Scheme 3-4).
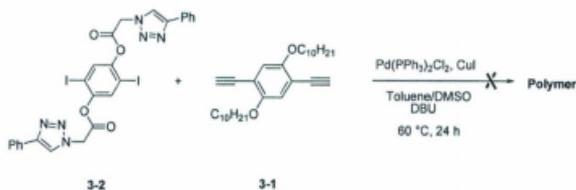
Scheme 3-4: Attempted polymerization to achieve polymer **3-1**.

Since the pre-functionalization approach was unsuccessful because of the low solubility of monomer **3-2**, a post-functionalization method was applied (Scheme 3-5). Compound **3-9** containing pendant bromide groups was used as a monomer instead of

monomer **3-1**. The polymerization of compound **3-9** with compound **3-1** afforded polymer **3-4** in which bromide groups were incorporated in the side chains of the polymer. Unfortunately, several trials to convert bromide groups to azido groups using NaN$_3$ were unsuccessful. As a result, the next step, click reaction with phenylacetylene, was not performed. Polymer **3-4** exhibited very low solubility in organic solvents. Presumably, for this reason, subsequent azidification of **3-4** was unsuccessful.
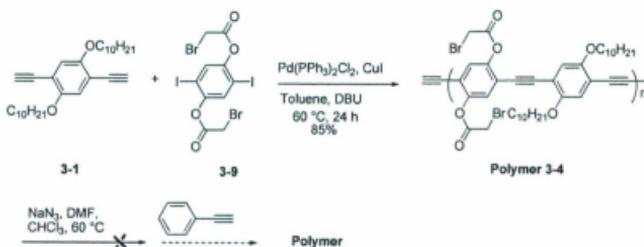
Scheme 3-5: Synthesis of polymer **3-4** and attempted azidification reaction to achieve the precursor to polymer **3-1**.

3.3.2 Synthesis of new precursors and polymers

Since the polymerization was unsuccessful using precursors **3-1** and **3-9** to achieve polymer **3-4**, some new precursors were synthesized. The esteric groups showed low stability after being introduced to the side chains of the polymer and they likely underwent hydrolysis process. Therefore, replacement of the esteric linkers by more stable groups such as alkoxy was attempted. Compound **3-12** was synthesized as the diiodo monomer for polymerization. 2,2′-(1,4-Phenylenebis(oxy))diethanol was

subjected to an Appel reaction in the presence of CBr$_4$ and PPh$_3$ in MeCN at room temperature to afford compound **3-11**. Then iodination of compound **3-11** with I$_2$/Hg(OAc)$_2$ in methylene chloride furnished compound **3-12** (Scheme 3-6).
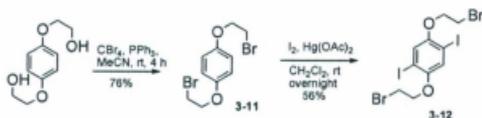
Scheme 3-6: Synthesis of compound **3-12**.

Compound **3-12** was subjected to the polymerization reaction with compound **3-1** employing different conditions. This polymerization was tuned by changing several factors. First, the base was changed from DBU to piperidine. Piperidine is a weaker base than DBU and decreases homocoupling side reactions, which introduce low solubility to the polymer products during the reaction. Compound **3-13** was used as an endcapping reagent in a catalytic amount (10 mol%) during the polymerization to increase the solubility of the polymer. Polymers with TMS groups at the ends of the polymer chain could not undergo further reactions such as cross coupling reactions. The resulting polymers could be purified by washing with MeOH, MeCN, water and hexanes and TLC analysis showed a single spot on the baseline of the TLC plate. Polymer **3-5** showed quite good solubility in organic solvents such as THF, CHCl$_3$ and CH$_2$Cl$_2$ (Scheme 3-7). Unfortunately, attempts to convert the bromide groups of **3-5** to azido groups under different conditions using NaN$_3$ were unsuccessful. Hence, the next step, click reaction with phenylacetylene, did not proceed.
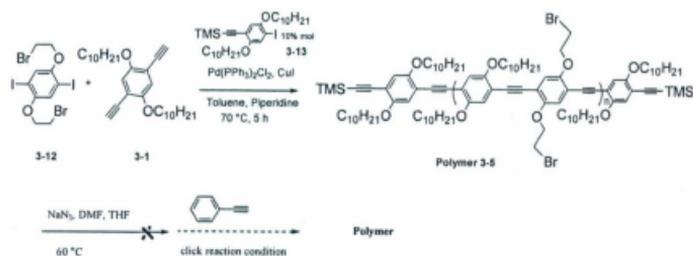
Scheme 3-7: Synthesis of polymer **3-5** and attempted azidification reaction to achieve the precursor to corresponding polymer.

Compound **3-13** was achieved by subjecting compound **3-4** to Sonogashira reaction with 0.7 molar equivalent of TMSA using Et$_3$N as base and Pd/Cu as catalysts (Scheme 3-8).
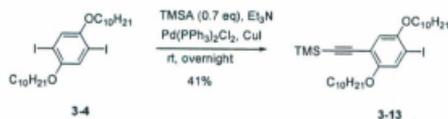
Scheme 3-8: Synthesis of compound **3-13**.

A pre-functionalization approach was attempted to perform the click reaction before polymerization. Bromide groups on compound **3-12** were converted to azido groups in the presence of sodium azide in DMF to afford compound **3-14** (Scheme 3-9). A click reaction was done with phenylacetylene in the presence of DIPEA as a base and a

catalytic amount of CuI in THF to furnish compound **3-15**, which was insoluble in most organic solvents except hot DMSO.
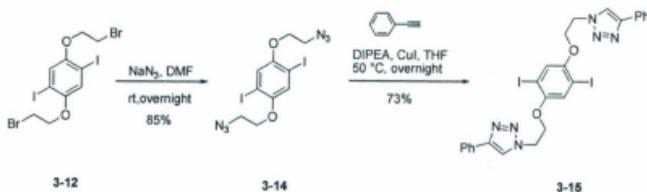
Scheme 3-9: Synthesis of compound **3-15**.

Since compound **3-15** showed very poor solubility in organic solvents, the polymerization step was not carried out (Scheme 3-10).
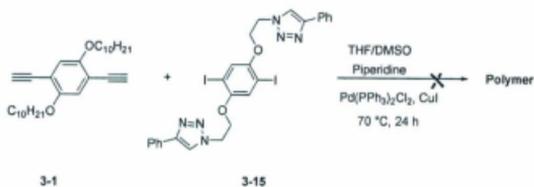
Scheme 3-10: Attempted polymerization of monomer **3-1** and monomer **3-15** to achieve the intended polymer.

Since the synthesized diiodo click reaction products suffered from low solubility, the polymerization step was thwarted by the low solubility problem. To solve this problem, an alternative method was tried, in which the diiodo click products were converted to

dialkynes. Removal of the iodide groups and introducing some extra carbons to the click reaction product resulted in dramatically enhanced solubility (Scheme 3-11).
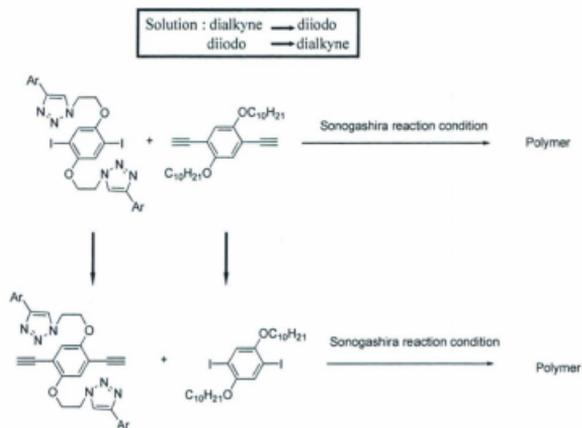
Scheme 3-11: Alternative method to solve the solubility problem of the monomer.

Instead of using compound **3-1** as the terminal alkyne for polymerization via Sonogashira coupling, the click product was converted the terminal alkyne. Compound **3-19** was synthesized as a dialkyne monomer for the polymerization. Compound **3-12** was subjected to Sonogashira reaction with TMSA to afford compound **3-16**. Then, the bromide groups were converted into azido groups in the presence of sodium azide to furnish compound **3-17** bearing two azido groups. A click reaction was done between compound **3-17** and phenylacetylene in the presence of DIPEA and CuI in THF to obtain

compound **3-18**. Column chromatography was run to obtain the pure compound, but it gave an extremely low yield of the product. Hence, instead of column chromatography, the crude product was washed with hexanes thoroughly and subjected to the desilylation reaction. Dialkyne **3-19** was made by the desilylation of compound **3-18** in the presence of K$_2$CO$_3$ and THF/MeOH at room temperature (Scheme 3-12). The solubility decreased after removing TMS groups and it appeared to be partially soluble in methylene chloride and chloroform and THF. However, it was completely soluble in DMF and DMSO.
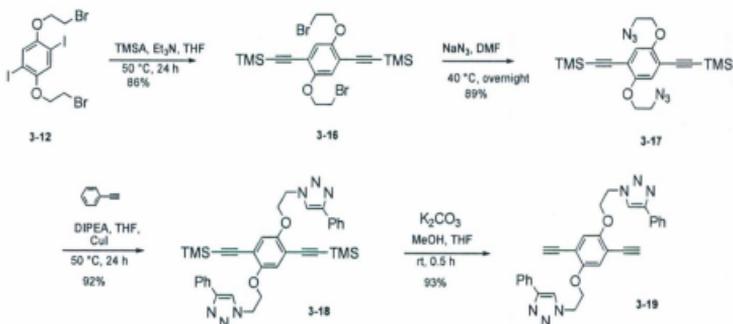
Scheme 3-12: Synthesis of compound **3-19** as a new monomer.

Polymerization was done using monomer **3-19** as dialkyne and monomer **3-4** as diiodo monomer, in the presence of Pd/Cu catalyst, THF, the endcapping reagent (compound **3-13**), and DIPEA as base (Scheme 3-13). Polymer **3-6** showed quite good solubility in organic solvents such as THF, chloroform, and methylene chloride.
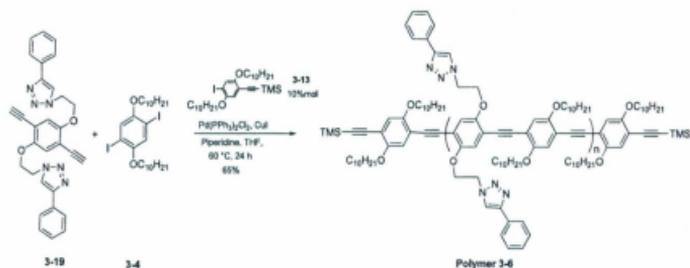
Scheme 3-13: Synthesis of polymer **3-6**.

3.3.3 Synthesis of modified polymers (polymer 3-7 and polymer 3-8) and related monomers

Based on the encountered solubility problem of monomers to synthesize polymer **3-1** and also the results of modification of polymer **3-1** to polymer **3-6**, two other target polymers were derived from polymer **3-2** and polymer **3-3** to polymer **3-7** and polymer **3-8** respectively. In the new polymers, the aromatic moieties, anthracene and pyrene, are attached to the backbone of the polymer via alkoxy groups. Furthermore, endcapping reagent (**3-13**) was used to introduce more solubility to the target conjugated polymers.

polymer 3-7
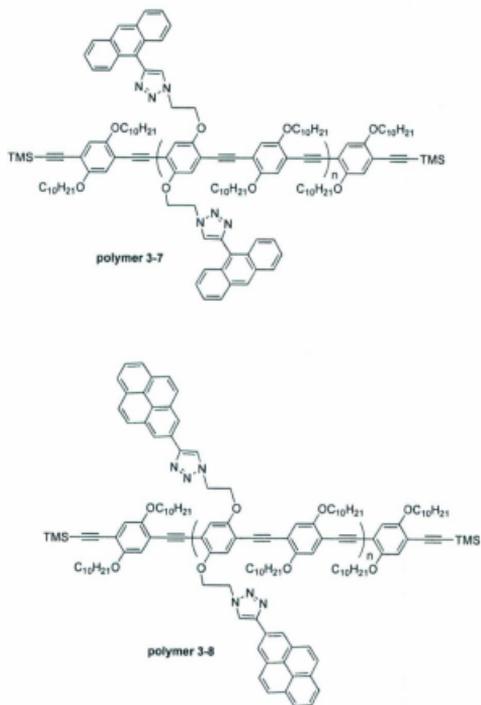
polymer 3-8

Figure 3-3: Molecular structures of modified polymers.

After successfully attaching phenyl rings to the side chains of the polymer, attempts to introduce anthracene and pyrene using the same synthetic procedure were conducted. Compound **3-21** was synthesized as a terminal alkyne. 9-Bromoanthracene was subjected to Sonogashira reaction with TMSA in THF and Et₃N in the presence of Pd(PPh₃)Cl₂ and

CuI as catalysts to furnish compound **3-20**. Desilylation of compound **3-20** in K$_2$CO$_3$ and

THF/MeOH afforded compound **3-21** (Scheme 3-14).
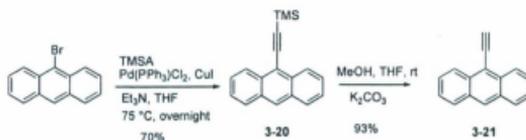
Scheme 3-14: Synthesis of compound **3-21**.

Compound **3-25** was also synthesized as another terminal alkyne. Pyrene was

brominated by HBr and H$_2$O$_2$ in MeOH/Et$_2$O mixture to afford compound **3-22**; however,

the product contained a small amount of unreacted pyrene which could not be separated

by column chromatography due to very close polarity. Then compound **3-22** was

subjected to Sonogashira reaction using 2-methylbut-3-yn-2-ol (compound **3-23**) in

piperidine and in the presence of Pd/Cu to afford compound **3-24**. Deprotection of

compound **3-24** by KOH in toluene furnished compound **3-25** (Scheme 3-15).
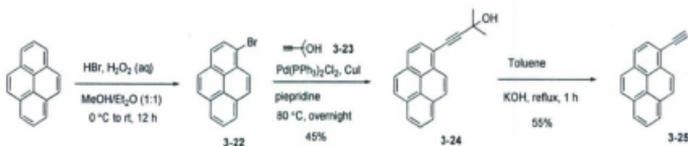
Scheme 3-15: Synthesis of compound **3-25**.

With compounds **3-17** and **3-21** in hand, a click reaction was applied to achieve the intended click product. The reaction did not proceed and the obtained reaction mixture showed many spots on the TLC plate. Various conditions, including changing the solvent from THF to DMF and using microwave instead of heating, did not lead to any improvement (Scheme 3-16).
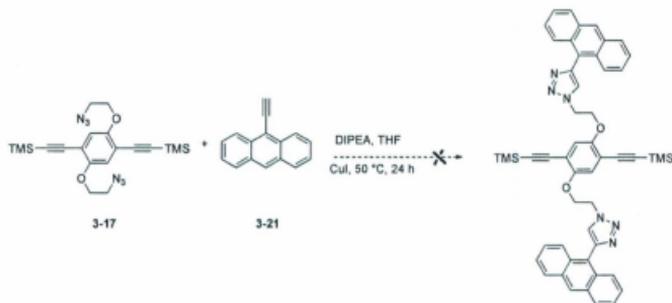
Scheme 3-16: Attempted click reaction to attach an anthracene system to the monomer.

The same observation was made during the click reaction of compound **3-25** with **3-17** (Scheme 3-17). Various conditions again were investigated including changing the solvent, temperature and employing microwave conditions, but the intended click product was not achieved.
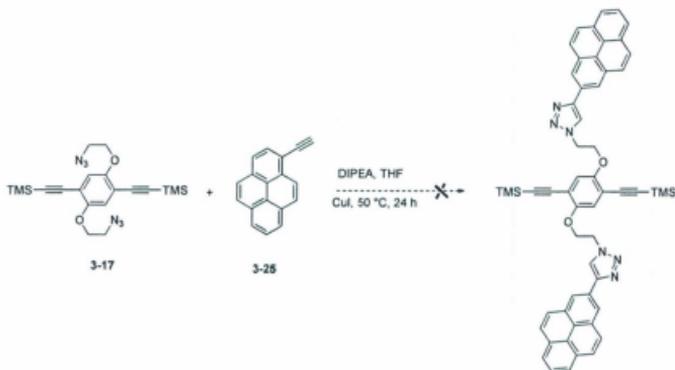
Scheme 3-17: Attempted click reaction to attach the pyrene to the monomer.

Since some precipitation was observed during the click reaction of **3-17** with **3-21**, it was assumed that the product was insoluble after the first click reaction, which hindered the intended second click reaction. To increase the solubility, compound **3-28** was synthesized and used as the diazido compound instead of compound **3-17**. The incorporation of long alkane chains in trimer **3-28** was then planned to gain more solubility.

Compound **3-16** underwent desilylation in the presence of K_2CO_3 in MeOH/THF to afford compound **3-26**. Sonogashira reaction of compound **3-26** with compound **3-13** in THF/Et$_3$N and Pd/Cu as catalysts, furnished compound **3-27**. Bromides were converted to azido groups using NaN$_3$ and THF/DMF as a solvent mixture to obtain compound **3-28** (Scheme 3-18).
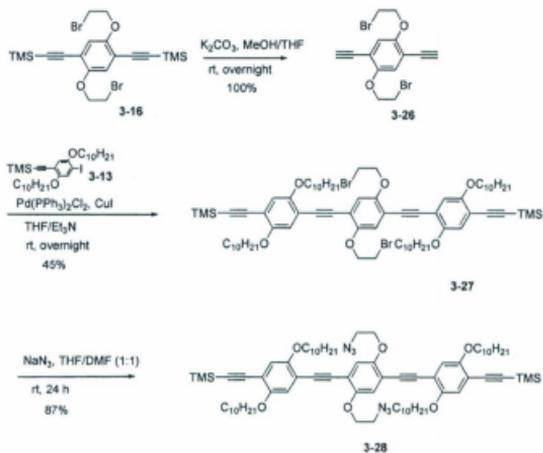
Scheme 3-18: Synthesis of compound **3-28**.

With highly soluble compound **3-28** in hand, a click reaction was conducted to achieve the intended click product (Scheme 3-19). Although various conditions such as changing the solvent, different temperatures, and microwave conditions were applied, none of them afforded the intended click product. The reaction mixture showed many spots on the TLC plate. Although the major spots were separated by column chromatography, their ^{1}H NMR spectra were not meaningful for structural elucidation.
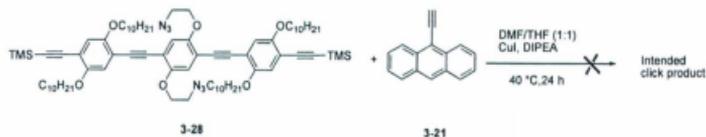
Scheme 3-19: Attempted click reaction to attach the anthracene on the monomer using trimer compound.

Using of anthracene and pyrene as the alkyne in click reaction did not afford the click product with the corresponding azide compounds. Hence, a new approach was applied; instead of attaching alkyne group to the anthracene, the azido group was incorporated into the structure (Scheme 3-20).
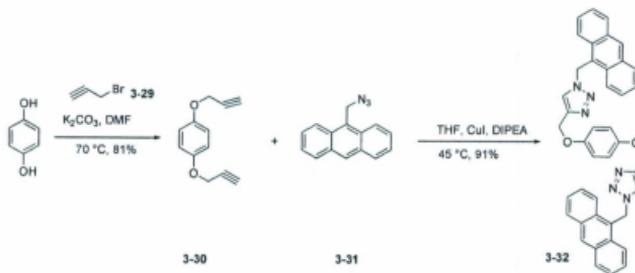
Scheme 3-20: Synthesis of compound **3-32**.

Compound **3-31** was prepared by a Ph.D student in our lab, Mr. Karimulla Mulla. Compound **3-30** was synthesized by the reaction of hydroquinone with propargyl bromide (compound **3-29**) in the presence of K_2CO_3 as base in DMF. By subjecting

compound **3-31** and **3-30** to the click reaction conditions using DIPEA as base, CuI as catalyst and THF as solvent, compound **3-32** was obtained in a high yield (Scheme 3-20). Compound **3-32**, however, is only soluble in hot DMSO which brings limitation during the polymerization step.

To increase the solubility of compound **3-32**, the chemical structure of compound **3-30** redesigned by incorporating TMSA groups to the structure of the molecule. Hence, with compound **3-36** in hand, a click reaction can be conducted with compounds **3-32** and **3-33** to achieve the intended click products. By desilylation of the click products, the related monomers could be obtained and the polymerization step was conducted by using more soluble monomers (Scheme 3-21).
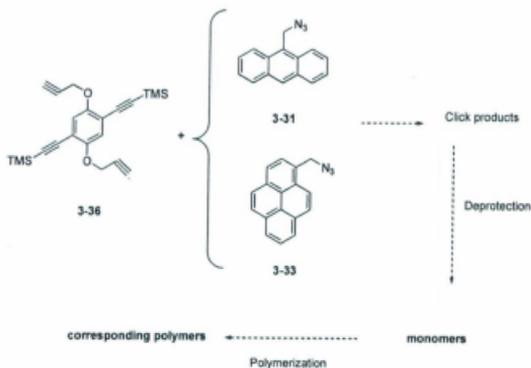
Scheme 3-21: Polymerization with new monomers.

By selecting compound **3-36** as a target precursor for click reaction with compounds **3-32** and **3-33**, the synthesis started from compound **3-6**. Sonogashira reaction of compound **3-6** with TMSA in THF and Et$_3$N and Pd/Cu afforded compound **3-34** in a high yield. The methoxy groups on compound **3-34** were converted to hydroxyl groups using BBr$_3$ in CH$_2$Cl$_2$ to obtain compound **3-35**. Unfortunately, compound **3-35** showed very low stability at room temperature and decomposed after working up the reaction mixture. As a result, the next step, which is the reaction with propargyl bromide to achieve target compound **3-36** was not undertaken (Scheme 3-22).
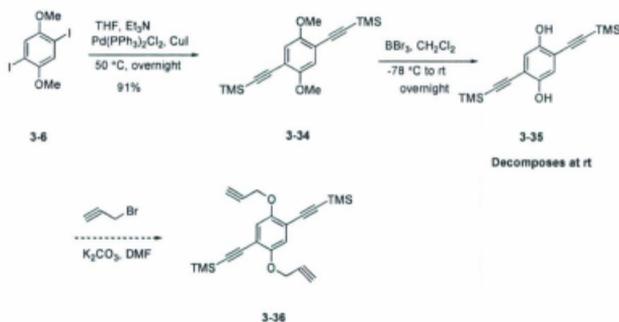
Scheme 3-22: Synthesis of compound **3-35**.

The decomposition of compound **3-35** prevented the next step to obtain compound **3-36**. However, this problem might be circumvented by doing the next step *in situ*, without purification of unstable compound **3-35**. This approach will be applied in the future work.

3.3.4 UV-Vis-NIR study of polymer 3-6 with SWNTs

In order to study the effectiveness of polymer **3-6** at dispersing SWNTs in organic solvents, UV-Vis-NIR spectroscopic analysis was conducted on a solution of the polymer in an organic solvent before and after addition of SWNTs. Polymer **3-6** was dissolved in CHCl$_3$ and SWNTs were added and the mixture was sonicated for half an hour to obtain a black suspension. The mixture was filtered through a cotton plug and the obtained black solution was examined by UV-Vis-NIR spectroscopy. Figure 3-4 shows the UV-Vis-NIR spectra of the polymer and polymer/SWNT mixture. If the polymer interacts with SWNTs and disperse into the organic solvent, the characteristic peaks (S$_{11}$ and M$_{11}$) will appear in absorption range between 500-1000 nm.[52]

This region (inset in Figure 3-4) shows the slight difference in absorbance comparing the spectra of polymer/SWNTs mixture and pure polymer. Furthermore, the absorption peak of the polymer is blue-shifted after mixing with SWNTs. These observations indicate that polymer **3-6** interacts with SWNTs weakly. This is expected because the phenyl rings on the backbone of the polymer can affect only a moderate degree of π-π interactions with SWNTs.
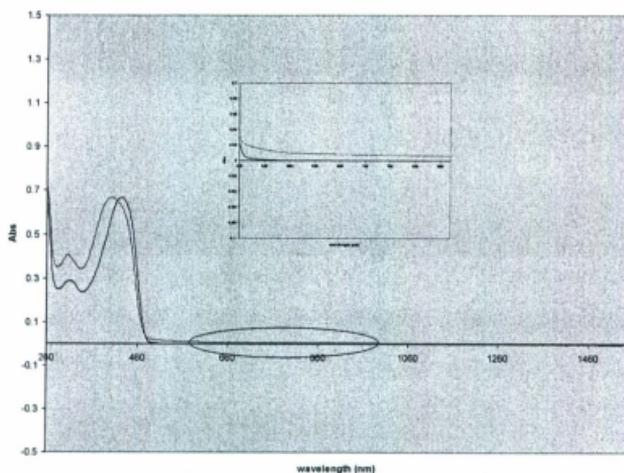
Figure 3-4: UV-Vis-NIR spectra of polymer **3-6** (blue line) and polymer/SWNT mixture (red line); inset shows the specified red circle area on the spectra.

3.4 Conclusions

Sonogashira cross coupling reaction has been used to synthesize some conjugated polymers. The low solubility of the obtained polymers and also related monomers in organic solvents, were the two main difficulties encountered during this project. To enhance the solubility of the synthesized polymers, the Sonogashira reaction conditions have been modified; the base was changed from DBU to milder bases such as piperidine and DIPEA. This modification in base was done in order to decrease the formation of

diyne defects during the polymerization process which make the obtained polymer less soluble in organic solvents. Cross-linking is another reason for the low solubility of the synthesized polymers, particularly in the solid state.[3] An endcapping reagent was used as part of the modification to decrease the cross-linking in the polymer.

Another main obstacle in this project was the low solubility of the designed monomers for polymerization process. Pre-functionalization and post-functionalization methods were unsuccessful and as a result, the structures of the target polymers were redesigned. In the click reaction, introducing triazole groups to the structure of small molecules brought about low solubility to the click products in organic solvents. This obstacle was removed by converting diiodo compounds of click products to dialkyne structures and as a result polymer 3-6 was successfully synthesized. Although triazole groups can be used as a linker, the low solubility of the obtained click products is a major difficulty in applying click chemistry to functionalization of conjugated polymers.

Designed target polymers; in which anthracene and pyrene groups had been incorporated in the side chain, were not obtained. The intermediate compound (3-35) decomposes at room temperature and, as a result, the next step could not be preceded. This problem could be solved by conducting the reaction in situ instead of isolating the unstable compound. The future work will focus on the obtaining of the target monomer to attach the π-rich compounds such as anthracene and pyrene to the backbone of the polymer and study the ability of obtained polymers to disperse SWNTs in organic solvents.

3.5 Experimental part

All reactions were carried out under a nitrogen atmosphere unless otherwise noted. All chemicals were of reagent grade. Chemicals and reagents were purchased from commercial suppliers and used as received unless noted otherwise. THF was distilled from sodium/benzophenone. Et_3N and toluene were distilled from CaH_2. Palladium catalyst, $Pd(PPh_3)_2Cl_2$, was prepared from $PdCl_2$ according to literature procedures. All reactions were performed in standard, oven-dried glassware. Evaporation and concentration were performed at H_2O-aspirator pressure. Flash column chromatography was carried out with silica gel 60 (230- 400 mesh). Thin-layer chromatography (TLC) was carried out with silica gel 60 F254 covered on plastic sheets and visualized by UV light or $KMnO_4$ stain. ^1H and ^{13}C NMR spectra were measured on the Bruker Avance 500 MHz or 300 MHz spectrometers. Chemical shifts (δ) are reported in parts per million (ppm) downfield from the signal of internal reference $SiMe_4$. Coupling constants (J) are given in Hertz. Mass spectra were obtained from an Agilent 1100 series LCMSD spectrometer. UV-Vis-NIR absorption spectra were recorded on an Agilent 8543 Diode Array Spectrophotometer interfaced with an HP computer.

1,4-Bis(decyloxy)benzene (3-3)[62]

3-3

Hydroquinone (5.01 g, 45 mmol), KOH (6.36 g, 113 mmol), EtOH (100 mL), and $C_{10}H_{21}Br$ (25.02 g, 113 mmol) were mixed. The resulting grey mixture was heated to 90

°C and refluxed for 60 h. It was then diluted with CH$_2$Cl$_2$, washed with NH$_4$Cl, H$_2$O, and brine and dried over MgSO$_4$. It was filtered through a short silica plug, washed with hexanes. The filtrate was concentrated in vacuo. The off-white solid was recrystallized from MeOH. The resulting colorless flakes were washed with cold MeOH to produce **3-3** as colorless flakes (10.62 g, 27.2 mmol, 60%). ^{1}H NMR (300 MHz, CDCl$_3$): δ 6.80 (s, 4H), 3.88 (t, $J = 6.59$ Hz, 4H), 1.78-1.68 (m, 4H), 1.44-1.37 (m, 28H), 0.86 (t, $J = 6.45$ Hz, 6H); ^{13}C NMR (75 MHz, CDCl$_3$), δ 153.22, 115.41, 68.69, 31.93, 29.62, 29.59, 29.45, 29.44, 29.35, 26.09, 22.71, 14.14.

1,4-Bis(decyloxy)-2,5diiodobenzene (3-4)[62]
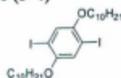
3-4

Compound **3-3** (8.05 g, 20.6 mmol), I$_2$ (13.12 g, 51.7 mmol), Hg(OAc)$_2$ (16.30 g, 51.3 mmol), and CH$_2$Cl$_2$ (200 mL) were mixed and stirred for 24 h. Then it was filtered and washed with Na$_2$S$_2$O$_3$, water, brine, and dried over MgSO$_4$. The solvent was removed *in vacuo*. The crude product was recrystallized from EtOH to afford the product as colorless flakes (6.89 g, 10.7 mmol, 52%). ^{1}H NMR (500 MHz, CDCl$_3$): δ 7.17 (s, 2H), 3.92 (t, $J = 6.44$ Hz, 4H), 1.82-1.77 (m, 4H), 1.52-1.46 (m, 4H), 1.36-1.32 (m, 24H), 0.88 (t, $J = 6.79$ Hz, 6H); ^{13}C NMR (75 MHz, CDCl$_3$), δ 152.89, 122.83, 86.33, 70.40, 31.94, 29.59, 29.57, 29.35, 29.31, 29.17, 26.06, 22.72, 14.15.

(2,5-Bis(decyloxy)-1,4-phenylenebis(ethyne-2,1-diyl)bis(trimethylsilane) (3-5)[62]
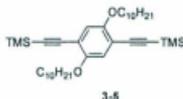
Compound **3-4** (6.52 g, 10.2 mmol), Pd(PPh₃)₂Cl₂ (0.73 g, 1.04 mmol), and CuI (0.42 g, 2.2 mmol) were added to an oven-dried round-bottom flask containing dry THF/Et₃N (100 mL, 1:1) under the protection of N₂. TMSA (2.54 g, 34.3 mmol) in dry THF was added dropwise and the reaction mixture was stirred at room temperature overnight. The solvents were removed in vacuo to give the crude product, which was purified by silica flash chromatography using hexanes/ethylacetate (3:1) to afford compound **3-5** as a pale pink solid (4.51 g, 7.7 mmol, 76%). ¹H NMR (500 MHz, CDCl₃): δ 6.91 (s, 2H), 3.96 (t, $J = 6.36$ Hz, 4H), 1.83-1.78 (m , 4H), 1.55-1.49 (m , 4H), 1.34-1.29 (m, 24H), 0.91 (t, $J = 6.80$, 6H), 0.28 (s, 18H).

1,4-Bis(decyloxy)-2,5-diethylbenzene (3-1)[62]
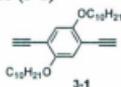
Compound **3-5** (3.2 g, 5.5 mmol) and K₂CO₃ (31.92 g, 23.1 mmol) were added to 20 mL of THF/MeOH (1:1) in a round-bottom flask and stirred for 1 h. The solvent was removed *in vacuo* and the residue was dissolved in CH₂Cl₂ and washed with water. The organic layer was dried over MgSO₄ and the solvent removed in vacuo to give **3-1** as a pale yellow solid (2.2 g, 5.0 mmol, 93%). ¹H NMR (500 MHz, CDCl₃): δ 6.95 (s, 2H),

3.97 (t, J = 6.63 Hz, 4H), 3.32 (s, 2H), 1.82-1.77 (m , 4H), 1.52-1.46 (m , 4H), 1.39-1.34 (m, 24H), 0.90-0.87 (t, J = 6.76 Hz , 6H).

1,4-Diiodo-2,5-dimethoxybenzene (3-6)[68]
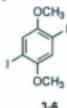
Commercially available 1,4-dimethoxybenzene (2.5 g, 18 mmol), I_2 (9.6 g, 38 mmol), Hg(OAc)$_2$ (11.8 g, 37.1 mmol), and CH_2Cl_2 (150 mL) were mixed and the mixture was stirred overnight. Then it was filtered through MgSO$_4$, washed with Na$_2$S$_2$O$_3$, H$_2$O, dried over MgSO$_4$ and evaporated in vacuo. The residue was recrystallized from EtOH (100 mL) to afford **3-6** as a colorless solid (4.40 g, 11.3 mmol, 62%). ^{1}H NMR (500 MHz, CDCl$_3$): δ 7.20 (s, 2H), 3.83 (s, 6H).

2,5-Diiodobenzene-1,4-diol (3-7)[68]
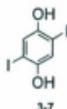
To a solution of compound **3-6** (4.3 g, 11.0 mmol) in methylene chloride (200 mL) under a dry ice bath was added BBr$_3$ (3.13 mL, 33.1 mmol). The mixture was allowed to warm to room temperature and stirred overnight. The resulting mixture was cooled in an ice bath. Then H$_2$O (100 mL) was added. The mixture was then filtered and washed with CH_2Cl_2. The filtrate was extracted with CH_2Cl_2 and the organic layer was dried over

MgSO$_4$ and evaporated to afford **3-7** as an off-white solid (3.3 g, 9.0 mmol, 82%). ^{1}H NMR (500 MHz, (CD$_3$)$_2$CO): δ 8.67 (s, 2H), 7.30 (s, 2H).

2,5-Diiodo-1,4-phenylene bis(2-bromoacetate) (3-9)

3-9
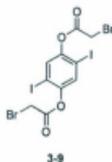
Compound **3-7** (2.0 g, 5.5 mmol) and 2-bromoacetic acid (1.77g, 12.7 mmol) were dissolved in 80 mL of methylene chloride. DMAP (102 mg, 0.83 mmol) was added and stirred for 5 min. DCC (2.6 g, 12.8 mmol) was dissolved in 5 mL of methylene chloride and slowly added. Then the mixture was stirred at room temperature for 30 minutes. Methylene chloride was added to the formed white slurry and filtered to remove the by-product, DCU (dicyclohexylurea). The filtrate was concentrated in vacuo and purified by column chromatography (20% hexanes/ 80% methylene chloride) to afford **3-9** as a pale yellow solid (2.9 g, 4.7 mmol, 86%). IR (neat): 1762, 1447, 1391, 1342, 1257, 1160, 1105, 1043, 930, 881, 803 cm^{-1}; ^{1}H NMR (500 MHz, CDCl$_3$): δ 7.58 (s, 2H), 4.11 (s, 4H); ^{13}C NMR (75 MHz, CDCl$_3$), δ 164.57, 149.22, 132.36, 89.34, 25.03; HRMS (EI, +eV) *m/z* calcd for C$_{10}$H$_6$Br$_2$I$_2$O$_4$ 601.6717, found 601.6765 (M$^+$).

2,5-Diiodo-1,4-phenylene bis(2-azidoacetate) (3-10)
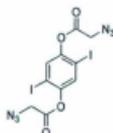
3-10

Compound **3-9** (2.5 g, 4.14 mmol) was dissolved in DMF (10 mL) and NaN$_3$ (810 mg, 12.8 mmol) was added and the mixture was stirred overnight at room temperature. To the reaction mixture were added cold water (10 mL) and then methylene chloride (15 mL). The organic layer was washed with water and brine and dried over MgSO$_4$. The solvent was evaporated *in vacuo* to furnish **3-10** as a colorless solid (1.814 g, 3.44 mmol, 83%). IR (neat): 2103, 1751, 1453, 1345, 1271, 1154, 1047, 936, 876, 790, 742 cm^{-1}; ^{1}H NMR (500 MHz, CDCl$_3$): δ 7.61 (s, 2H), 4.21 (s, 4H). ^{13}C NMR (75 MHz, CDCl$_3$), δ 165.84, 149.08, 132.51, 89.46, 50.61; HRMS (EI, +eV) *m/z* calcd for C$_{10}$H$_6$I$_2$N$_6$O$_4$ 527.8534, found 527.8539.

2,5-Diiodo-1,4-phenylenebis(2-(4-phenyl-1*H*-1,2,3-triazol-1-yl)acetate) (3-2)
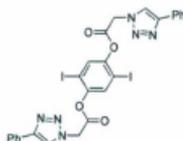
3-2

Phenylacetylene (93 mg, 0.909 mmol) was dissolved in dry THF (20 mL) and then CuI (11 mg, 0.058 mmol) and DIPEA (6 mg, 0.049 mmol) were added. Compound **3-10**

(200 mg, 0.379 mmol) was dissolved in THF (5 mL) and added slowly to the reaction mixture and the mixture was stirred overnight at room temperature. The formed slurry was filtered and washed with ethyl acetate, satd. NH$_4$Cl, water and hexanes and dried under vacuum to afford **3-2** as a colorless powder (202 mg, 0.277 mmol, 73%). ^{1}H NMR (500 MHz, DMSO-d_6): δ 8.65 (s, 2H), 7.94 (s, 2H), 7.89 (d, J = 7.39 Hz, 4H), 7.47 (t, J = 7.56 Hz, 4H), 7.37 (t, J = 7.37 Hz, 2H), 5.82 (s, 4H).

Polymer 3-4
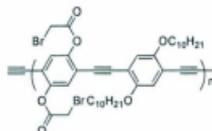
Polymer 3-4

Compound **3-1** (55 mg, 0.12 mmol), compound **3-9** (66 mg, 0.11 mmol), Pd(PPh$_3$)$_2$Cl$_2$ (1.5 mg, 0.01 mmol), and CuI (5 mg, 0.03 mmol) were dissolved in dry toluene (50 mL). Ten drops of DBU were then added and the contents were heated up to 60 °C. The reaction mixture was stirred for 24 h at this temperature and then cooled to room temperature. The solvent was evaporated off under vacuum and the residual solid mass was dissolved in CHCl$_3$ and washed sequentially with 1% HCl and satd. NH$_4$Cl solution to give a deep-red organic layer, which was concentrated to dryness. The solid was redissolved in CHCl$_3$ and the polymer **3-4** was precipitated out of MeOH as a deep-red solid (85 mg, 0.11 mmol, 85%). ^{1}H NMR (500 MHz, CDCl$_3$): δ 7.76 (m, 18H), 7.37 (m, 42H), 6.95 (m, 8H), 4.37 (m, 4H), 3.97 (m, 32H), 1.81 (s, 32H), 1.27 (m, 204H), 0.89 (m, 48H).

1,4-Bis(2-bromoethoxy)benzene (3-11)[63]

Carbon tetrabromide (20.5 g, 61.8 mmol) was slowly added in small portions to a solution of 1,4-bis(2-hydroxyethoxy)benzene (3.1 g, 15 mmol) and triphenylphosphine (16.1 g, 61.4 mmol) in 100 mL of dry acetonitrile at 0 °C with stirring, followed by allowing the reaction mixture to warm to room temperature. The resulting clear solution was stirred for another 4 h. Then 70 mL of cold water was added to the reaction, whereupon product **3-11** was precipitated as a colorless solid. The product was collected by vacuum filtration and thoroughly washed with methanol/water 60:40, and then recrystallized from methanol. Colorless flake-like crystals of **3-11** were collected after drying under vacuum (3.9 g, 12.0 mmol, 77%). ^{1}H NMR (500 MHz, CDCl$_3$): δ 6.86 (s, 2H), 4.25 (t, $J = 6.30$ Hz, 4H), 3.61 (t, $J = 6.30$ Hz, 4H); ^{13}C NMR (75 MHz, CDCl$_3$), δ 152.84, 116.10, 68.73, 29.28.

2,5-Diiodo-1,4-bis(2-bromoethoxy)benzene (3-12)[63]
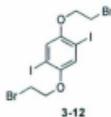
Compound **3-11** (3.0 g, 9.3 mmol), I$_2$ (9.165 g, 36.1 mmol), Hg(OAc)$_2$ (11.4 g, 35.6 mmol), and CH$_2$Cl$_2$ (150 mL) were mixed and the mixture was stirred overnight. Then it was filtered through MgSO$_4$, washed with Na$_2$S$_2$O$_3$, H$_2$O, dried over MgSO$_4$, and

evaporated *in vacuo*. The residue was recrystallized from EtOH (70 mL) to afford **3-12** as a colorless solid (16.5 g, 28.6 mmol, 56%). ^{1}H NMR (500 MHz, CDCl$_3$): δ 7.22 (s, 2H), 4.27 (t, *J* = 6.33 Hz, 4H), 3.66 (t, *J* = 6.29 Hz, 4H). ^{13}C NMR (75 MHz, CDCl$_3$), δ 152.78, 123.91, 86.64, 70.34, 28.52.

Polymer 3-5

Polymer 3-5
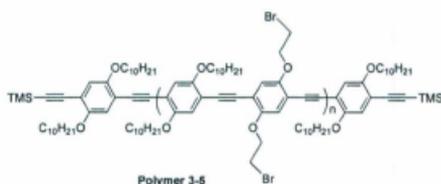
Compound **3-1** (55 mg, 0.12 mmol), compound **3-12** (63 mg, 0.11 mmol), compound **3-13** (6.5 mg, 0.012 mmol) as endcapping reagent, Pd(PPh$_3$)$_2$Cl$_2$ (1.5 mg, 0.01 mmol), and CuI (6 mg, 0.03 mmol) were dissolved in dry toluene/piperidine (5:3, 40 mL). The flask was purged with N$_2$ twice and cooled to -78 °C. The content was heated up to 60 °C. The reaction mixture was stirred for 5 h at this temperature and then cooled to room temperature. The solvent was evaporated off under vacuum and the residual solid mass was dissolved in CH$_2$Cl$_2$ and washed sequentially with 1% HCl and satd. NH$_4$Cl solution to give a deep-red organic layer, which was concentrated to dryness and dissolved again in CH$_2$Cl$_2$ and precipitated out of MeOH to yield polymer **3-5** (80 mg, 0.1 mmol) as a deep-yellow solid. ^{1}H NMR (500 MHz, CDCl$_3$): δ 7.04 (m, 2H), 7.01 (m, 2H), 4.19 (m, 4H), 4.04 (m, 4H), 2.86 (m, 4H), 1.87 (m, 4H), 1.51 (m, 6H), 1.25 (m, 32H), 0.87 (m, 8H), 0.27 (m, 1H); ^{13}C NMR (300 MHz, CDCl$_3$), δ 153.50, 153.45, 117.33, 117.23,

114.41, 114.35, 114.26, 69.71, 68.04, 57.93, 55.20, 31.93, 29.70, 29.63, 29.45, 29.37, 26.10, 26.00, 24.23, 14.13.

1,4-Bis(decyloxy)-2-iodo-5-(trimethylsilylethynyl)benzene (3-13)[62]
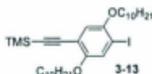
A mixture of 1,4-bis(decyloxy)-2,5-diiodobenzene (**3-4**) (2.02 g, 3.15 mmol), Pd(PPh$_3$)$_2$Cl$_2$ (88.0 mg, 0.12 mmol), and CuI (60.0 mg, 0.31 mmol) were added in 50 mL of dry THF/Et$_3$N (1:1). Then a solution of TMSA (216 mg, 2.20 mmol) in dry THF (5 mL) was added dropwise. The reaction mixture was then stirred at room temperature for 24 h. The solvent was removed under vacuum and the resulting solid mass was dissolved in CH$_2$Cl$_2$ and washed with H$_2$O. The organic layer was dried over MgSO$_4$, filtered and finally column chromatographed (hexanes/CH$_2$Cl$_2$, 10:1) to afford compound **3-13** (790 mg, 1.29 mmol, 41%) as a colorless liquid. ^{1}H NMR (500 MHz, CDCl$_3$): δ 7.25 (s, 1H), 6.83 (s, 1H), 3.95-3.92 (m, 4H), 1.82-1.75 (m, 4H), 1.52-1.46 (m, 4H), 1.32-1.27 (m, 24H), 0.88 (t, J = 6.57, 6H); ^{13}C NMR (75 MHz, CDCl$_3$), δ 154.93, 151.74, 123.87, 116.34, 113.46, 100.83, 99.47, 87.95, 70.14, 69.83, 31.97, 31.94, 29.69, 29.64, 29.62, 29.60, 29.47, 29.38, 29.35, 29.22, 26.15, 26.11, 26.05, 22.74, 14.17, 0.00.

1,4-Bis(2-azidoethoxy)-2,5-diiodobenzene (3-14)
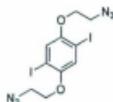
3-14

Compound **3-12** (3.5 g, 6.1 mmol) was dissolved in DMF (5 mL) and then NaN$_3$ (2.1 g, 32.1 mmol) was added. The reaction mixture was allowed to stir at room temperature overnight. To the reaction mixture were added cold water (5 mL) and then dichloromethane (15 mL). The organic layer was washed with water and brine and dried over MgSO$_4$. The solvent was evaporated in vacuo to furnish **3-14** as colorless needle-like crystals (2.6 g, 5 mmol, 87%). IR (neat): 2107, 1484, 1442, 1346, 1298, 1209, 1054, 926, 843, 762 cm^{-1}; ^{1}H NMR (300 MHz, CDCl$_3$): δ 7.23 (s, 2H), 4.10 (t, J = 4.90 Hz, 4H), 3.64 (t, J = 4.99, 4H); ^{13}C NMR (75 MHz, CDCl$_3$), δ 153.02, 123.21, 86.14, 69.05, 50.29; HRMS (EI, +eV) m/z calcd for C$_{10}$H$_{10}$I$_2$N$_6$O$_2$ 499.8949, found 499.8951 (M$^+$).

2,5-Diiodo-1,4-bis(2-(4-phenyl-1H- 1,2,3-triazol-1-yl)ethoxy)benzene (3-15)
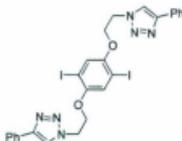
3-15

Phenylacetylene (99 mg, 0.98 mmol) was dissolved in dry THF (10 mL) and CuI (10 mg, 0.05 mmol), and DIPEA (8 mg, 0.06 mmol) were added to the mixture. Compound

3-14 (200 mg, 0.4 mmol) was dissolved in THF (2 mL) and added to the reaction mixture dropwise. The reaction mixture was stirred in 50 °C for 24 h. The white slurry was filtered and the residue was washed with ethyl acetate, satd. NH_4Cl, water and hexanes and dried under vacuum to afford a pale yellow fine powder (285 mg, 0.39 mmol, 73%).

(2,5-bis(2-bromoethoxy)-1,4-phenylene)bis(ethyne-2,1-diyl)bis(trimethylsilane) (3-16)
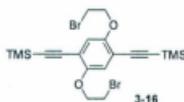
A mixture of **3-12** (800 mg, 1.39 mmol), $Pd(PPh_3)_2Cl_2$ (20 mg, 0.02 mmol), and CuI (26 mg, 0.14 mmol) were added in 15 mL of dry THF/Et_3N (1:1). To this constantly stirred mixture was then dropwise added a solution of TMSA (408 mg, 4.17 mmol) in THF (2 mL) and stirred at room temperature for 24 h. The solvent was removed and the resulting solid mass was dissolved in CH_2Cl_2 and washed with H_2O. The organic layer was then dried over $MgSO_4$, filtered and finally column chromatographed (hexanes/ethyl acetate 6:1) to give compound **3-16** as an off-white solid (613 mg, 1.19 mmol, 86%). IR (neat): 2956, 2150, 1499, 1396, 1211, 1072, 1025, 902, 840, 756 cm^{-1}; ^{1}H NMR (300 MHz, CDCl$_3$): δ 6.93 (s, 2H), 4.28 (t, J = 6.46 Hz, 4H), 3.63 (t, J = 6.49 Hz, 4H), 0.26 (s, 18H); ^{13}C NMR (75 MHz, CDCl$_3$), δ 153.75, 118.90, 115.02, 101.54, 100.15, 69.80, 28.83, 0.00; HRMS (EI, +eV) m/z calcd for $C_{22}H_{32}Br_2O_2Si_2$ 513.9995, found 513.9995 (M$^+$).

2,5-Bis(2-azidoethoxy)-1,4-phenylene)bis(ethyne-2,1-diyl)bis(trimethylsilane) (3-17)
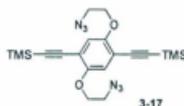
Compound **3-16** (600 mg, 1.36 mmol) was dissolved in DMF (10 mL) and NaN$_3$ (486 mg, 7.49 mmol) was added. The reaction mixture was allowed to stir at 40 °C overnight. To the reaction mixture were added cold water (5 mL) and dichloromethane (15 mL). The organic layer was washed with water and brine and dried over MgSO$_4$. The solvent was evaporated *in vacuo* to furnish **3-17** as colorless needle-like crystals (533 mg, 1.21 mmol, 89%). IR (neat): 2957, 2153, 2112, 1498, 1396, 1307, 1213, 1062, 1010, 939, 870, 833, 758, 696 cm^{-1}; ^{1}H NMR (300 MHz, CDCl$_3$): δ 6.94 (s, 2H), 4.14 (t, J = 4.88 Hz, 4H), 3.60 (t, J = 4.88 Hz, 4H), 0.25 (s, 18H). ^{13}C NMR (75 MHz, CDCl$_3$), δ 153.73, 118.13, 114.59, 101.39, 100.22, 68.73, 50.50, 0.00; HRMS (EI, +eV) *m/z* calcd for C$_{20}$H$_{28}$N$_6$O$_2$Si$_2$ 440.1812, found 440.1816 (M$^+$).

1,1'-(2,2'-(2,5-bis((trimethylsilyl)ethynyl)-1,4-phenylene)bis(oxy)bis(ethane-2,1-diyl))bis(4-phenyl-1H-1,2,3-triazole) (3-18)
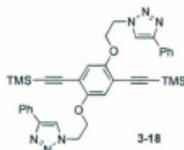
Phenylacetylene (255 mg, 2.50 mmol) was dissolved in dry THF (15 mL), and CuI (28 mg, 0.15 mmol) and DIPEA (21 mg, 0.16 mmol) were added to the mixture. Compound **3-17** (500 mg, 1.13 mmol) was dissolved in THF (5 mL) and added to the reaction mixture dropwise. The reaction mixture stirred in 50 °C for 24 h. The white slurry was filtered and the residue was washed with ethyl acetate. The filtrate was washed with saturated NH_4Cl, water and brine and dried under vacuum. The obtained solid was washed with hexanes, decanted and dried *in vacuo* to afford compound **3-18** as a pale yellow fine powder (670 mg, 1.04 mmol, 92%). IR (neat): 2961, 2142, 1498, 1402, 1260, 1214, 1023, 932, 864, 797, 756, 691 cm^{-1}; ^{1}H NMR (300 MHz, CD$_2$Cl$_2$): δ 8.13 (s, 2H), 7.74 (d, J = 7.78 Hz, 4H), 7.33 (t, J = 7.39 Hz, 4H), 7.24 (t, J = 7.49 Hz, 2H), 6.83 (s, 2H), 4.75 (t, J = 4.76 Hz, 4H), 4.28 (t, J = 4.77 Hz, 4H), 0.15 (s, 18H); ^{13}C NMR (75 MHz, CD$_2$Cl$_2$), δ 153.65, 148.18, 131.30, 129.21, 128.46, 126.13, 121.60, 117.93, 114.58, 101.88, 100.76, 68.39, 50.27, 1.21; HRMS (EI, +eV) *m/z* calcd for $C_{36}H_{40}N_6O_2Si_2$ 644.2751, found 644.2753 (M$^+$).

**1,1'-(2,2'-(2,5-diethynyl-1,4-phenylene)bis(oxy)bis(ethane-2,1-diyl))bis(4-phenyl-1H-1,2,3-triazole) (3-19)**

3-19
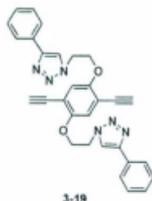
Compound **3-18** (600 mg, 0.93 mmol) and K$_2$CO$_3$ (629 mg, 4.56 mmol) were added to 15 mL of THF/MeOH (1:1) in a round-bottom flask and stirred for 0.5 h. The solvent was removed *in vacuo* and the residue was dissolved in ethylacetate and washed with water. The organic layer was dried over MgSO$_4$ and the solvent was removed *in vacuo* to give **3-19** as a pale yellow solid (433 mg, 0.86 mmol, 93%). IR (neat): 3290, 1666, 1565, 1496, 1396, 1353, 1269, 1224, 1156, 1041, 925, 869, 803, 759, 698 cm^{-1}; ^{1}H NMR (300 MHz, CD$_2$Cl$_2$): δ 8.14 (s, 2H), 7.74 (d, J = 7.14 Hz, 4H), 7.34 (t, J = 7.03 Hz, 4H), 7.24 (t, J = 7.22 Hz, 2H), 6.88 (s, 2H), 4.74 (t, J = 4.74 Hz, 4H), 4.27 (t, J = 4.97 Hz, 4H), 3.38 (s, 2H); ^{13}C NMR (75 MHz, CD$_2$Cl$_2$), δ 153.89, 147.93, 131.30, 129.23, 128.39, 125.89, 122.04, 118.17, 113.90, 83.78, 79.57, 68.34, 50.09; HRMS (EI, +eV) m/z calcd for C$_{30}$H$_{24}$N$_6$O$_2$ 500.1955, found 500.1958 (M$^+$).

Polymer 3-6

Polymer 3-6
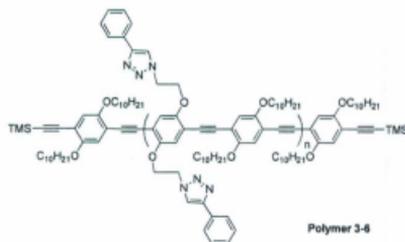
Compound **3-4** (70 mg, 0.11 mmol), compound **3-19** (60 mg, 0.12 mmol), compound **3-13** (6.5 mg, 0.012 mmol) as endcapping reagent, Pd(PPh$_3$)$_2$Cl$_2$ (1.5 mg, 0.01 mmol), and CuI (6 mg, 0.03 mmol) were dissolved in dry THF/piperidine (5:3, 40 mL). The flask

was purged with N_2 twice and cooled to -78 °C. The content was heated up to 60 °C. The reaction mixture was stirred for 24 h at this temperature and then cooled to room temperature. The solvent was evaporated off under vacuum and the residual solid mass was dissolved in CH_2Cl_2 and washed sequentially with 1% HCl and satd. NH_4Cl solution to give a deep-red organic layer, which was concentrated to dryness and dissolved again in CH_2Cl_2 and precipitated out of MeOH to yield polymer 3-6 (69 mg, 0.08 mmol, 65%) as a deep-yellow solid. IR (neat): 2921, 2851, 1562, 1498, 1459, 1423, 1369, 1269, 1210, 1040, 920, 857, 761, 693 cm^{-1}; ^{1}H NMR (300 MHz, CD_2Cl_2): δ 8.34 (m, 2H), 7.79 (m, 2H), 4.77 (m, 4H), 4.33 (m, 4H), 3.86 (m, 6H), 1.68 (m, 9H), 1.13 (m, 42H), 0.76 (m, 12H), 0.19 (m, 1H); ^{13}C NMR (75 MHz, CD_2Cl_2), δ 148.03, 147.98, 129.01, 128,15, 126.07, 125.77, 125.74, 125.72, 122.29, 122.24, 70.32, 70.06, 50.17, 32.34, 32.29, 30.03, 29.99, 29.74, 29.73, 26.50, 23.11, 23.08, 14.30.

(Anthracene-9-ylethynyl)trimethylsilane (3-20)[69]

3-20
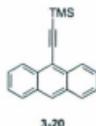
A mixture of 9-bromoanthracene (400 mg, 1.55 mmol), Pd(PPh$_3$)$_2$Cl$_2$ (11 mg, 0.01 mmol), and CuI (3 mg, 0.01 mmol) were added in 20 mL of dry THF/Et$_3$N (1:1). To this constantly stirred mixture was then dropwise added a solution of TMSA (471 mg, 4.80 mmol) in THF (2 mL) and stirred at 65 °C for 12 h. The solvent was removed and the resulting solid mass was dissolved in CH_2Cl_2 and washed with H_2O and brine. The organic layer was then dried over MgSO$_4$, filtered and finally column chromatographed

(CH$_2$Cl$_2$/hexanes 1:5) to give compound **3-20** as an orange solid (302 mg, 1.08 mmol, 70%). ^{1}H NMR (500 MHz, CDCl$_3$): δ 8.59-8.57 (d, J = 8.67 Hz, 2H), 8.45 (s, 1H), 8.03-8.02 (d, J = 8.08 Hz, 2H), 7.62-7.59 (m, 2H), 7.54-7.51 (m, 2H), 0.45 (s, 9H); ^{13}C NMR (75 MHz, CDCl$_3$), δ 132.62, 130.79, 128.36, 127.61, 126.50, 125.37, 116.84, 105.93, 101.26, 30.66, 0.00.

9-Ethynylanthracene (3-21)[69]

3-21

Compound **3-20** (50 mg, 0.18 mmol) and K$_2$CO$_3$ (100 mg, 0.72 mmol) were added to 5 mL of THF/MeOH (1:1) in a round-bottom flask and stirred at room temperature for 0.5 h. The solvent was removed in vacuo and the residue was dissolved in CH$_2$Cl$_2$ and washed with water. The organic layer was dried over MgSO$_4$ and the solvent was removed in vacuo to give **3-21** as a dark powder (33 mg, 0.16 mmol, 93%). ^{1}H NMR (300 MHz, CDCl$_3$): δ 8.59-8.56 (d, J = 8.73 Hz, 2H), 8.46 (s, 1H), 8.03-8.00 (d, J = 7.79 Hz, 2H), 7.62-7.56 (m, 2H), 7.53-7.48 (m, 2H), 3.99 (s, 1H); ^{13}C NMR (75 MHz, CDCl$_3$), δ 133.17, 131.03, 128.67, 128.24, 126.84, 126.56, 125.69, 116.02, 88.19, 80.13.

1-Bromopyrene (3-22)[70]

3-22

Pyrene (1 g, 5 mmol) was added to a mixture of MeOH/diethyl ether (40 mL, 1:1) and hydrobromic acid (440 mg, 48% aq, 5.4 mmol). Hydrogen peroxide (168 mg, 50 % wt aq, 4.94 mmol) was slowly added over a period of 15 min at 15 °C and stirred at room temperature for 12 h. The mixture was extracted with CH_2Cl_2 and washed with NaOH (1 M aq), water and brine. The organic layer was dried over $MgSO_4$, filtered and the solvent removed under vacuum. The residue was column chromatographed with hexanes to afford a mixture of compound **3-22** and pyrene as a yellow solid.

2-Methyl-4-(pyren-1-yl)but-3-yn-2-ol (3-24)[71]
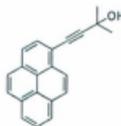
3-24

Compound **3-22** (1.05 g, 3.74 mmol) was dissolved in piperidine (25 mL) and 2-methylbut-3 yn-2-ol (942 mg, 11.21 mmol), $Pd(PPh_3)_2Cl_2$ (260 mg, 0.37 mmol), and CuI (145 mg, 0.76 mmol) were added and the mixture was stirred at 80 °C overnight. The solvent was rotavapped and the mixture was redissolved in ethyl acetate and washed with satd. $NaHCO_3$, water and brine. The residue was column chromatographed with (ethyl acetate/hexanes 1:5) to afford compound **3-24** (478 mg, 1.68 mmol, 45%) as an orange solid. ^1H NMR (300 MHz, CDCl$_3$): δ 8.51 (d, J = 9.12 Hz, 1H), 8.21-7.98 (m, 8H), 2.26 (s, 1H), 1.80 (s, 6H); ^{13}C NMR (75 MHz, CDCl$_3$), δ 131.93, 131.26, 131.23, 131.03, 129.66, 128.35, 128.15, 127.23, 126.23, 125.62, 125.58, 125.35, 124.42, 124.29, 117.20, 99.48, 81.27, 66.10, 31.79.

1-Ethynylpyrene (3-25)[71]

3-25

Compound **3-24** (342 mg, 1.20 mmol) was suspended in toluene (15 mL) and KOH (673 mg, 12.03 mmol) and refluxed for 1 h. The solvent was distilled off under vacuum and the residue redissolved in CH$_2$Cl$_2$, washed with HCl (1% aq), water and brine. The product **3-25** (149 mg, 0.66 mmol, 55%) was obtained after column chromatography with (ethyl acetate/hexanes 3:5) as a yellow solid. ^{1}H NMR (300 MHz, CDCl$_3$): δ 8.61-8.51 (d, J = 9.14, 1H), 8.24-8.01 (m, 8H), 3.62 (s, 1H); ^{13}C NMR (75 MHz, CDCl$_3$), δ 132.50, 131.60, 131.18, 130.99, 130.16, 128.56, 127.19, 126.29, 125.74, 125.69, 125.31, 124.38, 124.21, 116.51, 82.74, 82.60.

1,4-Bis(2-bromoethoxy)-2,5-diethynylbenzene (3-26)

3-26
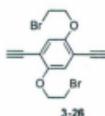
Compound **3-16** (152 mg, 0.29 mmol) and K$_2$CO$_3$ (243 mg, 1.76 mmol) were added to 10 mL of THF/MeOH (1:1) in a round-bottomed flask and stirred at room temperature for 0.5 h. The solvent was removed in vacuo and the residue was dissolved in CH$_2$Cl$_2$ and washed with water. The organic layer was dried over MgSO$_4$ and the solvent removed in vacuo to give **3-26** as a pale pink solid (108 mg, 0.29 mmol, 100%). IR (neat): 3258,

1492, 1275, 1216, 1071, 1013, 966, 897, 856 cm^{-1}; ^{1}H NMR (300 MHz, CDCl$_3$): δ 7.00 (s, 2H), 4.31 (t, J = 6.50 Hz, 4H), 3.65 (t, J = 6.70, 4H), 3.38 (s, 2H); ^{13}C NMR (75 MHz, CDCl$_3$), δ 153.66, 119.08, 114.20, 83.45, 78.95, 69.73, 28.52; HRMS (EI, +eV) m/z calcd for C$_{14}$H$_{12}$Br$_2$O$_2$ 369.9198, found 369.9209 (M$^+$).

Compound 3-27
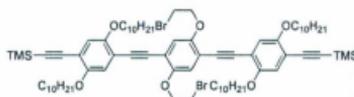
**3-27**

Compound **3-26** (82 mg, 0.22 mmol), Pd(PPh$_3$)$_2$Cl$_2$ (15 mg, 0.03 mmol), and CuI (19 mg, 0.1 mmol) in 10 mL of dry THF/Et$_3$N (1:1) at 0 °C were added to a 100 mL round-bottomed flask. To this constantly stirred mixture, a solution of 1,4-bis(decyloxy)-2,5-bis(ethynyl)benzene (compound **3-13**) (309 mg, 0.51 mmol) in Et$_3$N (5 mL) was added dropwise for 0.5 h. The reaction mixture was then stirred at room temperature for 12 h and the solvent was removed under vacuum. The resulting solid mass was dissolved in CH$_2$Cl$_2$ and washed with aq. HCl (1%), water and brine. The organic layer was dried over MgSO$_4$, filtered and solvent was removed to dryness and finally column chromatographed (hexanes/CH$_2$Cl$_2$, 4:1) to yield compound **3-27** (133 mg, 0.10 mmol, 45%) as a deep-yellow solid. IR (neat): 2918, 2848, 2153, 1501, 1384, 1275, 1214, 1023, 905, 849, 758 cm^{-1}; ^{1}H NMR (300 MHz, CDCl$_3$): δ 7.04 (s, 2H), 7.00 (s, 2H), 6.94 (s, 2H), 4.39-4.35 (t, J = 13.11, 4H), 4.03-3.96 (m, 8H), 3.69-3.65 (t, J = 13.10, 4H), 1.88-1.76 (m, 8H), 1.54-1.44 (m, 8H), 1.27-1.26 (m, 48H), 0.90-0.85 (m, 12H), 0.26 (s, 18H);

^{13}C NMR (75 MHz, CDCl$_3$): δ 154.19, 153.38, 153.25, 118.99, 117.26, 117.12, 115.33, 114.09, 113.94, 101.13, 100.39, 92.49, 90.48, 70.00, 69.62, 69.54, 31.93, 30.96, 29.69, 29.64, 29.49, 29.44, 29.37, 29.33, 28.93, 26.09, 25.97, 22.72, 14.15, 0.00; MALDI-TOF MS (dithranol as the matrix) m/z calcd for C$_{76}$H$_{116}$Br$_2$O$_6$Si$_2$ 1338.6672, found 1338.6706 (M)$^+$.

Compound 3-28
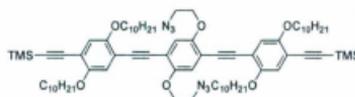
3-28

Compound **3-27** (99 mg, 0.07 mmol) was dissolved in a mixture of DMF/H$_2$O (10 mL) and NaN$_3$ (29 mg, 0.44 mmol) was then added. The mixture was stirred at 40 °C for 12 h. The solvent removed in vacuo and redissolved in CH$_2$Cl$_2$ and the organic layer was washed with H$_2$O and brine and dried over MgSO$_4$. The solvent was removed in vacuo to afford compound **3-28** (77 mg, 0.06 mmol, 87%) as a yellow solid. IR (neat): 2917, 2848, 2152, 2097, 1503, 1464, 1383, 1274, 1215, 1035, 899, 849, 755 cm^{-1}; ^{1}H NMR (300 MHz, CDCl$_3$): δ 7.04 (s, 2H), 6.99 (s, 2H), 6.93 (s, 2H), 4.23–4.20 (t, J = 10.10, 4H), 4.02–3.94 (m, 8H), 3.65–3.61 (t, J = 10.0, 4H), 1.51–1.44 (m, 8H), 1.54–1.44 (m, 8H), 1.27–1.25 (m, 48H), 0.90–0.84 (m, 12H), 0.26 (s, 18H); ^{13}C NMR (75 MHz, CDCl$_3$), δ 154.20, 153.43, 153.23, 118.21, 117.20, 117.04, 114.84, 114.04, 113.93, 101.19, 100.26, 92.29, 90.57, 69.56, 69.44, 68.85, 50.42, 31.92, 29.68, 29.64, 29.62, 29.49, 29.43, 29.39, 29.37, 29.33, 26.08, 22.70, 14.14, 0.00; MALDI-TOF MS (dithranol as the matrix) m/z calcd for C$_{76}$H$_{116}$N$_6$O$_6$Si$_2$ 1264.8489, found 1264.8539 (M)$^+$.

**1,4-Bis(prop-2-ynyloxy)benzene (3-30)**[72]

3-30

Hydroquinone (1.00 g, 9.09 mmol) was dissolved in DMF (15 mL) and K$_2$CO$_3$ (3.01 g, 21.8 mmol) was added and stirred at room temperature for 0.5 h. Propargyl bromide (2.38 g, 20 mmol) was added and the resulting mixture was stirred at 70 °C for 48 h. The reaction mixture cooled to room temperature and then ethyl acetate was added. The organic layer was washed with water and brine and dried over MgSO$_4$. Column chromatography using hexanes as eluent afforded compound **3-30** (1.369 g, 7.363 mmol, 81%) as a yellow solid. ^{1}H NMR (300 MHz, CDCl$_3$): δ 6.93 (s, 4H), 4.65 (d, J = 2.39 Hz, 4H), 2.51 (t, J = 2.39 Hz, 4H); ^{13}C NMR (75 MHz, CDCl$_3$), δ 152.43, 116.05, 78.80, 75.41, 56.53.

1,4-Bis((1-(anthracen-9-ylmethyl)-1H-1,2,3-triazol-4-yl)methyl)benzene (3-32)
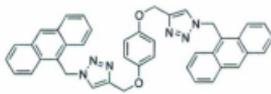
3-32

Compound **3-30** (20 mg, 0.11 mmol), 9-(azidomethyl)anthracene (52 mg, 0.22 mmol) were dissolved in THF (20 mL) and then CuI (5 mg, 0.03 mmol) and DIPEA (5 mg, 0.04 mmol) were added to the mixture. After stirring the mixture at 45 °C for 24 h, the slurry filtered and the precipitation was washed with NH$_4$Cl (satd.), CH$_2$Cl$_2$, water

and brine. The residue was dried under vacuum to afford compound **3-32** (67 mg, 0.10 mmol, 91%) as a yellow solid. IR (neat): 1505, 1220, 1013, 730 cm^{-1}; ^{1}H NMR (300 MHz, DMSO-d_6): δ 8.74 (s, 2H), 8.61 (d, J = 8.62 Hz, 4H), 8.17 (d, J = 8.14 Hz, 4H), 8.02 (s, 2H), 7.67-7.55 (m, 8H), 6.80 (s, 4H), 6.65 (s, 4H), 4.91 (s, 4H).

(2,5-Dimethoxy-1,4-phenylene)bis(ethyne-2,1-diyl)bis(trimethylsilane) (3-34)[72]
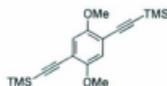
3-34

A mixture of compound **3-6** (800 mg, 2 mmol), Pd(PPh$_3$)$_2$Cl$_2$ (14 mg, 0.02 mmol), and CuI (78 mg, 0.41 mmol) were added in 15 mL of dry THF/Et$_3$N (1:1). To this constantly stirred mixture was then dropwise added a solution of TMSA (823 mg, 8.40 mmol) in THF (2 mL) and stirred at 50 °C for 12 h. The solvent was removed and the resulting solid mass was dissolved in ethyl acetate and washed with H$_2$O and brine. The organic layer was then dried over MgSO$_4$, filtered and finally column chromatographed (hexanes/ethyl acetate 5:1) to give compound **3-34** as an off-white solid (617 mg, 1.86 mmol, 91%). ^{1}H NMR (300 MHz, CDCl$_3$): δ 6.93 (s, 2H), 3.86 (s, 6H), 0.29 (s, 18H); ^{13}C NMR (75 MHz, CDCl$_3$), δ 154.16, 116.19, 113.41, 100.81, 100.43, 56.43, 0.00.

Page 133

missing from the
original book

Chapter 4

Conclusions and Future Work

The research presented in this dissertation is focused on the rational design, synthesis, and evaluation of conjugated polymers as fluorescent "turn-on" chemosensors and carbon nanotube (CNT) dispersants. "Click chemistry" has been exploited as an efficient and modular method to functionalize the conjugated polymers.

The efficiency of click chemistry in making polymer chemosensors has been demonstrated by the high sensitivity and selectivity of synthesized polymers in detecting metal ions. These polymers exhibit satisfactorily large fluorescence enhancement upon titration with metal ions compared to other reported polymer sensors in the literature. To better understand chemosensory systems involving click-functionalized conjugated polymers, detailed photophysical mechanisms need to be established and this work is currently ongoing in collaboration with Prof. David W. Thompson's group at Memorial University. At the moment, it is tentatively proposed that an internal charge transfer (ICT) mechanism dominates the sensor behavior instead of the photo-induced electron transfer (PET) mechanism, which already has been frequently adopted in the literature for explanation of turn-on systems based on conjugated polymers (Chapter 2). It should be noted that even though the PET mechanism has been widely used for design and rationalization, most of the reports did not provide conclusive evidence for its occurrence.

134

In this light, future work on mechanistic studies should lead to a significant progress in terms of fundamental understanding.

The ability of one of the synthesized polymers to detect harmful metal ions such as Cd^{2+} in aqueous solutions is worth some remarks. Development of this kind of polymer sensors can find practical use in industry and environmental science. The future work will focus on designing analogues of synthesized conjugated polymers employing click chemistry to show better sensor performance.

Although the click chemistry is efficient in preparation of chemosensors, a major setback should not be overlooked; that is, the click product suffers from low solubility in organic solvents (Chapter 3). The low solubility hinders the functionalization of conjugated polymers with various groups. In the case of developing effective functionalized polymers as CNT-dispersants, the target polymers in Chapter 3 were redesigned to circumvent this problem. Once the solubility problem is overcome, the future work will focus on the functionalizing of conjugated polymers with π-rich moieties such as anthracene and pyrene which can provide efficient π-π interactions with CNTs to disperse them in organic solvents. The ultimate goal will be aimed at finding suitable polymer dispersants to selectively disperse CNTs according to size, electronic type, and chirality.

Bibliography

1. Thomas III, S. W.; Joly, G. D.; Swager, T. M. *Chem. Rev.* **2007**, *107*, 1339-1386.

2. Bunz, U. H. *Chem. Rev.* **2000**, *100*, 1605-1644.

3. Giesa, R.; Schulz, R. C. *Macromol. Chem. Phys.* **1993**, *191*, 857.

4. Huisgen, R.; Szeimies, G.; Moebius, L. *Chem. Ber.* **1967**, *100*, 2494.

5. Rostovtsev, V. V.; Green, L. G.; Fokin, V. V.; Sharpless, K. B. *Angew. Chem. Int. Ed.* **2002**, *41*, 2596–2599.

6. Englert, B. C.; Bakbak, S.; Bunz, U. H. F. *Macromolecules* **2005**, *38*, 5868–5877.

7. Czarnik, A. W. *Acc. Chem. Res.* **1994**, *27*, 302-308.

8. Yang, J. S.; Swager, T. M. *J. Am. Chem. Soc.* **1998**, *120*, 11864.

9. De Silva, A. P.; Gunaratne, H. O. N.; Gunnlaugsson, T.; Huxley, A. J. M.; McCoy, C. P.; Rademacher, J. T.; Rice, T. E. *Chem. Rev.* **1997**, *97*, 1515-1566.

10. Mahmud, I. *Ph.D Dissertation* **2009**, Memorial Univeristy.

11. Fan, L.-J.; Zhang, Y.; Jones, W. E., Jr. *Macromolecules* **2005**, *38*, 2844-2849.

12. De Silva, A. P.; Gunaratne, H. O. N.; Gunnlaugsson, T.; Huxley, A. J. M.; McCoy, C. P.; Rademacher, J. T.; Rice, T. E. *Chem. Rev.* **1997**, *97*, 1515-1566.

13. Martínez-Máñez, R.; Sancenón F., *Chem. Rev.* **2003**, *103*, 4419-4476.

14. Valeur, B.; Leray, I., *Coord. Chem. Rev.* **2000**, *205*, 3-40.

15. McQuade, D. T.; Pullen, A. E.; Swager, T. M. *Chem. Rev.* **2000**, *100*, 2537.

16. Kim, J.; McQuade, D. T.; McHugh, S. K.; Swager, T. M. *Angew. Chem., Int. Ed.* **2000**, *39*, 3868.

17. Kim, I.-B.; Erdogan, B.; Wilson, J. N.; Bunz, U. H. F. *Chem. Eur. J.* **2004**, *10*, 6247.

18. Yang, J.-S.; Swager, T. M. *J. Am. Chem. Soc.* **1998**, *120*, 11864-11873.

19. Wang, H.; Lin, J.; Huang, W.; Wei, W. *Sensors And Actuators* B. **2010**, *150*, 798-805.

20. Fan, L. – J.; Zhang, Y.; Murphy, C. B.; Angell, S. E.; Parker, M. F. L.; Flynn, B. R.; Jones, W. E., Jr. *Coord. Chem. Rev.* **2009**, *253*, 410-422.

21. De Silva, A. P.; de Silva, S. A. *J. Chem. Soc. Chem. Commun.* **1986**, 1709.

22. de Silva, A. P.; Sandanayake, K. R. A. S. *Angew. Chem. Int. Ed. Engl.* **1990**, *29*, 1173.

23 Huston, M. E.; Haider, K. W.; Czarnik, A. W. *J. Am. Chem. Soc.* **1988**, 110, 4460.

24. McQuade, D. T.; Hegedus, A.H; Swager, T.M. *J. Am. Chem. Soc.* **2000**, *122*, 12389.

25. Fan, L.-J.; Zhang, Y.; Jones, W. E., Jr. *Macromolecules* **2005**, *38*, 2844.

26. Fan, L.-J.; Jones, W. E., Jr. *J. Am. Chem. Soc.* **2006**, *128*, 6784.

27. Huang, X.; Xu, Y.; Zheng, L.; Meng, J.; Cheng, Y. *Polymer* **2009**, *50*, 5996-6000.

28. Wang, H.; Lin, J.; Huang, W.; Wei, W. *Sensors and Actuators B* **2010**, *150*, 798-805.

29. (a) Kroto, H. W.; Heath, J. R.; O'Brien, S. C.; Curl, R. F.; Smalley, R. E. *Nature.* **1985**, 318. (b) Krätschmer, W.; Lamb, L. D.; Fostiropoulos, K.; Huffman, D. R. *Nature.* **1990**, 347.

30. (a) Iijima, S. Nature, **1991**, *354*, 56. (b) Iijima, S; Ichihashi, T. *Nature* **1993**, *363*, 603.

31. *Advanced Topics in the Synthesis, Structure, Properties and Applications*; Jorio, A.; Dresselhaus, G., Dresselhaus, M., Eds.; Springer: New York, 2008.

32. Odom, T. W.; Hafner, J. H.; Lieber, C. M. *Scaning Probe Microscopy Studies of Carbon Nanotubes*, Topics in Appl. Physics Series; *80*, 173-211, Springer-Verlag, Berlin Heidelberg, 2001.

33. Tasis, D.; Tagmatarchis, N.; Bianco, A.; Prato, M. *Chem. Rev.* **2006**, *106*, 1105-1136.

34. Umek, P.; Vrbanic, D.; Remskar, M.; Mertelj, T.; Venturini, P.; Pejovnik, S.; Mihailovic, D. *Carbon*.

35. Adu, C. K. W.; Sumanasekera, G. U.; Pradhan, B. K.; Romero, H. E.; Eklund, P. C. *Chem. Phys. Lett.* **2001**, *31*, 337.

36. (a) Dillon, A. C.; Jones, K. M.; Bekkedahl, T. A.; Kiang, C. H.; Bethune, D. S.; Heben, M. J. *Nature*. **1997**, *386*, 377-379. (b) Liu, C.; Fan, Y. Y.; Liu, M.; Cong, H. T.; Cheng, H. M.; Dresselhaus, M. S. *Science*. **1999**, *286*, 1127-1129.

37. Chambers, A.; Park, C.; Baker, T. K.; Rodriguez, N. M. *J. Phys. Chem.* **1998**, *102*, 4253-4256.

38. Pederson, M.; Broughton, J. *Phys. Rev. Lett.* **1992**, *69*, 2689-2692.

39. Kam, N. W. S.; O'Connel, M.; Wisdom, J. A.; Dai, H. *PNAS*. **2005**, *102*, 11600-11605.

40. Kymkis, E.; Amaratunga, G. A. J. *J. Appl. Phys.* **2003**, *80*, 465-472.

41. Ago, H.; Petritsch, K.; Shaffer, M. S. P.; Windle, A. H.; Friend, R. H. *Advanced Material*. **1999**, *11*, 1281-1285.

42. Arnold, M. S.; Stupp, S. I.; Hersam, M. C. *Nano Lett.* **2005**, *5*, 713-718.

43. Park, T. J.; Banerjee, S.; Hemraj-Benny, T.; Wong, S. S. *J. Mater. Chem.* **2006**, *16*, 141-154.

44. Chen, J.; Hamon, M. A.; Hu, H.; Chen, Y. S.; Rao, A. M.; Ecklund, P. C.; Haddon, R. C. *Science*. **1998**, *282*, 95-98.

45. Pan, H. L.; Liu, L. Q.; Guo, Z. X.; Dai, L. M.; Zhang, F. S.; Zhu, D. B.; Czerw, R.; Carroll, D. L. *Nano Lett*. **2003**, *3*, 29-32.

46. Campidelli, S.; Sooambar, C.; Dis, E. L.; Ehli, C.; Guldi, D. M.; Prato, M. *J. Am. Chem. Soc.* **2006**, *128*, 12544-12552.

47. Li, H.; Cheng, F.; Duft, A. M.; Adronov, A. *J. Am. Chem. Soc.* **2005**, *127*, 14518-14524.

48. (a) Wang, X.; Liu, Y.; Oiu, W.; Zho, D. *J. Mater. Chem.* **2002**, *12*, 1636. (b) Cao, L.; Chen, H.–Z.; Zhou, H.-B.; Zhu, L.; Sun, J.-Z.; Zhang, X.-B.; Xu, J.-M. *Adv. Mater*. **2003**, *15*, 909. (c) Murakami, H.; Nomura, T.; Nakashima, N. *Chem. Phys. Lett.* **2003**, *378*, 481.

49. Hasobe, T.; Fukusumi, S.; Kamat, P. V. *J. Am. Chem. Soc.* **2005**, *127*, 11884-11885.

50. Nakayama-Ratchford, N.; Bangsaruntip, S.; Sun, X.; Welsher, K.; Dai, H. *J. Am. Chem. Soc.* **2007**, *129*, 2448-2449.

51. Herranz, M. A.; Ehli, C.; Campidelli, S.; Gutierrez, M.; Hug, G. L.; Ohkubo, K.; Fukuzumi, S.; Prato, M.; Martin, N.; Guldi, D. M. *J. Am. Chem. Soc.* **2008**, *130*, 66-73.

52. Itkis, M. E.; Perra, D. E.; Niyogi, S. M.; Hamon, M. A.; Hu, H.; Zhao, B.; Haddon, R. C. *Nano Lett.* **2003**, *3*, 309.

53. Yi, W.; Malkovskiy, A.; Xu, Y.; Wang, X-Q.; Sokolov, A. P.; Lebron-Colon, M.; Meador, M. A.; Pang, Y. *Polymer*. **2010**, *51*, 475-481.

54. Nish, A.; Hwang, J.-Y.; Doig, J.; Nicholas, R. J. *Nature Nanotech.* **2007**, *2*, 640.

55. Chen, F.; Yang, B.; Chen, Y.; Li, L-J. *Nano Lett.* **2007**, *7*, 3013.

56. Rice, N. A.; Soper, K.; Zhou, N.; Merschrod, E.; Zhao, Y. *Chem. Commun.* **2006**, 5937- 4939.

57. Delozier, D. M.; Watson, K. A.; Smith, J. G.; Clancy, T. S.; Connel, J. W. *Macromolecules.* **2006**, *39*, 1731-1739.

58. Pu, K.-Y.; Liu, B. *Adv. Funct. Mater.* **2009**, *19*, 277.

59. Shen, D.; Wang, L.; Pan, Z.; Cheng, S.; Zhu, X.; Fan, L. *Macromolecules* **2010**, *44*, 1009–1015.

60. Grabowski, Z. R.; Rotkiewicz, K.; Rettig, W. *Chem. Rev.* **2003**, *103*, 3899.

61. *Guidelines for drinking water quality (second ed.),* Health Criteria and Other Supporting Information *vol. 2*, World Health Organization, Geneva, 1998, 281–283.

62. Zhao, Y.; Shirai, Y.; Slepkov, A. D.; Cheng, L.; Alemany, L. B.; Sasaki, T.; Hegmann, F. A.; Tour, J. M. *Chem. Eur. J.* **2005**, *11,* 3643-3658.

63. Pinto, M. R.; Kristal, B. M.; Schanze, K. S *Langmuir.* **2003**, *19,* 6523-6533.

64. Shao, M.; Zhao, Y. *Tetrahedron Lett.* **2010**, *51*, 2892-2895.

65. Miki, Y.; Momotake, A.; Arai, T. *Org. Biomol. Chem.* **2003**, *1*, 2655-2660.

66. Numata, M.; Fujisawa, T.; Li, C.; Haraguchi, S.; Ikeda, M.; Sakurai, K.; Shinkai, S. *Supramolecular Chemistry,* **2007**, *19*, 107-113.

67. Wang, J.; Wang, D. L.; Miller, E. K.; Moses, D.; Bazan, G. C.; Heeger, A. J. *Macromolecules* **2000**, *33*, 5153-5158.

68. Sierra, C. A.; Lahati, P. M. *Chem. Mater.* **2004**, *16*, 55-61.

69. Nierth, A.; Kobitski, A. Y.; Nienhaus, U.; Jasxhke, A. *J. Am. Chem. Soc.* **2010**, *132*, 2646-2654.

70. He, C.; He, Q.; Chen, Q.; Shi, L.; Cao, H.; Cheng, J.; Deng, C.; Lin, T. *Tetrahedron letters.* **2010**, *51*, 1317-1321.

71. Crip, G. T.; Jiang, Y.-L.; *Synth. Commun.* **1998**, *28*, 2571.

72. Zhao, Y.-L.; Liu, L.; Zhang, W.; Sue, C.-H.; Li, Q.; Milijanic, O. S.; Yaghi, O. M.; Stoddart, J. F. *Chem. Eur. J.* **2009**, *15*, 13356-13380.

Appendix 2-1

Steady State Measurements

UV-Visible spectra were recorded on an Agilent 8543 Diode Array Spectrophotometer interfaced to an HP computer. Data manipulations were conducted using software supplied by the manufacturer. Spectroscopic experiments were conducted using 1cm sealed quartz fluorescence cuvettes supplied by Aldrich.

Emission spectra were measured on Photon Technology International (PTI) Quantamaster 6000 spectrofluorometer equipped with a continuous xenon arc lamp as the excitation source. The emitting light was collected at $90°$ to the excitation beam and detected by a Hammamatsu R-928 photomultiplier tube (PMT) in photon counting mode. The PMT was housed in a water-cooled PMT housing supplied by Products for Research Inc. All emission spectra were corrected for instrumental light loss using correction factors supplied by PTI.

Reagents

De-ionized water was obtained from a Sybron/Barnstead apparatus. Spectral grade THF and DMSO solvents (Sigma Aldrich > 99% pure) were used as received. Titrations were performed by using triflate salts of corresponding analyte (unless otherwise noted) purchased from sigma Aldrich in 99% purity and used as received. Trifluoroacetic acid (TFA) was used in the titration as a source of H^+ was purchased from sigma Aldrich in 99% purity.

Titrations

Fixed molar solutions of **triflate/perchlorate salts** in THF and/or H$_2$O were prepared by gravimetric methods. Concentrated solution of the triflate and perchlorate salts in THF and/or H$_2$O were injected into the cuvette containing sensor to acquire the emission and absorption spectra. Addition of aliquots of metal salts resulted spectral changes in absorption and emission spectra assigned to the reactions, sequential binding reactions of polymer under investigation with cations.

Emission quantum yields were measured in N$_2$ saturated THF and H$_2$O solutions at 295 ± 3 K. The absorbance of the samples < 0.5 at the excitation wavelength, $\lambda_{exc} = 350$ nm to prevent distortion of the emission spectral data by inner-filter effects. The radiative quantum yields for all compounds (λ_{em}) were determined using quinine bisulfate in 0.1 M aqueous sulfuric acid solution as the actinometer ($\lambda_{std} = 0.52$ at $\lambda_{ex} = 350$ nm) and calculated using equation **S-1**.

$$\phi_{em} = \phi_{std}\left(\frac{A_{std}}{A_{un}}\right)\left(\frac{I_{un}}{I_{std}}\right)\left(\frac{n_{un}}{n_{std}}\right)^2 \qquad \textbf{[S-1]}$$

Where A is a solution absorbance, I the emission intensity, n the refraction index of the solvent and the subscripts un and std refer to the unknown and standard respectively.

Titration of PPE-1 with various metal cations

(A)

(B)

(C)
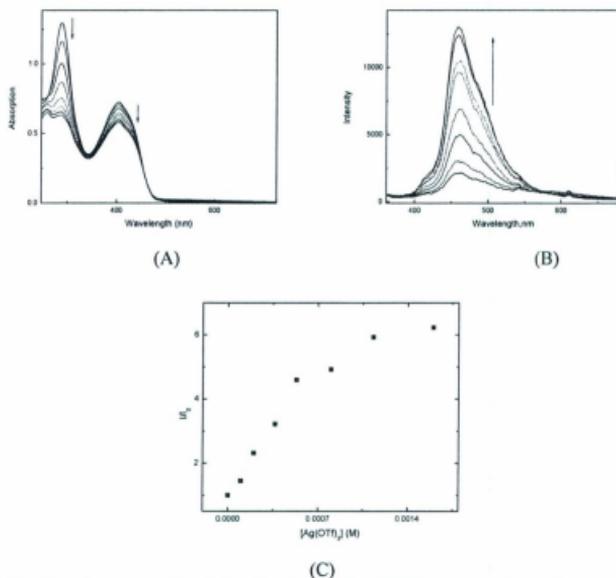
Fig-S1: Showing absorption (A) and emission (B) of PPE-1 obtained simultaneously as a function of increasing aliquots of Ba(OTf)$_2$ in the following manner in THF at 298 ± 2 K. 0.0, 1.0×10^{-4}, 2.0×10^{-4}, 3.66×10^{-4}, 5.33×10^{-4}, 8.0×10^{-4}, 1.13×10^{-3}, 1.60×10^{-3} (All in M). [Ba(OTf)$_2$] = 0.1 M; λ_{ex} = 380 nm. The arrows indicate the direction of response after addition of analyte. (C) shows the Stern - Volmer plot calculated from emission titration at 475 nm.

(A)

(B)

(C)
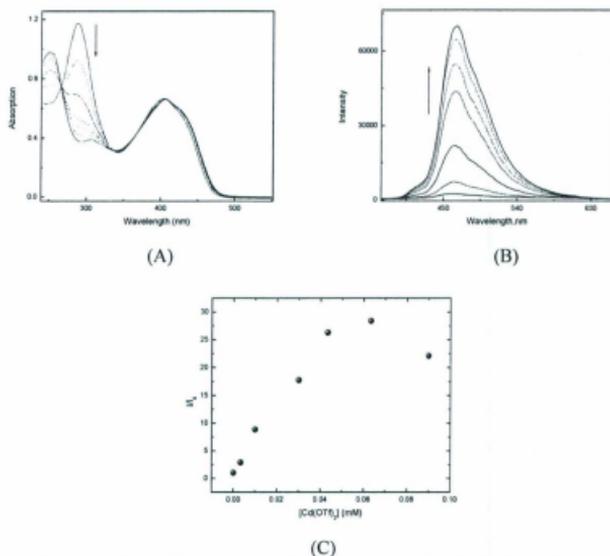
Fig-S2: Showing absorption (A) and emission (B) of PPE-1 obtained simultaneously as a function of increasing aliquots of $Cd(ClO_4)_2$ in the following manner in THF at 298 ± 2 K. 0.0, 3.33 × 10⁻⁶, 1.0 × 10⁻⁵, 3.0 × 10⁻⁵, 9.0 × 10⁻⁵, 4.33 × 10⁻⁵, 6.33 × 10⁻⁵ . [Cd(ClO₄)₂] = 0.01 M; λ_{ex} = 380 nm. The arrows indicate the direction of response after addition of analyte. (C) shows the Stern - Volmer plot calculated from emission titration at 475 nm.

(A)

(B)

(c)
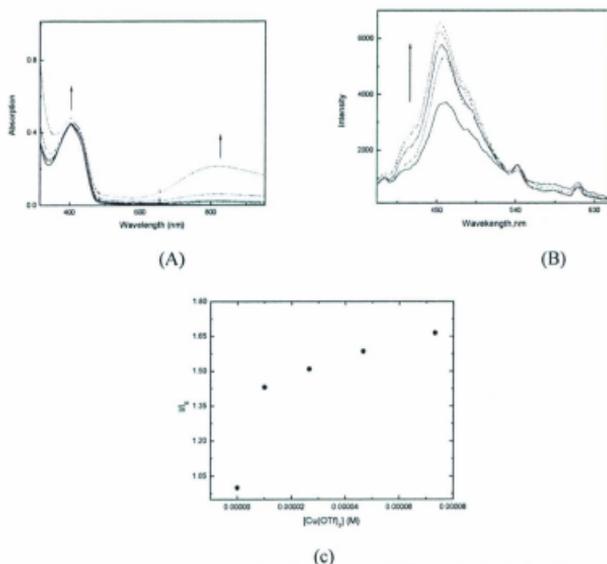
Fig-S3: Showing absorption (A) and emission (B) of PPE-1 obtained simultaneously as a function of increasing aliquots of Cu(OTf)$_2$ in the following manner in THF at 298 ± 2 K. 0.0, 1.0 × 10^{-5}, 2.66 × 10^{-5}, 4.66 × 10^{-5}, 7.33 × 10^{-5} . [Cu(OTf)$_2$] = 0.01 M; λ_{ex} = 380 nm. The arrows indicate the direction of response after addition of analyte. (C) shows the Stern - Volmer plot calculated from emission titration at 475 nm.

(A)

(B)

(C)
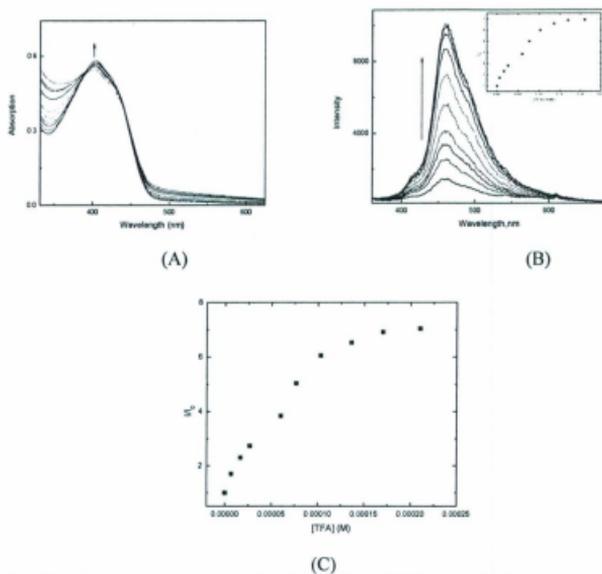
Fig-S4: Showing absorption (A) and emission (B) of PPE-1 obtained simultaneously as a function of increasing aliquots of TFA in the following manner in THF at 298 ± 2 K. 0.0, 6.66 × 10^{-6}, 1.66 × 10^{-5}, 2.66 × 10^{-5}, 6.0 × 10^{-5}, 7.66 × 10^{-5}, 1.03 × 10^{-4}, 1.36 × 10^{-4}, 1.70 × 10^{-4}, 2.1 × 10^{-4} [TFA] = 0.01 M. λ_{ex} = 380 nm. The arrows indicate the direction of response after addition of analyte. (C) shows the Stern - Volmer plot calculated from emission titration at 475 nm.

(A)

(B)

(C)
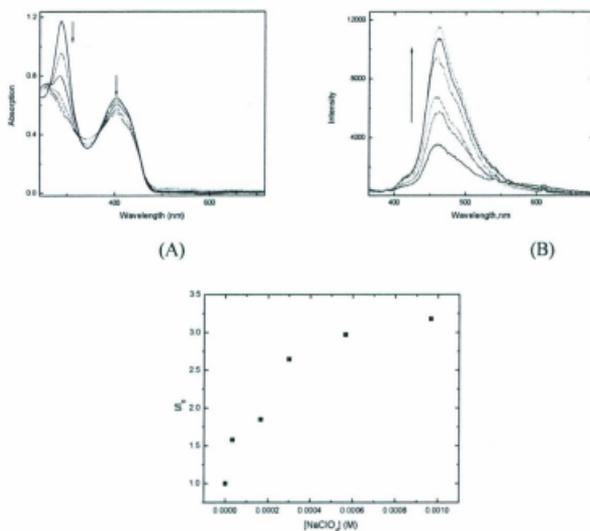
Fig-S5: Showing absorption (A) and emission (B) of PPE-1 obtained simultaneously as a function of increasing aliquots of NaClO$_4$ in the following manner in THF at 298 ± 2 K. 0.0, 3.33 × 10^{-5}, 1.66 × 10^{-4}, 3.0 × 10^{-4}, 5.66 × 10^{-4}, 9.66 × 10^{-4} [NaClO$_4$] = 0.1 M. λ_{ex} = 380 nm. The arrows indicate the direction of response after addition of analyte. (C) shows the Stern - Volmer plot calculated from emission titration at 460 nm.

(A)

(B)

(C)
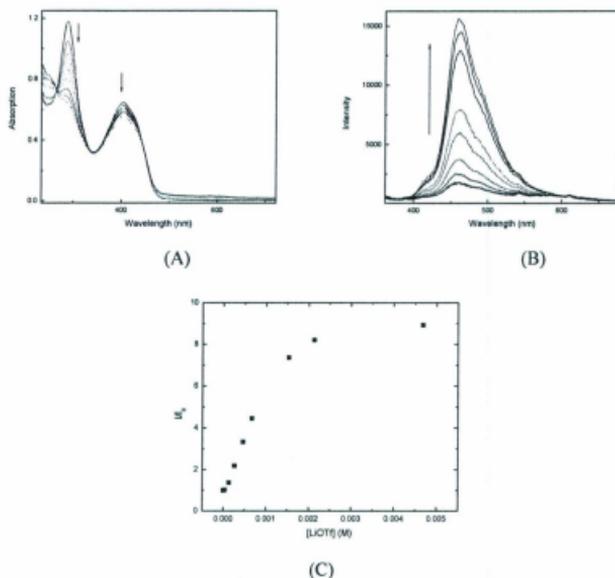
Fig-S6: Showing absorption (A) and emission (B) of PPE-1 obtained simultaneously as a function of increasing aliquots of LiOTf in the following manner in THF at 298 ± 2 K. 0.0, 3.33×10^{-5}, 1.33×10^{-4}, 2.66×10^{-4}, 4.66×10^{-4}, 6.66×10^{-4}, 1.53×10^{-3}, 2.13×10^{-3}, 4.68×10^{-3}. [LiOTf] = 0.1 M. λ_{ex} = 380 nm. The arrows indicate the direction of response after addition of analyte. (C) shows the Stern - Volmer plot calculated from emission titration at 475 nm.

(A)

(B)
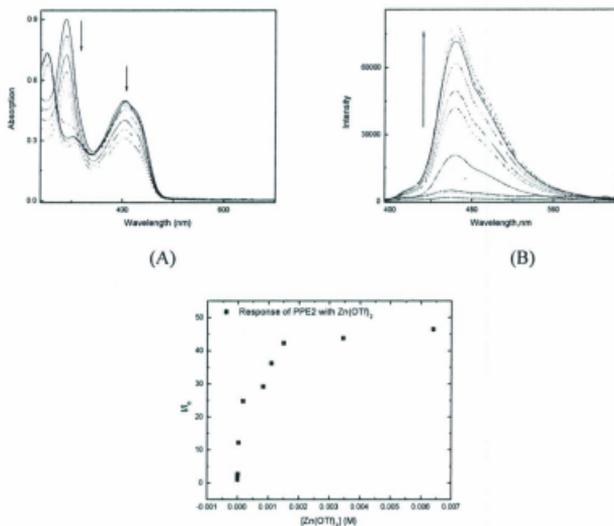
(C)

Fig-S7: Showing absorption (A) and emission (B) of PPE-1 obtained simultaneously as a function of increasing aliquots of [Zn(OTf)$_2$] in the following manner in THF at 298 ± 2 K. 0.0, 3.33 × 10^{-6}, 1.0 × 10^{-5}, 3.0 × 10^{-5}, 1.70 × 10^{-4}, 8.33 × 10^{-4}, 1.10 × 10^{-3}, 1.50 × 10^{-3} and 3.45 × 10^{-3} and 6.20 × 10^{-3} M. [Zn(OTf)$_2$] = 0.01 M. λ_{ex} = 380 nm. The arrows indicate the direction of response after addition of analyte. (C) shows the Stern - Volmer plot calculated from emission titration at 475 nm.
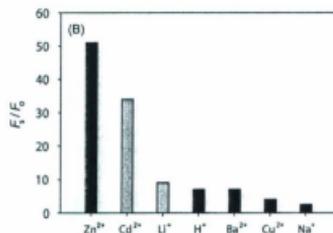
Fig-S8: Comparison of fluorescence enhancement of PPE-1 at 475 nm in response to various cations, calculated from emission titration data showing obtained in THF at 298 ± 2 K. Noticeably, the greatest enhancement is for Zn^{2+} and Cd^{2+}.

Titration of PPE-1 with Cd^{2+} in $H_2O/DMSO/SDS$ mixture.
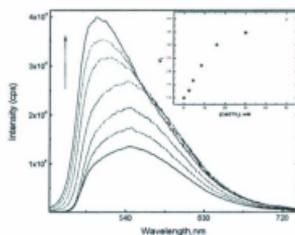
Fig-S9: Showing the emission spectrum of PPE-1 obtained as a function of increasing aliquots of $Cd(ClO_4)_2$ in 1:1 v/v of deionized $H_2O/DMSO$ with 0.5 mg/ml of SDS added as surfactant at 298 ± 2 K. $[Cd(ClO_4)_2]$ = 1.0 M. λ_{ex} = 425 nm. The arrows indicate the direction of response after addition of analyte. Inset showing Stern - Volmer plot calculated from emission titration data at 505 nm.

PPE-4 in water with cations

(A)

(B)

(C)
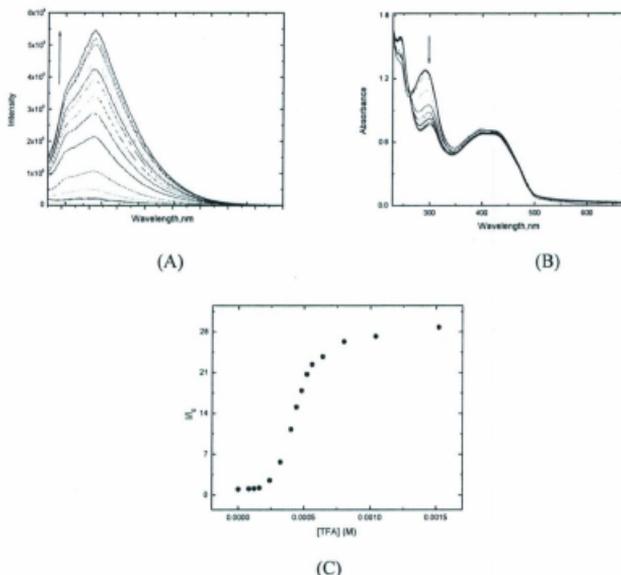
Fig-S10: Showing the emission (A) and absorption (B) spectra of PPE-4 obtained simultaneously as a function of increasing aliquots of TFA in the following manner; 0.0, 1.2×10^{-4}, 1.6×10^{-4}, 1.8×10^{-4}, 2.4×10^{-4}, 3.2×10^{-4}, 4.0×10^{-4}, 4.4×10^{-4}, 4.8×10^{-4}, 5.2×10^{-4}, 5.6×10^{-4}, 6.4×10^{-4}, 8.0×10^{-4}, 1.04×10^{-3}, 1.52×10^{-3} and 2.0×10^{-3} M titrated in deionized H_2O at 298 ± 2 K. [TFA] = 0.1 M. λ_{ex} = 400 nm. The arrows indicate the direction of response after addition of analyte. (C) shows the Stern - Volmer plot calculated from emission titration at 490 nm.

(A)

(B)

(C)
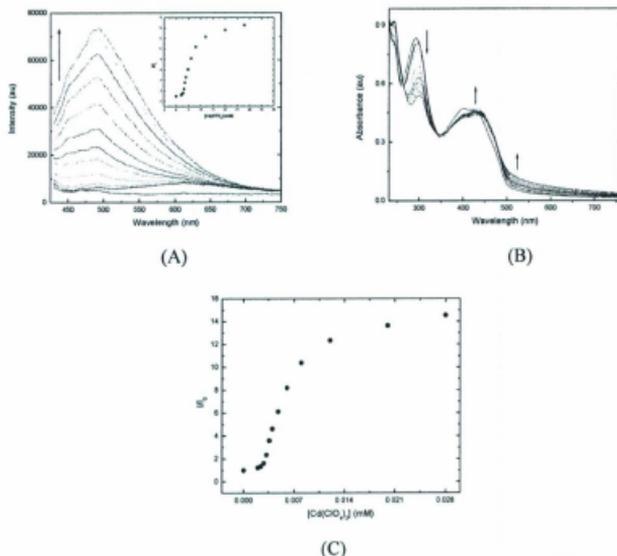
Fig-S11: Showing the emission (A) and absorption (B) spectra of PPE-4 obtained simultaneously as a function of increasing aliquots of Cd(ClO$_4$)$_2$ in the following manner; 0, 2.0, 2.4, 2.8, 3.2, 3.6, 4.0, 4.8, 6.0, 8.0, 12, 20 and 28 mM titrated in deionized H$_2$O at 298 ± 2 K. [Cd(ClO$_4$)$_2$] = 1.0 M. λ_{ex} = 400 nm. The arrows indicate the direction of response after addition of analyte. (C) shows the Stern - Volmer plot calculated from emission titration at 490 nm.

(A)

(B)
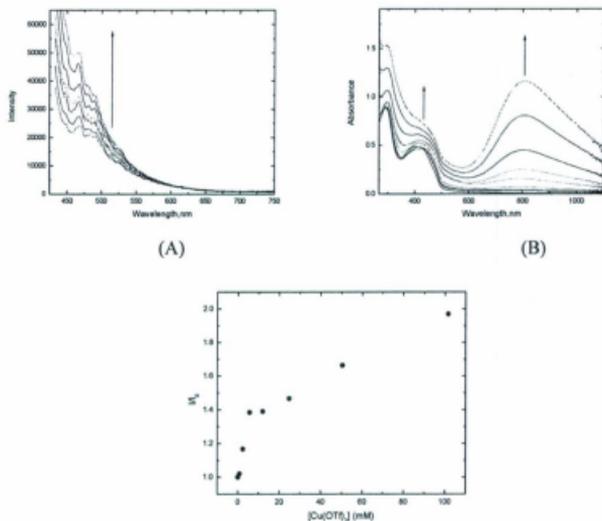
(C)

Fig-S12: Showing the emission (A) and absorption (B) spectra of PPE-4 obtained simultaneously as a function of increasing aliquots of Cu(OTf)$_2$ in the following manner; 0.0 , 0.8, 2.4, 5.6, 12, 24.8, 50.4 and 101.6 titrated in deionized H$_2$O at 298 ± 2 K. [Cu(OTf)$_2$] = 1.0 M. λ_{ex} = 400 nm. The arrows indicate the direction of response after addition of analyte. (C) shows the Stern - Volmer plot calculated from emission titration at 465 nm.
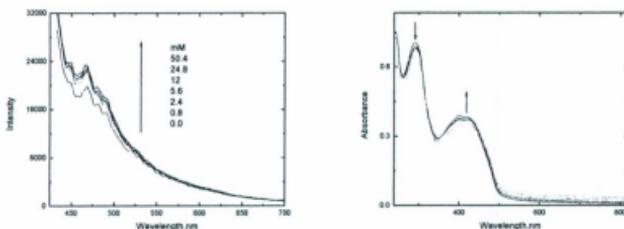
Fig-S13: Showing the emission (left) and absorption (right) spectra of PPE-4 obtained simultaneously as a function of increasing aliquots of LiOTf) in deionized H_2O at 298 $\pm$ 2 K. [LiOTf] = 1.0 M. λ_{ex} = 400 nm. The arrows indicate the direction of response after addition of analyte. A Stern - Volmer plot couldn't be calculated due to weak response.
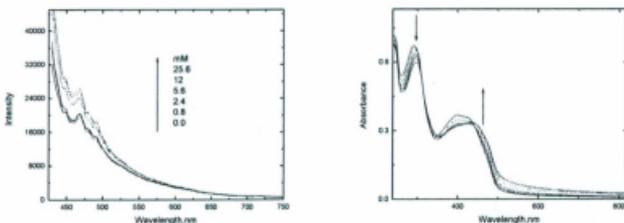

Fig-S14: Showing the emission (left) and absorption (right) spectra of PPE-4 obtained simultaneously as a function of increasing aliquots of Zn(OTf)$_2$ in deionized H_2O at 298 $\pm$ 2 K. [Zn(OTf)$_2$] = 1.0 M. λ_{ex} = 400 nm. The arrows indicate the direction of response after addition of analyte. A Stern - Volmer plot couldn't be calculated due to weak response.
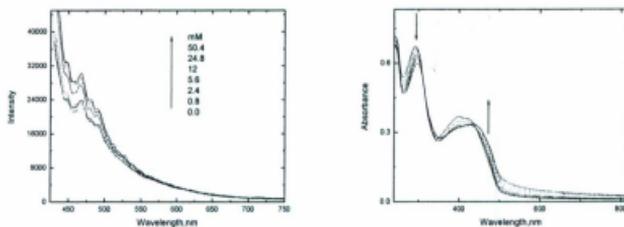
Fig-S15: Showing the emission (left) and absorption (right) spectra of PPE-4 obtained simultaneously as a function of increasing aliquots of Ba(OTf)$_2$ in deionized H$_2$O at 298 ± 2 K. [Ba(OTf)$_2$] = 1.0 M. λ_{ex} = 400 nm. The arrows indicate the direction of response after addition of analyte. A Stern - Volmer plot couldn't be calculated due to weak response.
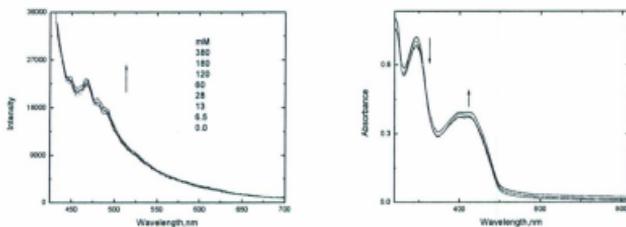

Fig-S16: Showing the emission (left) and absorption (right) spectra of PPE-4 obtained simultaneously as a function of increasing aliquots of NaClO$_4$ in deionized H$_2$O at 298 ± 2 K. NaClO$_4$ = 1.0 M. λ_{ex} = 400 nm. The arrows indicate the direction of response after addition of analyte. Stern - Volmer plot couldn't be calculated due to weak response.
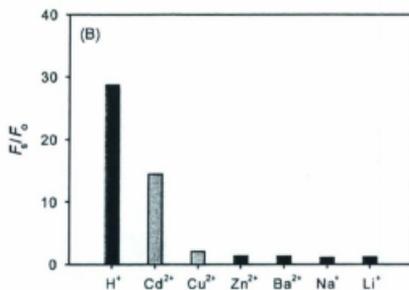
Fig-S17: A Comparison of fluorescence enhancement of PPE-4 at 490 nm in response to various cations and TFA, calculated from emission titration data. Noticeably, the greatest enhancement was for Cd^{2+}.

### Titration of PPE-3 with Cd^{2+} and TFA
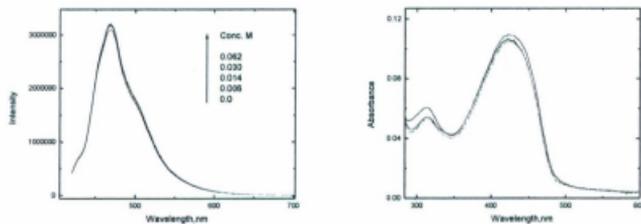
Fig-S18: Showing the emission (left) and absorption (right) spectra of PPE-3 obtained as a function of increasing aliquots of $Cd(ClO_4)_2$ in THF at 298 ± 2 K. $[Cd(ClO_4)_2] = 1.0$ M. $\lambda_{ex} = 400$ nm.
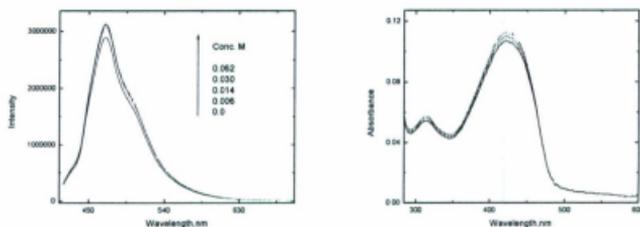
Fig-S19: Showing the emission (left) and absorption (right) spectra of PPE-3 obtained as a function of increasing aliquots of TFA in THF at 298 ± 2 K. [TFA] = 1.0 M. λ_{ex} = 400 nm.
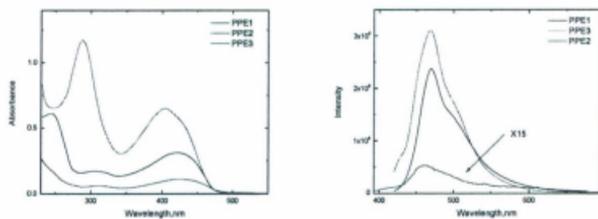

Fig-S20: A comparison of absorption (left) and emission spectra (right) of PPE-1, PPE-2 and PPE-3. For lucidity emission of PPE-1 was enhanced by 15 times.

Binding Constants
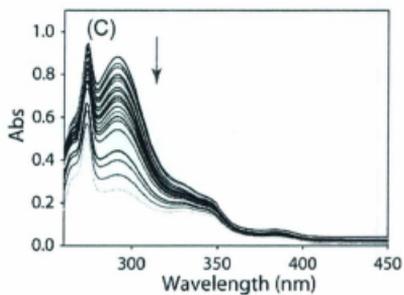
Fig-S21: Showing the UV-Vis titration of **monomer 2-11** obtained as a function of increasing aliquots of Cd(ClO$_4$)$_2$ in DMSO at 298 ± 2 K. [Cd(ClO$_4$)$_2$] = 0.1 M. Data from above spectrum was employed in calculation of association constants using global kinetic analysis. The arrows indicate the direction of response after addition of analyte. [2-11] = 0.0154 mM.
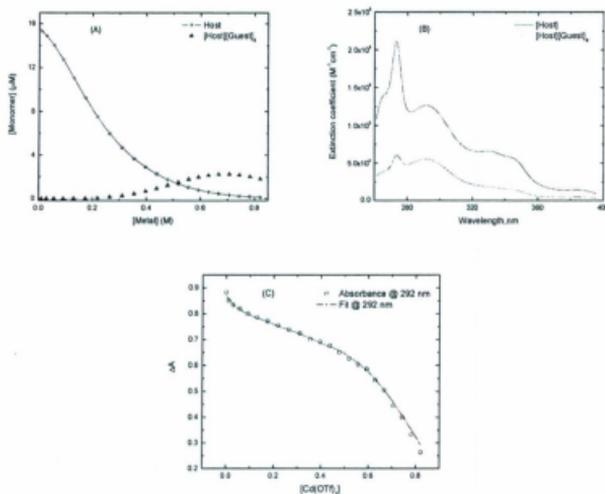
Fig-S22: (A) Concentration profiles of colorful species involved, extracted from the global fit by using ML$_4$ model of binding. (B) Deconvoluted absorption spectra of prevailing colorful species at different stages of titration experiment. (C) Change in absorbance at 292 nm after each addition of [Cd(ClO$_4$)$_2$] and the corresponding fit.

Compound	Binding model	Association constant (log β)
Monomer	ML$_4$	1.10 ± 0.06

Table of Quantum yields

Compound	φ_{Yield}
Monomer 2-11	0.0099
PPE-1	0.038
PPE-2	0.74
PPE-3	0.29
PPE-4	0.0024